MCR-74-52
Contract NAS9-12685

CR 134269

Final Report

May 1974

Flight Prototype Regenerative Particulate Filter System Development

Prepared for:
National Aeronautics
and Space Administration
Johnson Space Center
Houston, Texas

MARTIN MARIETTA

Contract NAS9-12685
DRL Number T-744
DRL Line Item 4
DRD Number MA-183T
MCR-74-52

FINAL REPORT

FLIGHT PROTOTYPE REGENERATIVE PARTICULATE FILTER SYSTEM DEVELOPMENT

May 1974

PREPARED BY:

DONALD C. GREEN
PAUL J. GARBER

APPROVED BY:

Victor A. DesCamp

VICTOR A. DESCAMP
PROGRAM MANAGER

MARTIN MARIETTA CORPORATION
P.O. BOX 179
DENVER, COLORADO 80201

FOREWORD

This document presents the results of work performed by the Martin Marietta Corporation's Denver Division for the National Aeronautics and Space Administration, Johnson Space Center. This final report was prepared as partial fulfillment of Contract NAS9-12685, Flight Prototype Regenerative Particulate Filter System. The NASA Technical Monitor was Mr. Albert F. Behrend, Jr. of the Crew Systems Division, Environmental Control and Life Support Systems Branch.

ABSTRACT

This report describes the effort accomplished under Contract NAS9-12685 to design, fabricate, and test a flight prototype Filter Regeneration Unit used to regenerate (clean) fluid particulate filter elements. This report describes the design of the filter regeneration unit and the results of tests performed in both one-gravity and zero-gravity. The filter regeneration unit uses a backflush/jet impingement method of regenerating fluid filter elements that is highly efficient (98.7 to 100%). A vortex particle separator and particle trap were designed for zero-gravity use, and the zero-gravity test results are discussed. The filter regeneration unit was designed for both inflight maintenance and ground refurbishment use on Shuttle and future space missions.

DISTRIBUTION LIST

COPIES	RECIPIENT
	National Aeronautics and Space Administration Johnson Space Center Houston, Texas 77058
1	Mr. Jack H. Goldstein Mail Code BC72 R&T Procurement Branch
4	Mrs. Retha Shirkey Mail Code JM6 Technical Library Branch
1	Mr. John T. Wheeler Mail Code JM7 Management Service Division
10	Mr. Albert F. Behrend, Jr. Mail Code EC3 Environmental Control and Life Support Systems Branch

CONTENTS

ABBREVIATIONS AND SYMBOLS

Abbreviations

AC	AC Road Dust, AC Spark Plug, Division of General Motors Corporation
ACS	American Chemical Society
Dia	Diameter
Hz	frequency, Hertz
N/A	Not Applicable
R.H.	Relative Humidity
VAC	Volts Alternating Current
VDC	Volts Direct Current
ΔP	Pressure drop
P	Pressure
T	Temperature
ϕ	Phase, electrical

British Units

amp	current, ampere
ft	length, feet
in	length, inches
FPM	velocity, feet per minute
GPM	flow rate, gallons per minute
gal	volume, gallons
psi	pressure, pounds per square inch
psia	pressure, pounds per square inch, absolute
psid	pressure, pounds per square inch, differential
psig.	pressure, pounds per square inch, gage
rpm	angular velocity, revolutions per minute
°F	temperature, degrees Farenheit
#/hr	flow rate, pounds per hour

International Units

°C	temperature, degrees Centigrade
cm	length, centimeters
m/sec	velocity, meters per second
gm	mass, gram
°K	temperature, degrees Kelvin
kg	mass, kilogram
kg/m^3	density, kilogram per cubic meter
kg/sec	flow rate, kilogram per second
m	length, meter

Abbreviations and Symbols Continued--

mg	mass, milligram
mm	length, millimeter
ml	volume, milliliter
m^3/sec	flow rate, cubic meters per second
N/m^2	pressure, newtons per square meter
$N \cdot s/m^2$	Dynamic viscosity, newton-second per square meter
μ	length, microns
rad/sec	angular velocity, radians per sec

I. SUMMARY AND RESULTS

A. INTRODUCTION

The objective of this contract was to design, fabricate, and test flight prototype hardware that will be used to regenerate (clean) fluid particulate filters. The technique for the backflush/jet impingement method of cleaning filters was developed on a prior contract (NAS9-11984). The purpose of this contract was to use the design information gained during the development contract to proceed with a flight prototype design that was more compact, portable, lighter, compatible with the system fluid (water), and less complex. The development of this item is applicable to the potable water, process water, and the thermal water systems for the Space Shuttle and future long duration manned space missions.

Current liquid filter designs for space application are not suitable for Space Shuttle or long duration orbital missions because of the extended use times required. In addition, present Apollo/Skylab inplace (nonreusable) fluid filters are not suitable for inflight maintenance and regeneration.

Since filter replacement represents 20% or more of the scheduled maintenance of a fluid system, techniques must be employed whereby the elements can be changed out or regenerated (cleaned) in place. It is not practical to expect that, for every filter replacement, the system be drained, purged, filled and bled in addition to the replacement of filter elements.

Because of the demand for a better method of maintaining filters, the Filter Regeneration System was developed. The filter regeneration unit and regenerative filter provide a system that utilizes a backflush/jet impingement concept to clean and recondition fluid system filters. The Filter Regeneration system has demonstrated a cleaning efficiency of 98.7 to 100%.

B. SYSTEM DESCRIPTION

The filter regeneration unit, Figures I-1 and I-2, is a self-contained, compact, portable device that connects to the filter

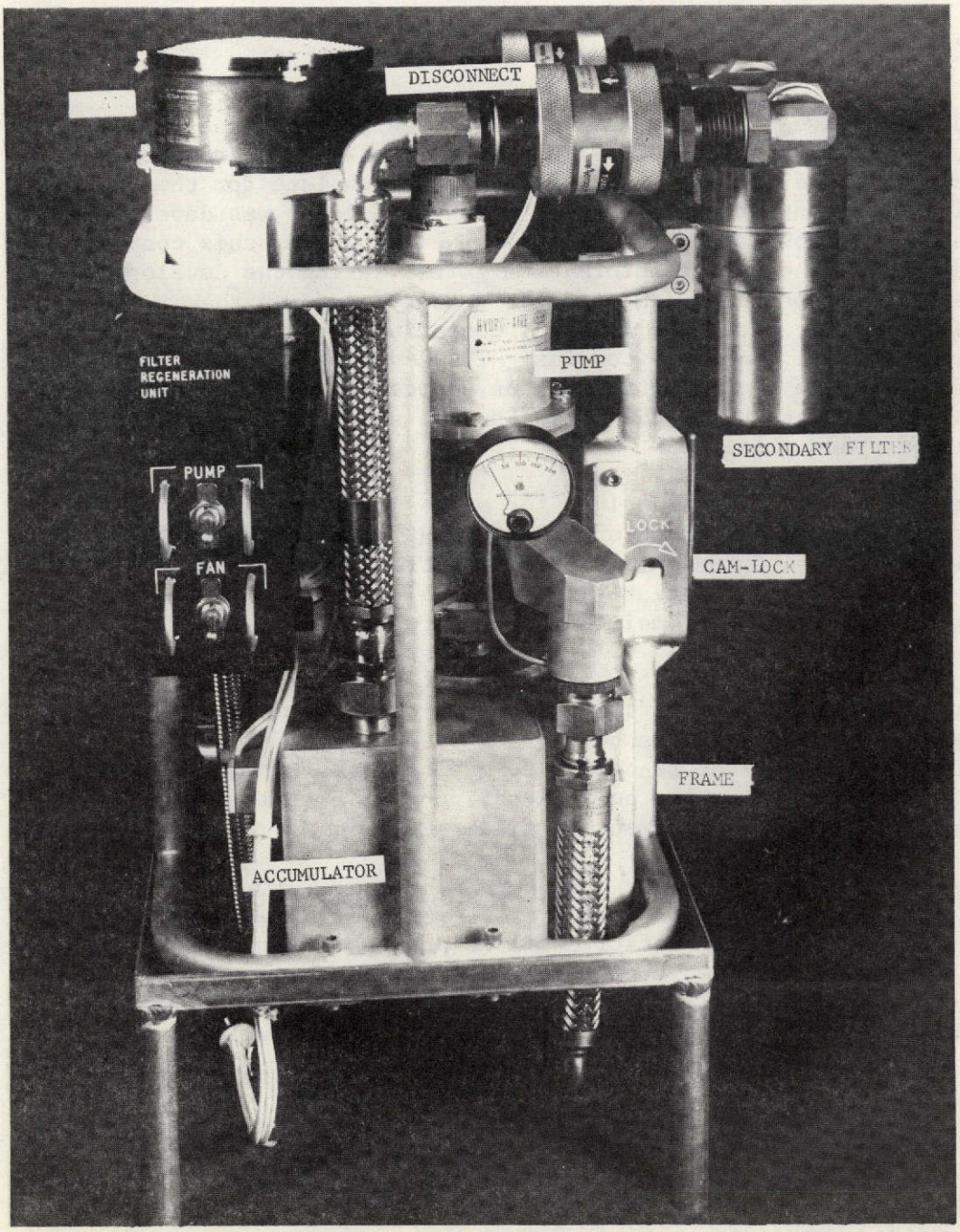

Figure I-1 Filter Regeneration Unit, Front View

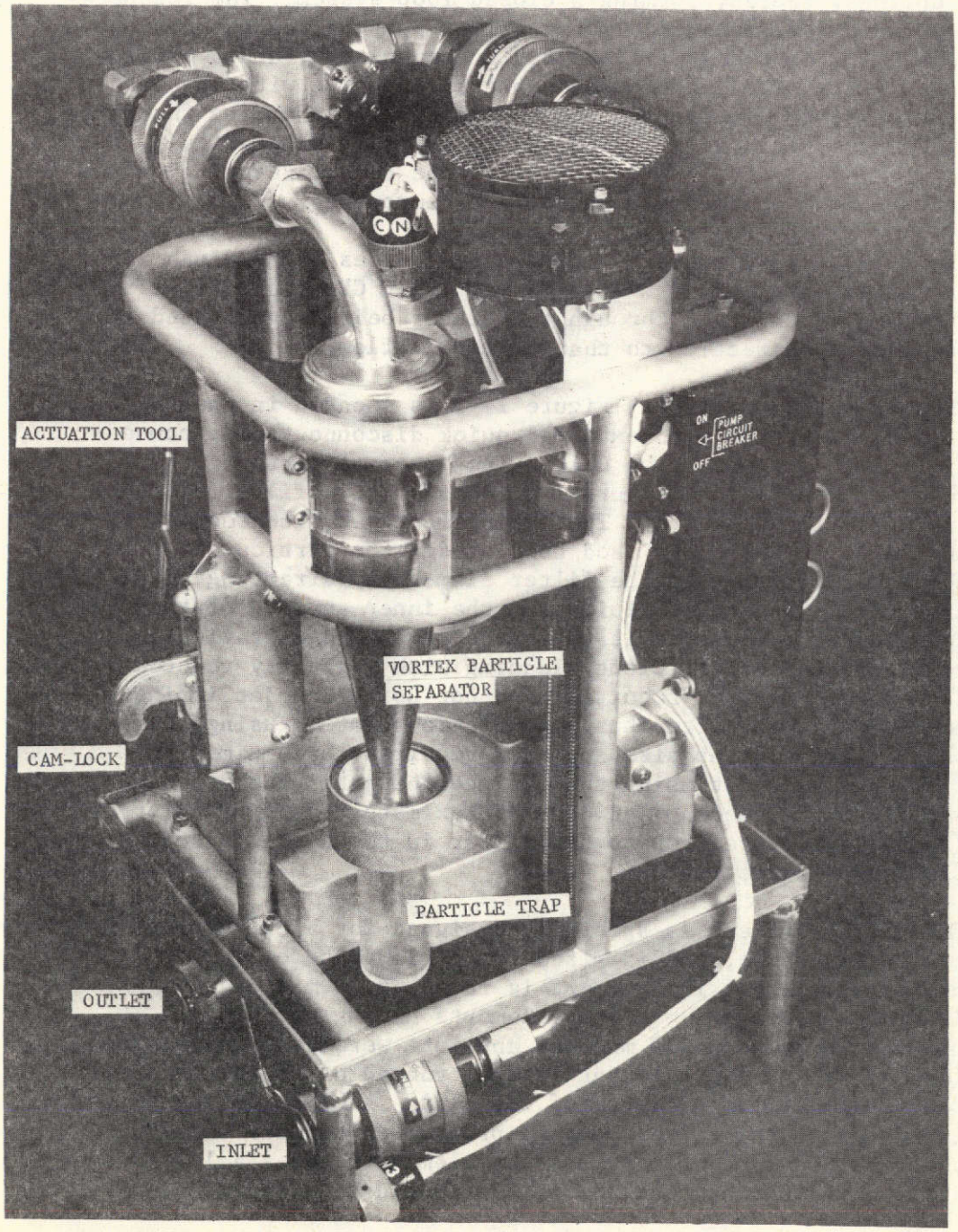

Figure I-2 Filter Regeneration Unit, Side View

to be regenerated by a set of self-sealing quick disconnect couplings, thereby forming a closed loop system. The regeneration unit contains an AC motor driven pump, a vortex particle separator, secondary filter, fluid accumulator, and a cooling fan. All of the system components are passive with the exception of the motor/pump and the fan, thus enhancing the overall system reliability. The system is shown schematically in Figure I-3, and the following gives the detail description and operation of the overall system and components.

The high speed AC motor driven pump provides a backflush rate of approximately 7.44×10^{-4} m^3/sec (11.8 GPM), and flow from the pump is directed through the filter being regenerated in the reverse direction to that of normal flow.

The regenerative filter, Figure I-4, is located in the respective fluid system with external quick disconnects for connection to the regeneration unit. The internal parts of the regenerative filter, Figure I-5, consist of a filter element and an impingement jet. The impingement jet, located within the filter element, is used to dislodge the particulate from the outer surfaces of the filter element by directing small, high velocity jets of fluid onto the inner surface of the filter element. This jet is the basis of the regeneration process and enables efficient cleaning with a greatly reduced flow rate from that required when not using the jet impingement techniques. Previous regeneration systems using the same filter element size and area required three times the flow rate when not using the impingement jet. This special backflush impingement jet adds approximately a 13.79×10^3 N/m^2 (2 psid) pressure drop to the filter in the normal system fluid flow direction.

The filter element is specially designed for backflushing and continuous reuse, and is sized for a flow rate of 6.31×10^{-4} m^3/sec (10 GPM). The element is rated at 20 microns nominal and 40 microns absolute. Filter elements having a rating of 10 microns nominal and 25 microns absolute were also successfully tested. The filter element is constructed of stainless steel for extended life and ease of cleaning. A differential pressure indicator on the filter housing provides a visible indication when the pressure drop across the element reaches a loaded condition, indicating that the filter should be cleaned.

During the two-minute regeneration cycle, the backflush flow through the regenerative filter removes the particles from the filter element and carries them into the vortex particle separator

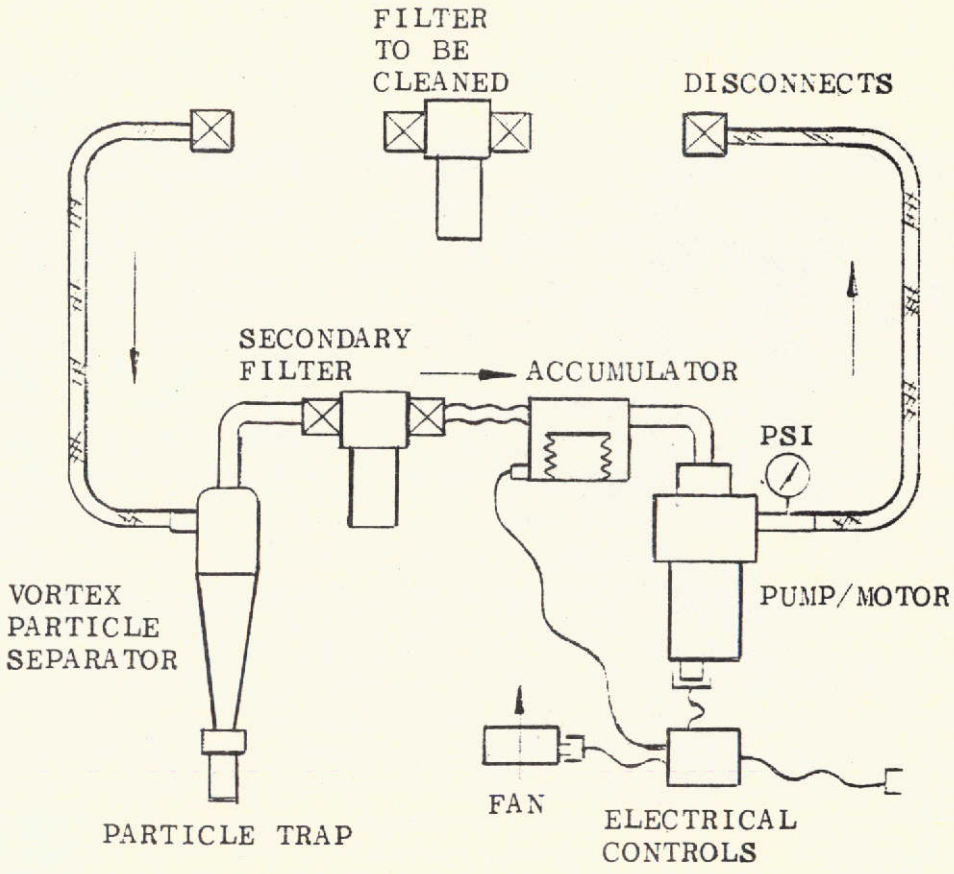

Figure I-3 Filter Regeneration Unit Schematic

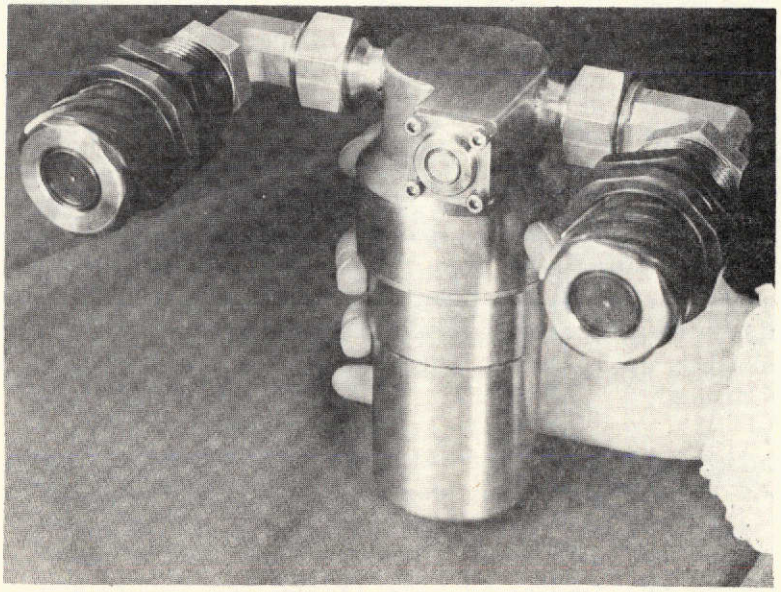

Figure I-4 Regenerative Filter

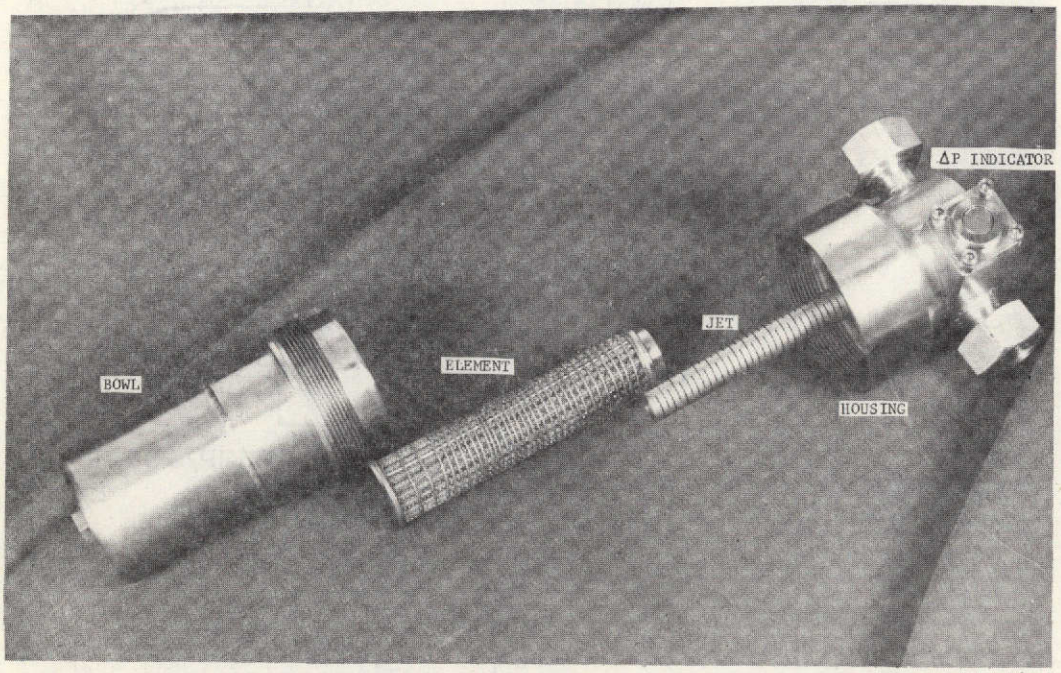

Figure I-5 Regenerative Filter - Disassembled

where the particles are removed from the fluid by centrifugal action. The particle separator is a key element in the regeneration unit and is used as a means of removing and collecting large amounts of contaminant.

The vortex particle separator, Figure I-6, is a passive component with no moving parts. The separator employs a vortex action where the particles are thrown to the outer surface of the separator and eventually are forced down to the zero-g trap where they are accumulated and prevented from re-entering the normal flow. The particle trap is sized so that little or no change-out is required during a normal mission. The trap can be removed with no loss of fluid and can be either replaced or simply rinsed.

Any remaining particles that were not removed by the vortex action flow out of the separator and into the secondary filter where all 10 micron or larger particles are filtered out of the fluid. The secondary filter insures that no fine particles are transmitted to the inside surface of the regenerative filter that could possibly contaminate the spacecraft system. The secondary

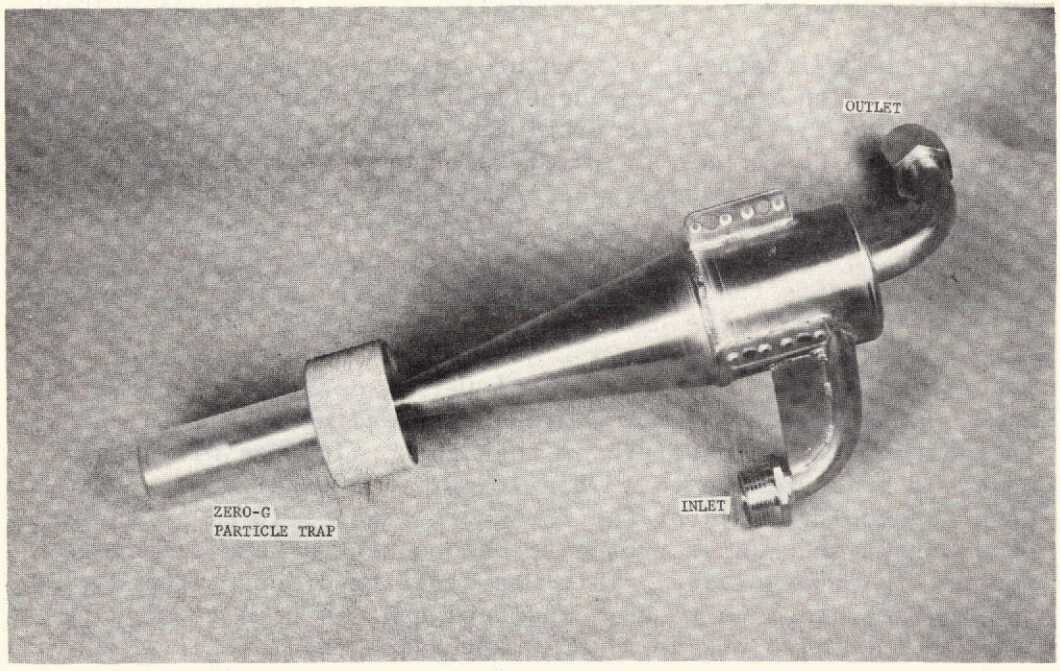

Figure I-6 Vortex Particle Separator

filter periodically requires maintenance and since it is identical to the regenerative filter, it can also be regenerated with the regeneration unit. Thus, the regeneration unit is self-sufficient and does not require any additional servicing equipment for particle removal.

Fluid flow from the secondary filter enters the accumulator prior to passing through the motor pump. The accumulator provides makeup fluid to the system that may be lost when the quick disconnects are disconnected and connected. The accumulator houses a small bellows which, when pressurized, provides a positive pressure on the pump inlet preventing cavitation during the regeneration cycle. The storage volume of the fluid contained by the accumulator is also used as a heat sink for the regeneration unit. The cooling fan mounted on the unit is used to remove heat during and after the regeneration cycles.

The filter regeneration unit is basically a servicing unit which provides a better method of performing maintenance on fluid systems. Even though it is a maintenance tool in itself, the

unit was designed with maintainability as a prime consideration.

Some of the maintainability features include open access to all six sides of the unit, component level of maintenance, and commonality in fasteners and fittings. All of the components, but one, can be removed by itself without removing any other components. This feature was accomplished by an open frame design which allows free access from all sides and by strict attention to detail in the placement of the components. The one exception is that the fan must be removed from its bracket in order to remove the particle separator.

The fluid fittings are a face seal O-ring design that permits each component to be removed without spreading the fluid tubes. In addition, tests have proven that these fittings will seal water at pressures up to 1378×10^3 N/m^2 (200 psig) with only hand tightening. All of the fasteners are No. 10 Allen socket head screws which have proven to be one of the best fasteners for use in zero-gravity. This was reaffirmed during the Skylab inflight maintenance tasks. The tool that is used to actuate the cam-lock also has an Allen wrench designed into it which can be used to remove all of the fasteners. The Allen screws mate with floating nut plates which minimize alignment problems during assembly and allow greater tolerances in equipment interfaces.

The particle trap on the separator can be removed by hand and does not require any additional tools. The trap is fabricated from clear Lexan, and the crew member can easily see when it requires servicing. When the secondary filter becomes loaded, as indicated by the ΔP indicator, it too can be regenerated with the regeneration unit.

C. TEST RESULTS

Four categories of testing were conducted on this program; 1) component testing, 2) subsystem testing, 3) system performance testing, and 4) zero-gravity testing on the NASA KC-135 aircraft. Including supporting tests to these major categories, there was approximately 175 tests run on the Flight Prototype Filter Regeneration unit.

1. Component Tests - The four major components of the prototype filter regeneration unit tested included the regenerative filter, the vortex particle separator, the fluid accumulator, and the fluid disconnects. A total of 30 tests were run on these components to determine individual performance data.

Four performance tests were conducted on the prototype regenerative filter using a known quantity of graded AC coarse road dust as the test contaminant and water as the working fluid. AC road dust was used because it is a known and graded contaminant, and thus decreases the error and variables incurred during testing. A 20 micron nominal, 40 micron absolute filter element was used and the loading flow rate was 4.29×10^{-4} m^3/sec (6.8 GPM). Regeneration efficiencies of 90.8 - 95.0% were obtained using a backflush flow rate of 7.29×10^{-4} m^3/sec (11.5 GPM) for 5 minutes. Testing demonstrated that the filter element was cleaned to its original condition or better each time. The pressure drop of the flight prototype filter is 22×10^3 N/m^2 (3.2 psid) lower than that for the development regenerative filter. The cleaner and more efficient design of the prototype regenerative filter is the result of larger inlet and outlet ports and optimization of flow design characteristics within the unit.

A total of six efficiency tests were conducted on the prototype separator. By passing a known quantity of graded AC coarse road dust through the separator at a flow rate of 7.29×10^{-4} m^3/sec (11.5 GPM) an overall average separator efficiency of 85.4% was obtained. The pressure drop of the prototype separator at a flow rate of 6.31×10^{-4} m^3/sec (10 GPM) was 12.41×10^3 N/m^2 (18 psid) lower than that of the development particle separator. This decrease in pressure drop was achieved by increasing the inlet/outlet port sizes and placing straightener vanes in the outlet flow tube to direct the flow more evenly.

The flight prototype accumulator provides good mixing of the water and maintains thermal control during the operating cycle. A plexiglass flow model of the accumulator was constructed and tested for ΔP and flow mixing qualities during the development phase. The pressure drop obtained with the plexiglass model at a flow rate of 6.31×10^{-4} m^3/sec (10 GPM) was 5.51×10^3 N/m^2 (8.0 psid) for the bellows in the normal position and 6.62×10^3 N/m^2 (9.6 psid) for the bellows fully extended. The pressure drop of the prototype accumulator at this flow rate was much lower than those of the plexiglass model: 2.41×10^3 N/m^2 (3.5 psid) for the bellows extended and 2.62×10^3 N/m^2 (3.8 psid) for the bellows in the normal position. The amount of fluid change out versus time was measured by mixing food dye with the accumulator water and visually recording the time it took to completely change out the water in the accumulator. At a flow rate of 4.31×10^{-4} m^3/sec (6.8 GPM) the water was completely changed out in 20 seconds. This flow provides a good heat sink to maintain thermal control during operation. The prototype accumulator bellows was pressurized to 10.34×10^3 N/m^2 (15 psig) and had an operating pressure of 24.13×10^3 N/m^2 (35 psig). This pressure was sufficient to prevent pump cavitation and maintain unit pressure if a small leakage occurred during connection and disconnection of the filters to the unit.

Evaluation testing was performed on five commercially available fluid quick disconnects during the development phase to determine performance in one-g and ease of crewman usage in zero-g. From the development tests, two disconnects (Aeroquip and Seaton-Wilson) were selected for the zero-gravity tests because of their superior characteristics. During the zero-g tests, both types were connected and disconnected at pressures of 34.47 to 37.92×10^3 N/m^2 (50 to 55 psig) with no loss of fluid or pressure. Due to the difficulty of connection of the Seaton-Wilson quick disconnect at pressures approaching 413.6×10^3 N/m^2 (60 psig), the Aeroquip quick disconnect was considered most acceptable for the filter regeneration system. The disconnects used with the prototype regeneration unit are 1.59 cm (5/8 inch) disconnects and have a pressure drop, at 6.31×10^{-4} m^3/sec (10 GPM) of 41.36×10^3 N/m^2 (6 psid) in the nipple to coupler flow direction and 51.15×10^3 N/m^2 (8 psid) in the coupler to nipple flow direction.

Filter bubble-point tests were conducted to determine any deterioration of the individual filter elements used throughout the testing program. By comparing the pressure required

to force a gas bubble through the largest pore of a clean filter with the pressure required after loading and subsequent cleaning, any deterioration can be detected. There was no significant change in bubble-point pressure readings for any of the filter elements tested; therefore, it was concluded that no deterioration took place as a result of the filter regenerations.

2. Subsystem Tests - Subsystem tests were conducted using the filter and separator in combination. The filter was first loaded with AC coarse road dust at a flow rate of 4.29×10^{-4} m^3/sec (6.8 GPM). The filter was then connected upstream of the separator in the backflush direction. During the development program, a regeneration cycle of 30 minutes at a backflush rate of 7.2×10^{-4} m^3/sec (11.5 GPM) was used to obtain subsystem efficiencies of 87%. It was noted that the cleaning of the filter appeared to be accomplished during the first few moments of operation. During the flight prototype subsystem tests, the regeneration time was reduced to 5 minutes resulting in a regeneration efficiency of 89.7%. The regeneration cycle was further reduced, during the system tests, to two minutes. The average efficiency for the 2 minute prototype unit runs was 92%. A further reduction from two minutes to one minute was attempted during the zero-g tests of the flight prototype subsystem. The results showed that a one-minute cyclic regeneration cycle was not sufficient to clean the filter elements.

The ΔP of the development subsystem at 6.31×10^{-4} m^3/sec (10 GPM) was 3.93×10^3 N/m^2 (57 psid). The ΔP of the prototype subsystem was 2.48×10^3 N/m^2 (36 psid) for the same flow rate. The lower ΔP of the prototype subsystems is the result of larger flow passages, and a larger outlet passage with straightener vanes in the separator.

3. System Tests - A total of fifteen one-g performance tests were conducted on the prototype unit to determine its overall efficiency, the optimum run cycle, and to check out the system's integrity. These tests were performed with regeneration cycles of 5 minutes, 2 minutes, 1 minute, and 20 second intervals for a total of two minutes run time. The average regeneration efficiency for the 2 minute runs was 92.6%. This compared with the 93.8% efficiency obtained during the development program using a 30 minute regeneration cycle. The average regeneration efficiency for the 5 minute test (90.6%) was lower than that of the 2 minute cycle. Since the temperature rise of the

unit was much higher with the 5 minute continuous run than for the two minute run, the 2 minute cycle was selected as the optimum in order to minimize the temperature rise. The one minute continuous runs were conducted with no appreciable loss in efficiency. The 20 second cyclic tests, with a 2 minute total run time, showed an average efficiency drop of 7%. The prototype unit ran smoothly without any flaws throughout the testing program with the exception of a slight leak which developed in the inlet disconnect. The disconnects should be kept clean and well lubricated to prevent binding and possible leakage.

In order to keep the regeneration unit at a safe operating temperature during successive regenerations, fan cooling should be used before and after shutdown. This run time should also be continuous since the efficiency was decreased in the cyclic test.

4. Zero-Gravity Tests - During the development program, four regenerative filters were cleaned using the development unit in a zero-g environment. The regeneration of the filters was conducted in 20-second increments for a total time of 5 minutes. The average regeneration efficiency of the development unit in zero-g was 81.65%. This efficiency was slightly higher than the 80.47% regeneration efficiency obtained during the one-g intermittent test run prior to the zero-g tests. The average zero-g regeneration efficiency is, however, 12.23% lower than the average one-g, continuous cycle, 5 minute tests. This lower efficiency was caused by the cyclic mode of operation required by the KC-135 parabolas, and the two-g downward force executed by the test aircraft during pullout which compacts the particles. High speed (400 frames/sec) movie coverage showed that the majority of the contaminant entered the separator within 2 seconds after the start of the cleaning cycle and immediately went into the trap and was prevented from reentering the separator. The maintainable filter was disconnected and connected a number of times in zero-g. There was no fluid pressure on the filter and connection and disconnection operations were performed easily by the operator.

A total of eight filters were regenerated in zero-g using the flight prototype unit. Five filters were regenerated with a total cumulative regeneration cycle of two minutes each, and three filters were cleaned with a one minute cycle each. The average regeneration efficiency of the two minute tests is 72.5%. This was considerably higher than the 45.3% efficiency obtained with the one-minute runs. A one minute, cyclic,

regeneration cycle is not sufficient to clean the fluid filters in either one-g or zero-g environments.

All human factors tasks were completed successfully with no fluid leakage upon removal of the separator trap from the unit, and no difficulties were experienced in removing or reattaching the prototype unit to the interface panel.

II. CONCLUSIONS AND RECOMMENDATIONS

A. CONCLUSIONS

1. A flight prototype filter regeneration unit that efficiently cleans fluid particulate filters has been built and tested.

2. The time required to regenerate filters with the filter regeneration unit has been reduced from 30 minutes (during the development program) to 2 minutes without loss in cleaning efficiency. Tests were conducted at one minute durations and the results were excellent in one-gravity, however, at zero-gravity with 20 second intermittent operation the one minute backflush did not prove satisfactory.

3. The flight prototype unit is a lightweight, compact, portable unit. Certain design changes have been realized during the course of this program and it is believed that the overall weight could be further reduced by 3.17 to 4.5 kg (7 to 10 pounds).

4. The filter regeneration unit achieves a system efficiency of 94% while flowing at a backflush flowrate of 7.44×10^{-4} m^3/sec (11.8 GPM) for 2 minutes.

5. The filter regeneration unit is suitable for either in-flight maintenance (zero-g) or for ground refurbishment purposes.

6. The physical structure of the filter elements did not deteriorate nor did the micron ratings increase as a result of successive backflush processes with the filter regeneration unit.

B. RECOMMENDATIONS

In the performance of a contract in an area of new technology, such as filter regeneration and inflight maintenance, it is incumbent upon the participants to identify those areas of technology that require future development. In addition, this contract requires that recommendations be provided for additional areas of investigation based on the results of the contractual effort. The formulation of programs such as Space Shuttle and other future manned missions depends upon

the proper development of future technology so that a solution to problems is developed on a timeline consistent with its needs.

Space maintenance and filter regeneration are of prime importance to the fulfillment of the long-duration mission, and require proper development to meet those future requirements. Two specific areas of future technology follow, and it is recommended that further effort be continued in these areas.

1. Maintainable/Regenerable Filter - A maintainable filter was delivered under contract NAS9-11984 whereby the filter element could be removed from the system without stopping operation of the spacecraft system and without incurring spillage or leakage during the disconnect operation. The testing performed on this filter has demonstrated that the basic design is solid and that a maintainable filter can be built that has the characteristics of minimum leakage and spillage. In addition, it has been demonstrated that filters can be efficiently regenerated.

The combination of a maintainable filter that could be removed from the system and then regenerated would combine the best attributes of inflight refurbishment and regenerative systems. Preliminary design layouts have been prepared that show three alternate methods of combining regeneration within a maintainable filter, thus proving the feasibility of such a component.

The filter design should reflect minimum pressure drop and flight weight along with minimal or no leakage and spillage. The filter should exhibit good human factors design for use by a crew member in either zero-g or one-g. A flight prototype should be fabricated and tested in the system environment that it would experience on the Space Shuttle.

2. Maintainable Components - During the performance of this contract, it again became apparent that existing component designs do not have provisions for inflight maintenance. Solutions are required for: (1) system isolation so that components can be removed from the system when they fail; (2) a disconnect design that has minimum pressure drop, minimum spillage, reduced envelope size, and increased reliability; and (3) a solution for solving fluid system leaks in a zero-g environment. In these areas, there are no existing components or methods that satisfactorily fulfill the requirement. Future long-duration missions will require, as a minimum, inflight main-

tenance and the ability to isolate, repair and remove components from a system. Technology and developed hardware are lagging in this field and require additional emphasis.

3. Efficient Lightweight Motor/Pump - During the procurement phase of this program it was found that no lightweight motor/pump combination existed that would meet the flow and pressure requirements of this contract. Further search revealed that there were only two vendors with pumps that could be modified to meet these pressure requirements. These pumps were originally designed for other aircraft and spacecraft coolant systems. Both pumps contained non-compatible materials and were relatively inefficient. Development of a lightweight efficient motor/pump assembly is required. The materials in contact with the fluid should be compatible with water. Reliability, long life, and maximum efficiency should be prime criteria for the pump. Additional criteria should include minimum transfer of waste heat into the water system.

III. PROGRAM DESCRIPTION

The Flight Prototype Filter Regeneration System program was performed within a 23 month period. The objective of this program was to design, fabricate, and test a flight prototype filter regeneration unit. The design was based upon the experience gained during the development program on Contract NAS9-11984. The filter regeneration unit is applicable to the Space Shuttle and future manned spacecraft missions and can be used for inflight maintenance or as a ground refurbishment unit. The fluid systems to be considered for the baseline were the potable water, process water, and thermal water systems. Two major items of hardware were delivered on this program: (1) a filter regeneration unit, and (2) a regenerative filter assembly.

The program was performed in the following six tasks:

TASK I: Zero-G Testing of the Development Unit

TASK II: Flight Prototype Design and Analysis

TASK III: Flight Prototype Fabrication

TASK IV: Performance Testing

TASK V: Hardware Delivery

TASK VI: Documentation and Final Presentation

1. Task I: Zero-G Testing of the Development Unit - Zero-G tests were conducted on the development regeneration unit developed under Contract NAS9-11984. The primary objective of these tests was to determine the fluid dynamic characteristics and system performance under zero-g conditions. A secondary objective was to evaluate the aspects of human factors in the design and operation of the unit. Fluid disconnects and the Maintainable Filter were also tested to evaluate their performance in zero-g. A zero-g test procedure and zero-g test report were issued as part of this task, and a presentation of the test results was presented at the conclusion of the task.

2. Task II: Flight Prototype Design and Analysis - Design analyses, tradeoff studies, and the detailed design for the flight prototype filter

regeneration system were performed.

The first task was to establish the design baseline for the unit, which included system flow rates, pressures, materials, filtration levels, etc. After the baseline was established, a tradeoff study was conducted to determine the relative merits of a portable vs fixed regeneration unit. Preliminary design analysis was also performed to size the unit, determine pressure drops, and determine line sizes. Preliminary design layouts were prepared to define the configuration. A Preliminary Design Review was conducted at the conclusion of the preliminary design phase.

Design analyses were conducted on the flight prototype unit to size system flow rates, determine pressure drops, determine assembly weights, perform stress analysis, and to determine pump performance requirements. The detailed design drawings for the regeneration unit were then prepared, and a final design review was conducted.

Long lead procurement searches were conducted, and a procurement specification for the motor/pump was prepared and issued to prospective vendors.

3. Task III: Flight Prototype Fabrication - All of the necessary procurement, fabrication, and assembly was completed under this task. Verification tests and calibration of hardware were also performed during this period.

4. Task IV: Performance Testing - Those tests necessary to evaluate the performance of the components, subassemblies, and the filter regeneration unit assembly were conducted under this task. Zero-g tests were also conducted for the flight prototype filter regeneration unit.

The component tests included leak checks, proof pressure, pressure drop, contaminant build-up, regeneration efficiencies, air flow velocities, vortex particle separation efficiencies, accumulator flow distribution, and motor/pump acceptance tests.

The subsystem tests included the combined loading/efficiency tests of the filter/vortex separator as a subassembly; and the temperature rise tests for the pump circuit.

Performance and temperature rise tests were conducted for the complete assembly. In addition, one-gravity tests were conducted prior to the zero-g tests to confirm the procedures and to gain comparison data. Ground system loading tests were also conducted at NASA-JSC prior to the zero-g tests.

5. Task V: Hardware Delivery - All of the hardware that was produced under this program was shipped to NASA-JSC and demonstrated. Predelivery and confirmation tests were also conducted on the unit prior to shipment. Major items of deliverable hardware were the Filter Regeneration Unit, the Regenerative Filter, and the Demonstration panel/container.

6. Task VI: Documentation and Final Presentation - Fifty-three documentation submittals were made during this program. The major documentation items included a program plan, a test plan, zero-g test procedures, detail drawings, Familiarization and Operations Manual, progress reports, and a final report. A final presentation was conducted at NASA-JSC at the conclusion of the program.

IV. FILTER REGENERATION SYSTEM

A. SYSTEM DESCRIPTION

The filter regeneration unit and regenerative filter provide a system that utilizes a backflush/jet impingement concept to clean and recondition fluid system filters. The filter regeneration unit, Figure IV-1, is a self-contained, compact, portable device that connects to the filter to be regenerated by a set of self-sealing quick disconnect couplings thereby forming a closed loop system. The fluid filters are regenerated in place without removing the filter or filter element from the system. The schematic of the regeneration system, Figure IV-2, shows the relationship of the major components of the filter regeneration unit. The backflush flow through the unit is indicated by the arrows. The regeneration unit contains an AC motor driven pump, a vortex particle separator, secondary filter, fluid accumulator, and a cooling fan. All of the system components are passive, except for the motor/pump and the fan, thus enhancing the overall system reliability.

The high speed AC motor driven pump provides a backflush rate of approximately 7.44×10^{-4} m^3/sec (11.8 GPM). The centrifugal pump operates at 2303 rad/sec (22,000 RPM) providing a high flow rate with minimum component weight. The pump reaches maximum flow and pressure in 0.14 seconds, producing instantaneous high velocity flow for the regeneration process. Fluid flow from the pump is directed through the filter being regenerated in the reverse direction to that of normal flow. The regenerative filter, Figure IV-3, is located in the respective fluid system with external quick disconnects for connection to the regeneration unit. Figure IV-4 shows a disassembled view of the filter body. The external parts of the stainless steel filter assembly consist of a bowl, housing, P indicator, and the quick disconnects. The internal parts consist of a filter element and an impingement jet. The regenerative filter must be fully charged with fluid prior to connecting it to the regeneration unit to avoid induction of air into the backflush system. The inclusion of too much air will reduce operating efficiency.

The impingement jet, located within the filter element, is used to dislodge the particulate from the outer surface of the filter element by directing small, high velocity jets of fluid

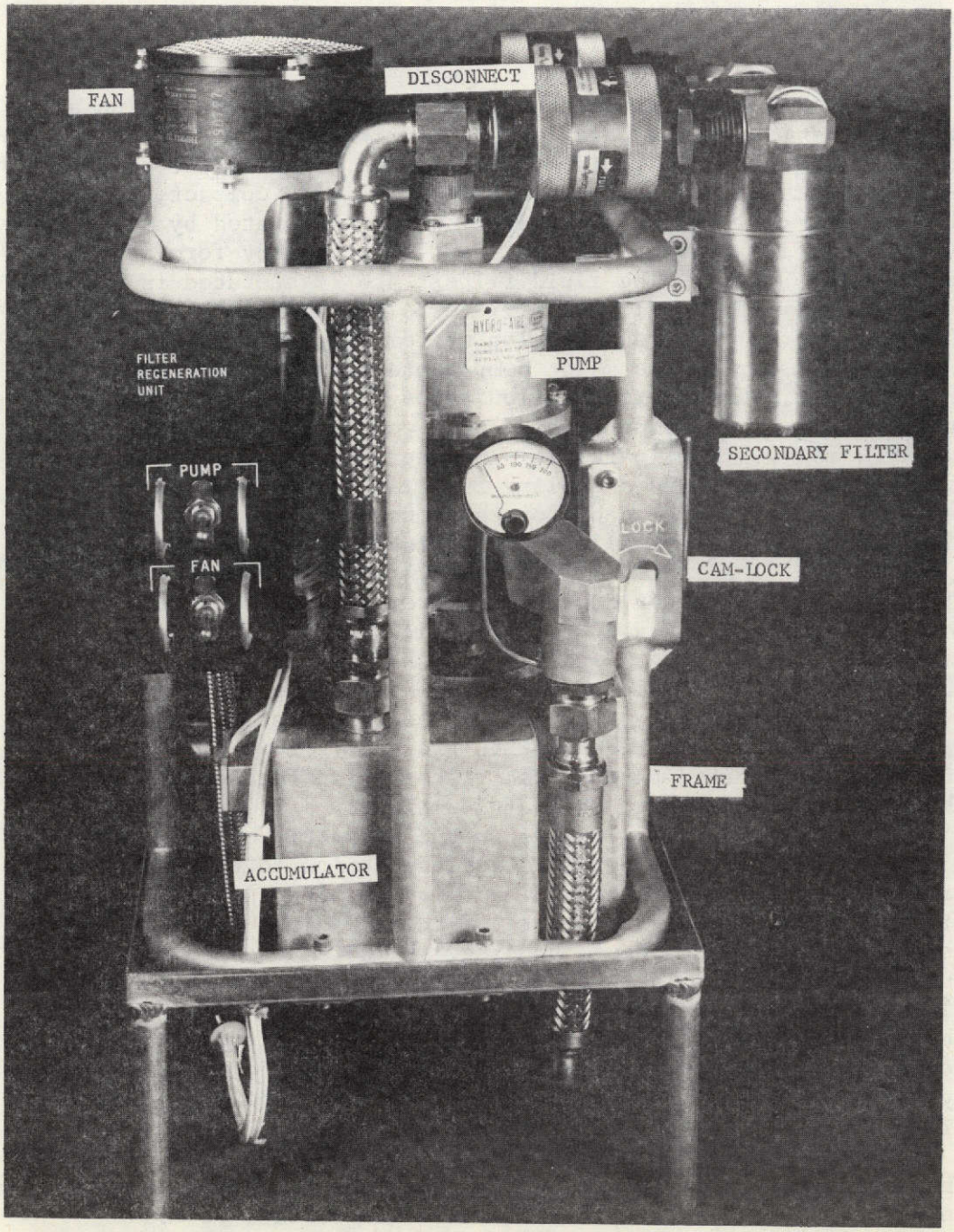

Figure IV-1 Filter Regeneration Unit

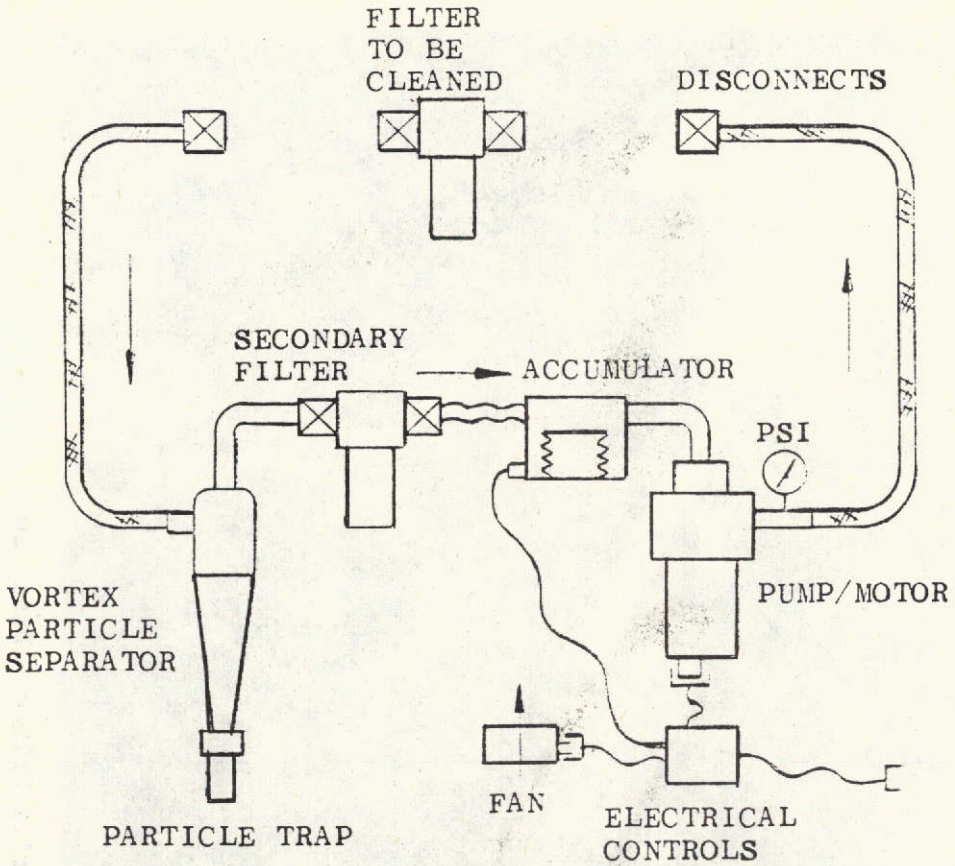

Figure IV-2 Filter Regeneration Unit Schematic

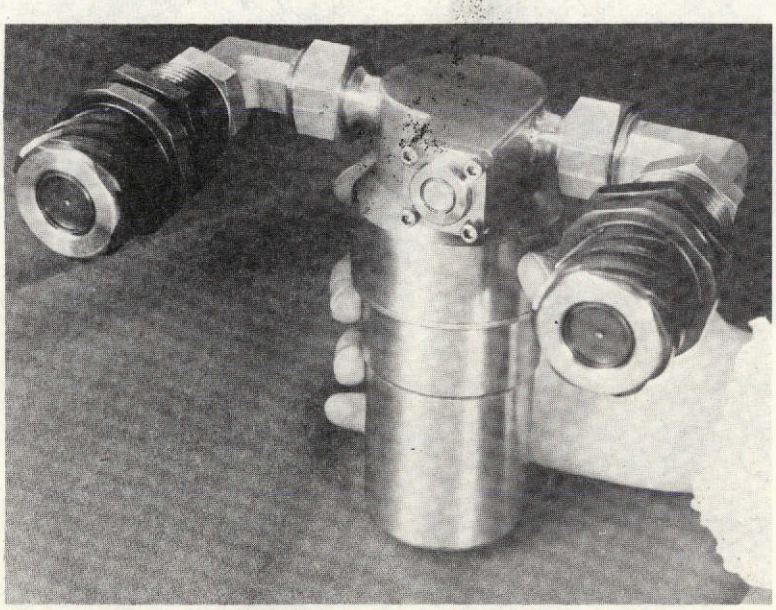

Figure IV-3 Regenerative Filter

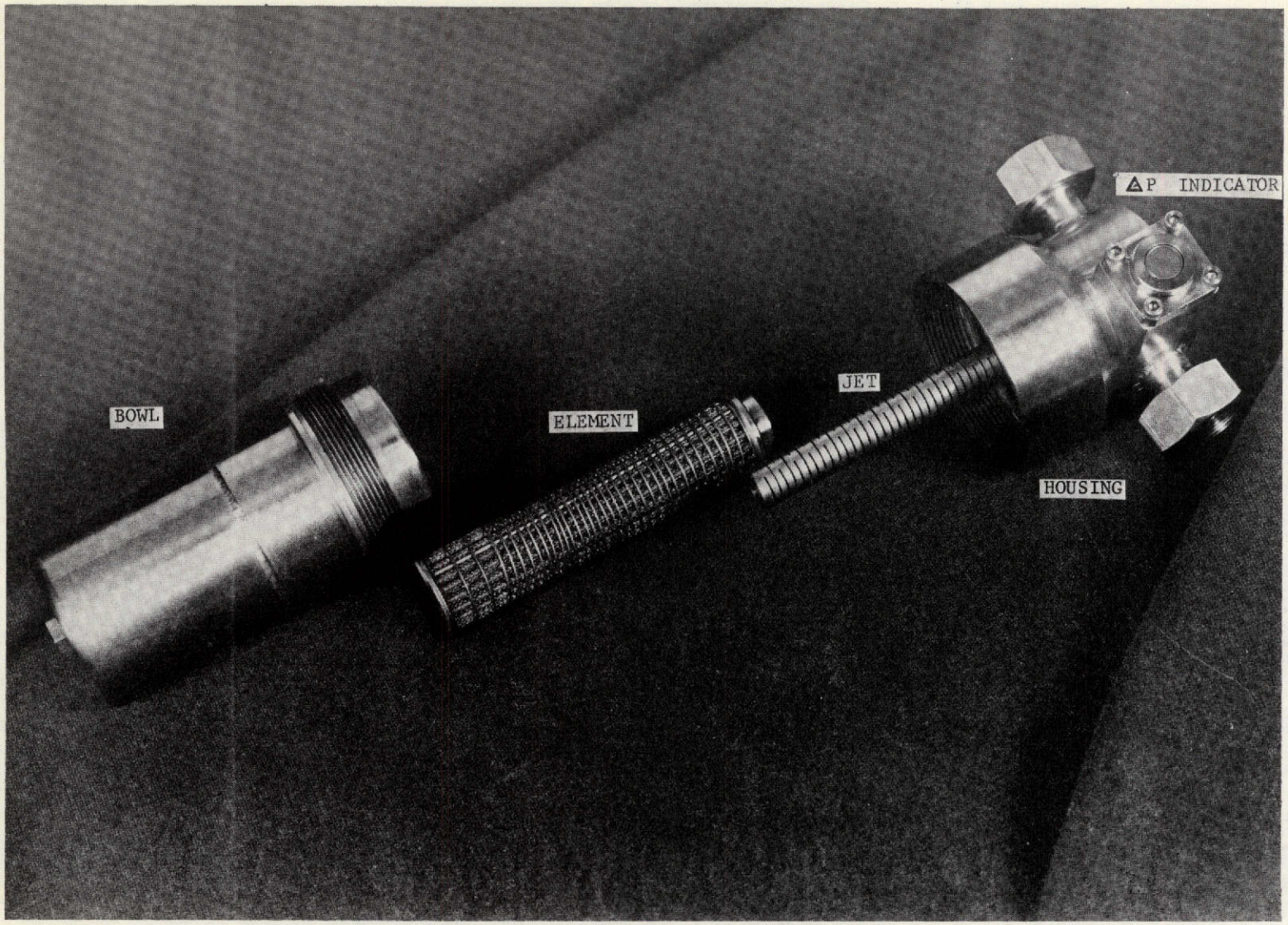

Figure IV-4 Regenerative Filter - Disassembled

onto the inner surfaces of the filter element. This jet is the basis of the regeneration process and enables efficient cleaning with a greatly reduced flow rate from that required when not using the jet impingement technique. This special backflush impingement jet adds very little pressure drop, 1.38×10^4 N/m^2 (2 psid), to the filter in the normal system fluid flow direction.

The filter element is specially designed for backflushing and continuous reuse and is sized for a flow rate of 6.31×10^{-4} m^3/sec (10.0 GPM). The element is rated at 20 microns nominal and 40 microns absolute.

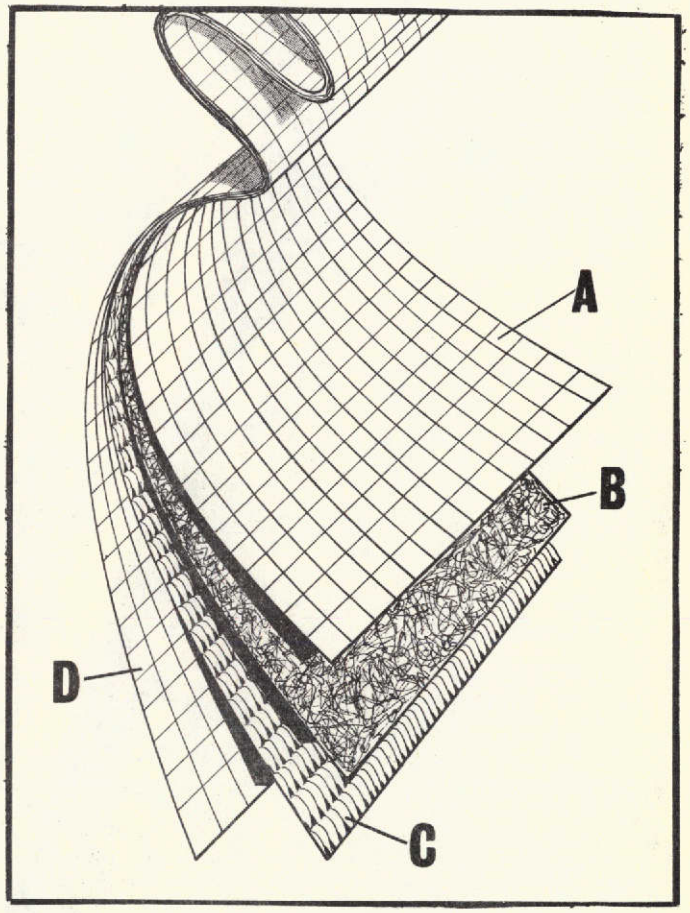

Figure IV-5 Filter Element Material Composition

The filter element is constructed of stainless steel for extended life and ease of cleaning. The pleated composite material, Figure IV-5, consists of (A) a coarse outside stainless steel screen which prevents impingement of high velocity particles on the precision filter cloth, (B) a first stage fine wire depth cloth consisting of fine stainless steel fibers in a random but controlled matrix which provides the main filtration with a high dirt holding capacity and high particle removal efficiency, (C) a second stage woven stainless steel wire mesh which provides a backup filtration media as well as uniform pore size to ensure absolute particle control, and (D) a coarse inside stainless steel screen to provide separation to the inside of the

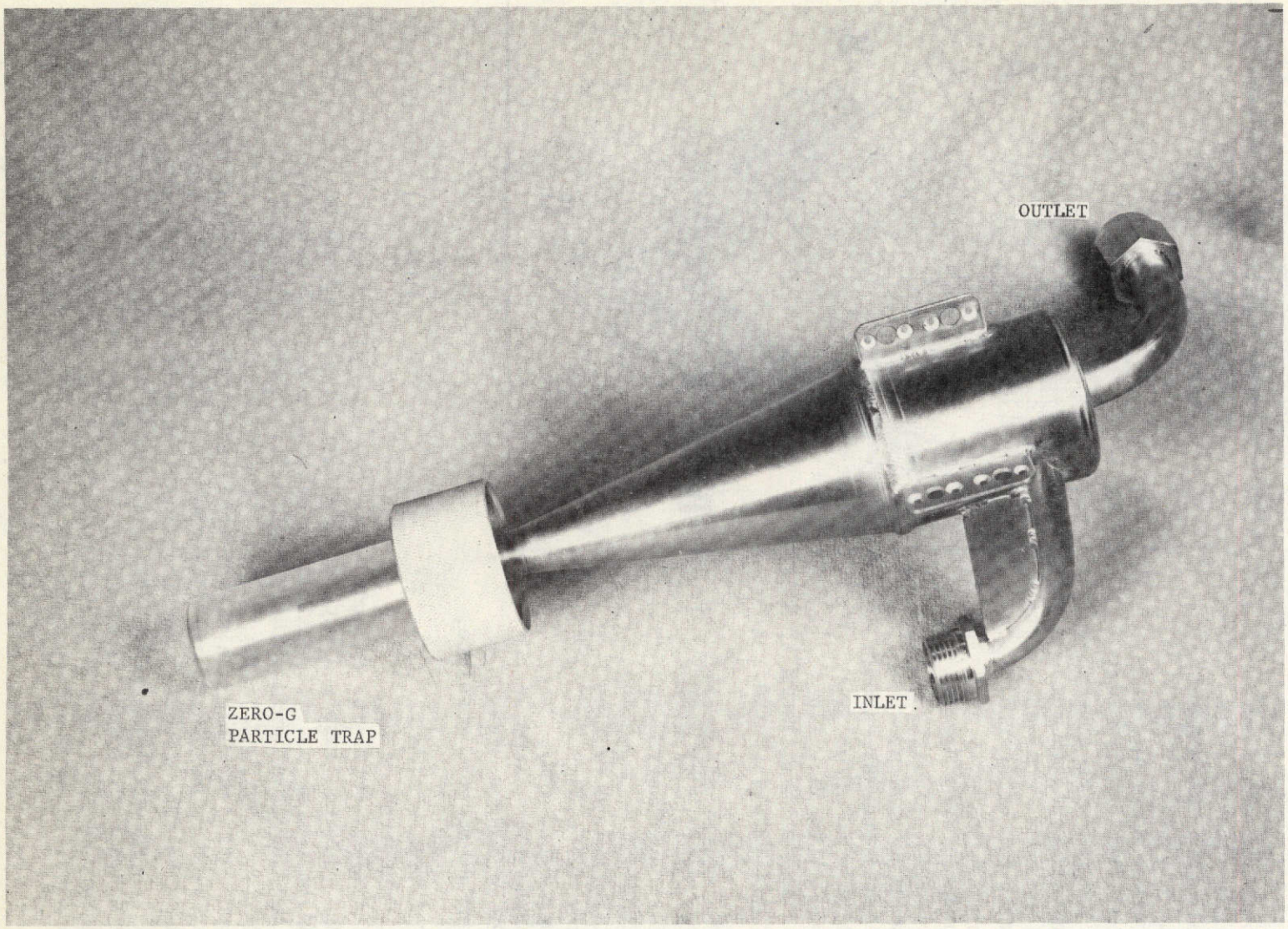

Figure IV-6 Flight Prototype Vortex Particle Separator

pleats and additional strength for long life. The filter element also contains an outer stainless steel retaining spring which prevents deformation when backflushing. A differential pressure indicator on the filter housing provides a visible indication when the pressure drop across the element reaches a loaded condition (approximately 13.8×10^4 N/m^2, 20 psid), indicating that the filter should be cleaned.

During the two-minute regeneration cycle, the backflush flow through the regenerative filter removes the particles from the filter element and carries them into the vortex particle separator, Figure IV-6, where 88% to 93% of the particles are removed from the fluid by centrifugal action. The particle separator is a key element in the regeneration unit and is used as a means of removing and collecting most of the backflushed effluent from the regenerative filter element. The vortex particle separator is a passive component with no moving parts. The separator employs a vortex action where the particles are thrown to the outer surface of the separator and eventually are forced down to the trap where they are accumulated and prevented from re-entering the normal flow, Figure IV-7. The particle trap, which consists of a particle ejector and trap bowl, is shown in Figure IV-8. The particle ejector tube has a slot milled on a tangent to the inside diameter of the vortex chamber. The circular motion of the fluid entering the trap throws the suspended particles out through the tangential slot. When the flow stops, the particle trap prevents the particles from re-entering the separator when in a zero-g environment. The particle trap presently holds 17 grams of particulate but could be sized so that little or no change-out is required during a normal mission. The trap can be

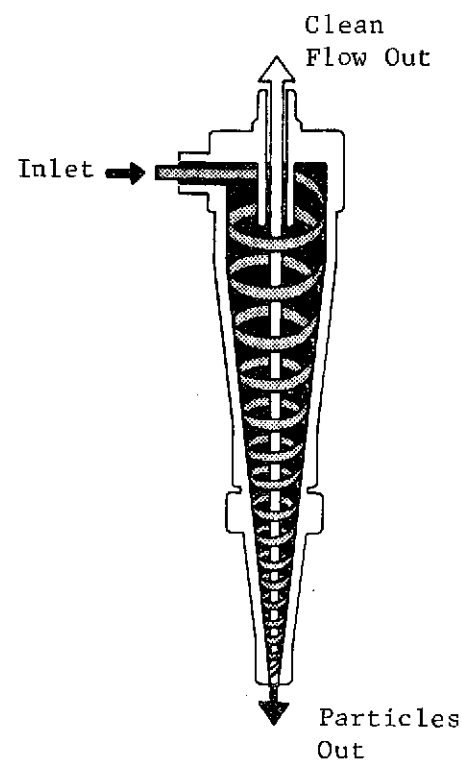

Figure IV-7 Vortex Particle Separator Principle

removed without any loss of system pressure or fluid and can either be replaced or simply rinsed. Care must be taken to insure that the trap is fully charged with fluid prior to reattaching the particle separator.

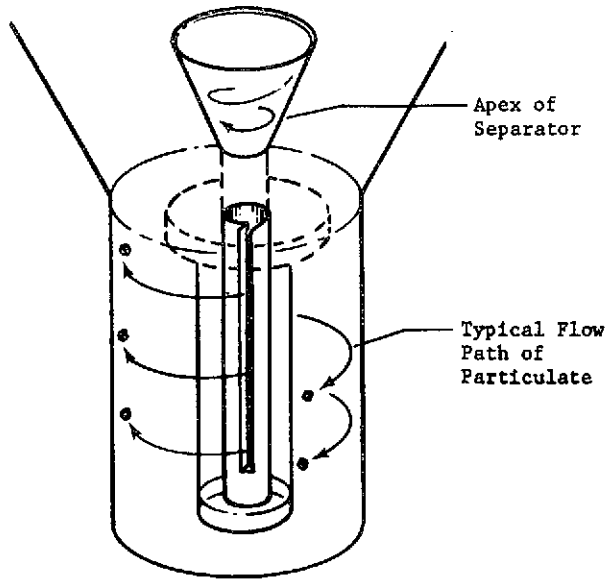

Figure IV-8 Separator Trap

Any remaining particles that were not removed by the vortex action flow out of the separator and into the secondary filter where all 10 micron or larger particles are filtered out of the fluid. The secondary filter insures that no fine particles are transmitted to the inside surface of the regenerative filter that could possibly contaminate the spacecraft system. The secondary filter periodically requires maintenance and since it is identical to the regenerative filter, it can also be regenerated. Thus, the regeneration unit regenerates its own filters and does not require any additional servicing equipment to remove the particles collected.

Fluid flow from the secondary filter enters the accumulator prior to passing through the motor pump. The accumulator provides makeup fluid to the system in the event of fluid loss when the quick disconnects are disconnected and connected. The accumulator houses a bellows which, when pressurized, provides a positive pressure on the pump inlet preventing cavitation during the regeneration cycle. The storage volume of fluid contained by the accumulator is also used as a heat sink for the regeneration unit. The cooling fan mounted on the unit is used to remove heat during and after the regeneration cycles.

B. HARDWARE DESCRIPTION

The major components of the Filter Regeneration System include the AC motor driven pump which provides the proper backflush flow rate, the vortex particle separator which removes the contaminant backflushed from the regenerative filter, the secondary filter which prevents fine particles from reaching the inside surface of the filter element being regenerated, the accumulator which provides system fluid make-up in the event of fluid loss, the cooling fan which directs air flow down onto the unit, and the quick disconnects for connection to the filters being regenerated.

1. Motor/Pump Assembly - The motor/pump provides the flow rate and pressure required for the backflush operation. The motor/pump assembly, Figure IV-9, consists of the motor, pump, inlet and outlet ports, pressure gage, and electrical connector. The motor housing is aluminum. The pump housing is an aluminum alloy with a hard anodize finish. The journal bearings are carbon graphite. The canned type induction motor is a two-pole machine designed for 3.75 shaft horsepower at 2303 rad/sec (22,000 RPM) and a duty cycle of 5 minutes ON, 30 minutes OFF. The pressure balanced centrifugal impeller is of the closed radial type for maximum efficiency.

The operating current, required for a backflush flow rate of 7.44×10^{-4} m^3/sec (11.8 GPM) is 10.6 amperes per phase. There is an inrush start-up current of 53 amperes which is present for 0.13 seconds. At the operating flow rate of 7.44×10^{-4} m^3/sec (11.8 GPM) the normal discharge pressure with $207_2 \times 10^3$/ N/m^2 (30 psig) inlet pump pressure is 1379×10^3 N/m^2 (200 psig). The pressure is indicated on the pressure gage mounted on the pump.

2. Regenerative Filter - The regenerative filter, which removes particulate contaminant from spacecraft fluid subsystems, is specially designed for regeneration (cleaning) with the regeneration unit. The regenerative and secondary filters are identical in design except for the filtration ratings of their respective filter elements. The filter assembly, Figure IV-10, consists of a housing, Δ P indicator, impingement jet, filter element, and a filter bowl. The regenerative filter has a set of external quick disconnects for connection to the regeneration unit.

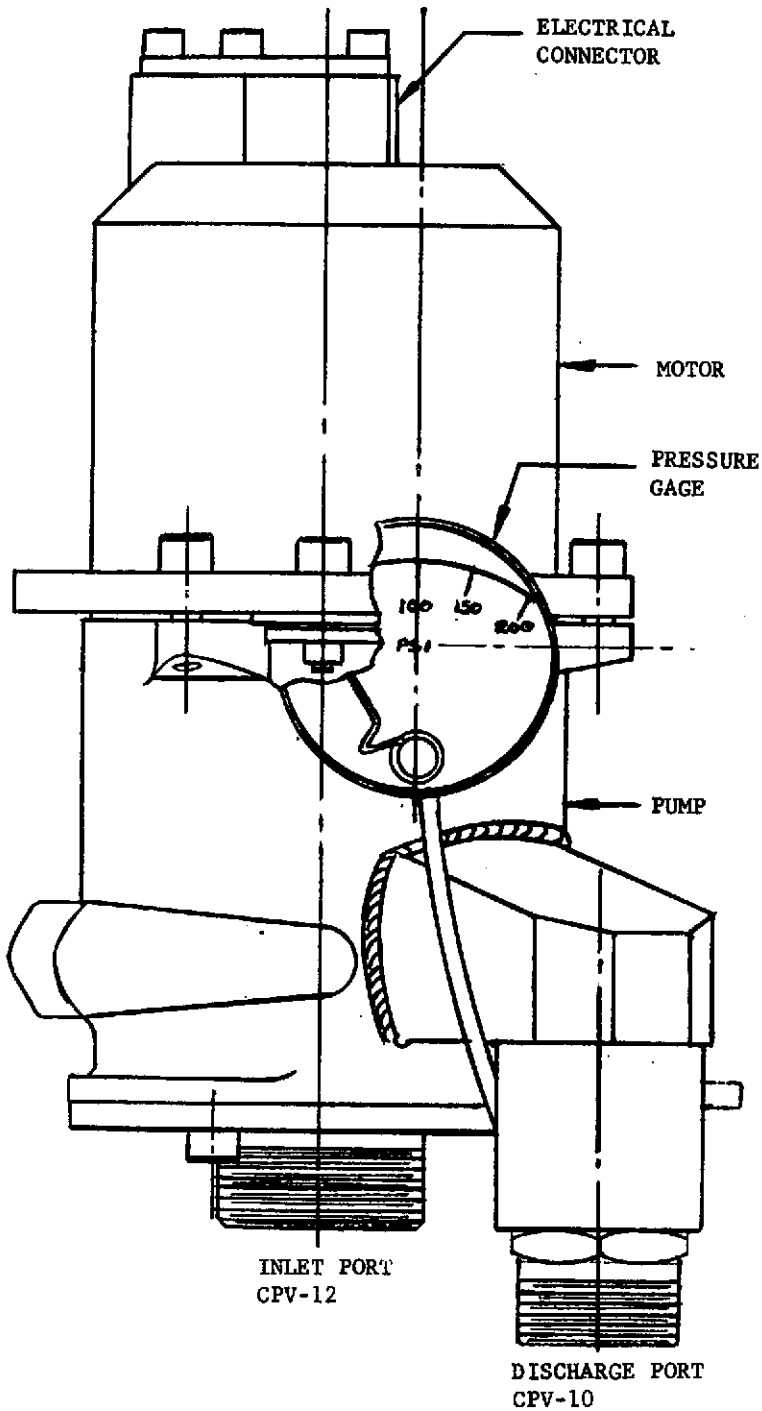

Figure IV-9 Motor/Pump Assembly

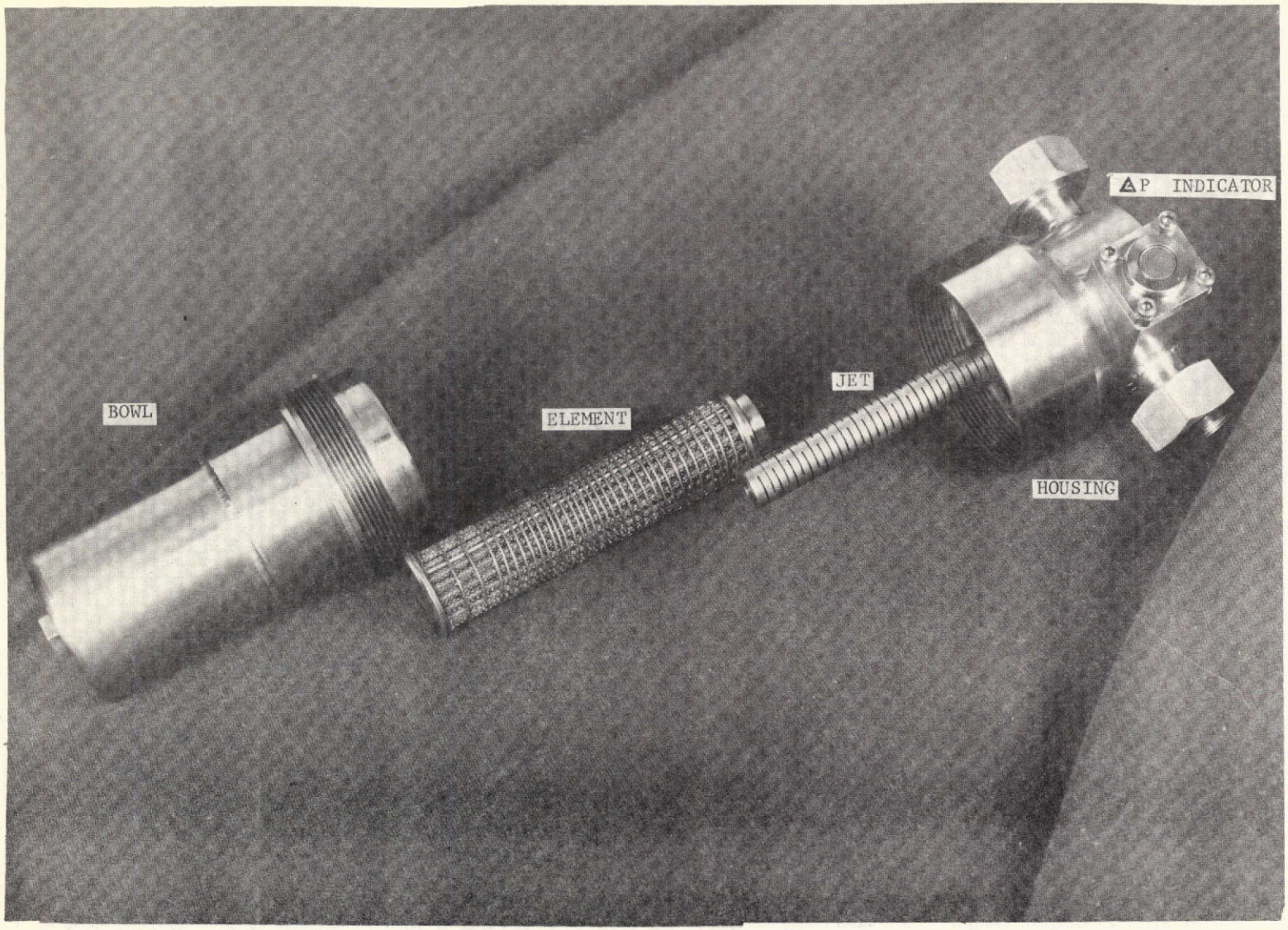

Figure IV-10 Regenerative Filter - Disassembled

The filter elements for both the secondary and regenerative filters are designed for backflushing and continuous reuse. They are sized for a flow rate of 6.31×10^{-4} m^3/sec (10.0 GPM). The regenerative filter element is rated at 20 microns nominal and 40 microns absolute. The secondary filter element is rated at 10 microns nominal and 25 microns absolute. A pressure drop across the filter of 138×10^3 N/m^2 (20 psid) indicates a fully loaded filter that requires cleaning. Both elements are constructed of stainless steel for extended life and ease of cleaning.

The backflush impingement jet is located within the inside diameter of the filter element. It adds very little pressure drop to the filter in the normal flow direction and improves the cleaning efficiency during the backflush operation. The alternating slots direct small high velocity jets of fluid onto the inner surface of the filter element, facilitating particle removal.

3. Vortex Particle Separator - The vortex particle separator is used to remove the contaminant particles that are backflushed from the regenerative filter. The vortex particle separator, shown in Figure IV-11, is a simple passive device which separates chemically inactive mixtures of substances of differing densities by the action of centrifugal forces induced by swirling flows. The particle separator operates at a backflush flow rate of 7.44×10^{-4} m^3/sec (11.8 GPM) and is designed for a particle size separation range of 10-200 microns. The separation efficiency of the separator at 7.44×10^{-4} m^3/sec (11.8 GPM) is approximately 86.7%.

The operation of the vortex separator involves the tangential injection of the fluid and entrained particles at the inlet of the cylindrical section causing a vortex motion. The vortex motion creates centrifugal forces up to or greater than 10,000 times the force of gravity. The centrifugal forces cause the heavier substances to move to the outside wall of the separator. The lighter fluid remains in the center of the cylinder and is withdrawn from the overflow at one end of the cylinder. The heavier substance is moved along the wall downwards in a spiral motion towards the underflow outlet of the conical section by a decreasing static pressure gradient and is discharged out the tube into the separator trap. The particle trap which consists of a particle ejector tube and a trap bowl, collects the contaminant particles and prevents them from reentering the separator after shutdown.

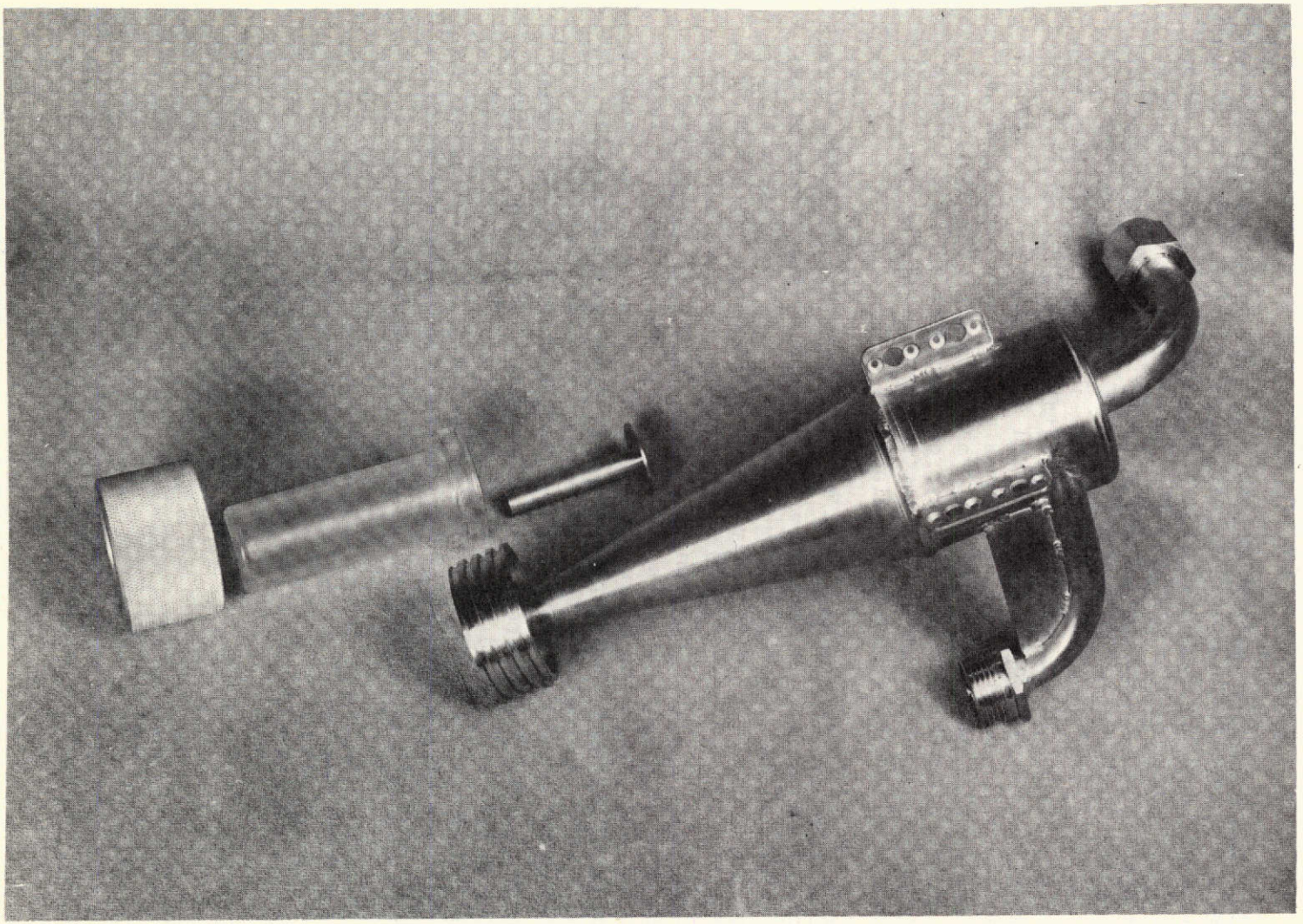

Figure IV-11 Vortex Particle Separator - Disassembled

4. Accumulator - The accumulator provides makeup fluid to the system in the event of fluid loss when the quick disconnects are disconnected and connected and also provides a convenient means for pressurizing the system. The accumulator is also used as a heat sink to maintain thermal control while operating the regeneration unit. The water volume of the accumulator is 2.52×10^{-3} m^3 (154 cu. inches). The stainless steel accumulator, Figure IV-12, consists of an inlet port, an outlet port, a flow deflector, bellows, and an air valve. The flow deflector is utilized to obtain maximum fluid mixing which is important in minimizing the temperature rise of the system. During operation the bellows is pressurized to 103.4×10^3 N/m^2 (15 psig) which maintains a positive pressure on the pump inlet, thereby preventing pump cavitation.

5. Fluid Quick Disconnects - The fluid quick disconnects permit connection and disconnection of the secondary and regenerative filters to the regeneration unit without loss of system fluid or pressure. The self-sealing quick disconnects are designed for 20.682×10^6 N/m^2 (3000 psig) maximum pressure and easily connect and disconnect with one hand. Figure IV-13 shows an external view of the quick disconnect coupling with the "TURN" to connect "PULL" to disconnect markings. The quick disconnect coupling, Figure IV-14, consists of two parts: the nipple half which is connected to the regenerative and secondary filters; and the coupler half which is connected to the regeneration unit fluid lines. When these two halves are separated, the valves are closed and the "O" rings provide an unexposed and fully protected seal. When connecting, the coupling halves align and mate without a cavity thereby preventing air entrapment on connection or fluid spillage on disconnection.

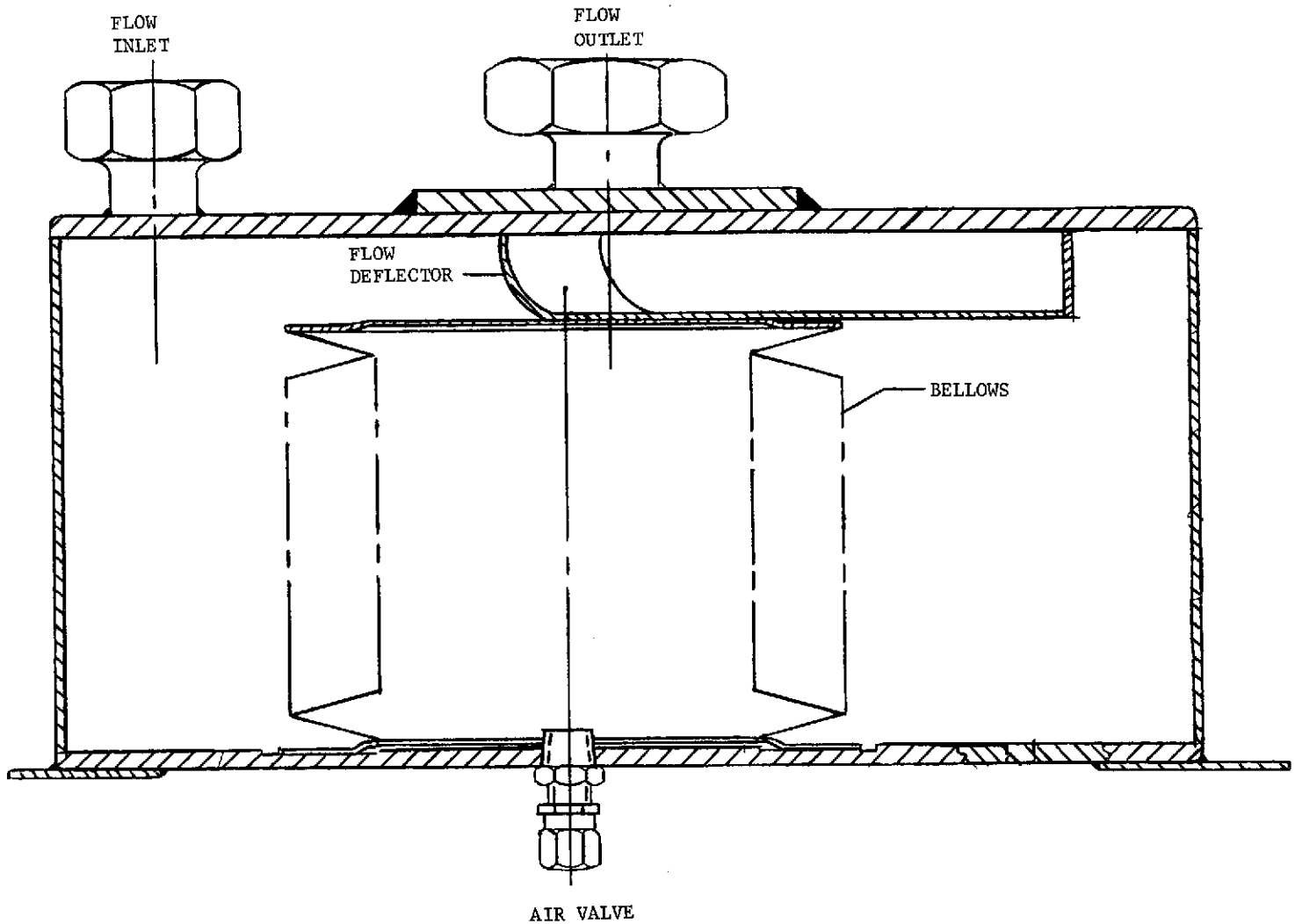

Figure IV-12 Accumulator

Figure IV-13 Quick Disconnect Coupling

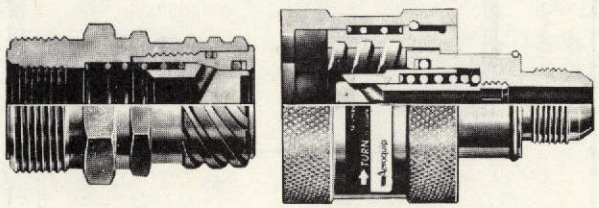

Nipple Coupler

Figure IV-14 Quick Disconnect - Uncoupled

C. INTERFACE REQUIREMENTS

The following data provides interface data for the flight prototype regeneration unit. The location of the disconnects on the interface panel is shown in Figure IV-15.

1. Filter Regeneration Unit - Interface Data

Fluid Media	water
Flow Rate:	
Operating	7.44×10^{-4} m^3/sec (11.8 GPM)
Minimum	6.62×10^{-4} m^3/sec (10.5 GPM)
Maximum	8.20×10^{-4} m^3/sec (13 GPM)
Discharge Pressure:	
Normal Operating	140.6×10^3 N/m^2 (200 psig)
Minimum Operating	105.5×10^3 N/m^2 (150 psig)
Maximum Operating	161.7×10^3 N/m^2 (230 psig)
* at an inlet pressure of	21.1×10^3 N/m^2 (30 psig)
Static Pressure	21.1×10^3 N/m^2 (30 psig)
Maximum Water Temperature:	65.5°C (150°F)
Power Source	200 vac
Frequency	400 Hz
Phase	3
Operating Current/Phase	10.6 amps
Maximum Current/Phase	11. amps
Inrush Start Current	53 amps

Inrush Current Time Period	0.14 sec
Power Consumption at Maximum Flow	3100 watts
Electrical Connector	5-Pin, Plug, Cannon P/N 81D58P14-5PB
Backflush Cycle Duration	2 minutes/filter
Weight of Regeneration Unit	16.69 kg (36.8 lbs)
Regeneration Unit Envelope Dimensions	29.7 x 30.7 x 47.2 cm (11.7 x 12.1 x 18.6 inches)
Distance between Disconnect Centerlines	15.40 cm (6.063 inches)
Spacecraft filter P/N	849FRS00007-010
Spacecraft Filter Rating	20 micron nominal 40 micron absolute
Regeneration Unit Quick-Disconnect Coupling P/N	Aeroquip P/N 3205-10, Style I
Spacecraft Filter Quick-Disconnect Nipple P/N	Aeroquip P/N 3202-10, Style I

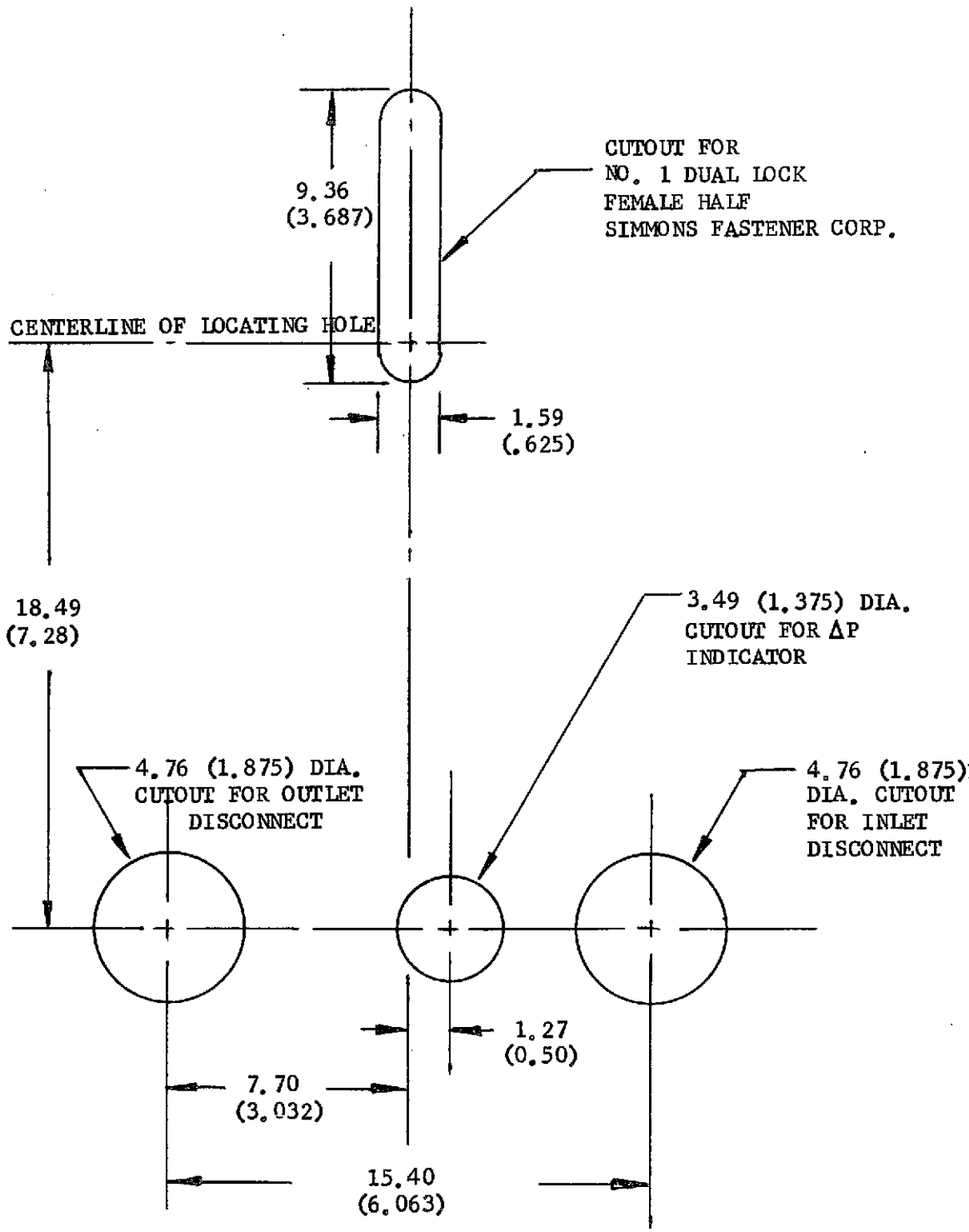

FIGURE IV-15 INTERFACE PANEL DIMENSIONS

V. TEST PROGRAM

A test program was conducted, as part of this contract, to verify the performance of the regenerative fluid filter system and its components. The tests were broken down into component tests, bubble-point tests, subsystem tests, system tests, and zero-g tests. Including supporting tests to these major categories there were approximately 175 tests run on the Flight Prototype Filter Regeneration Unit.

Performance tests were performed on the filter and separator as separate components (component tests), and as a unit (subsystem tests), prior to their installation in the prototype filter regeneration unit. These tests were performed in the same ground test system as the development tests, and thus provide a direct comparison with previous data. Following the assembly of the filter regeneration unit, one-g tests were performed on the closed loop system to determine regeneration efficiency, overall efficiency, thermal capacity, and regeneration unit performance. Final testing included zero-g cyclic testing on the KC-135 aircraft of the closed loop system.

The filter regeneration prototype tests were performed using AC coarse road dust as the contaminant. All testing was accomplished with water that was filtered on the inlet of the test circuit to remove all particles larger than 2 microns in size. The AC road dust (Figure V-1) is a composite of screened and graded dust particles, primarily quartz, and is a natural road dust from Arizona. The basic composition in each size range is:

Particle Size (microns)	Percent by Weight
0 to 5	12 $\pm$ 2
5 to 10	12 $\pm$ 3
10 to 20	14 $\pm$ 3
20 to 40	23 $\pm$ 3
40 to 80	30 $\pm$ 3
80 to 200	9 $\pm$ 3

The number of particles of a given size per 1.0 mg of road dust is shown in Figure V-2. It may be observed from the above data that approximately 60% (by weight) of the particles are below 40 microns. This is below the 50 micron cutoff specified for the process water, thermal water, and thermal freon systems. The large percentage

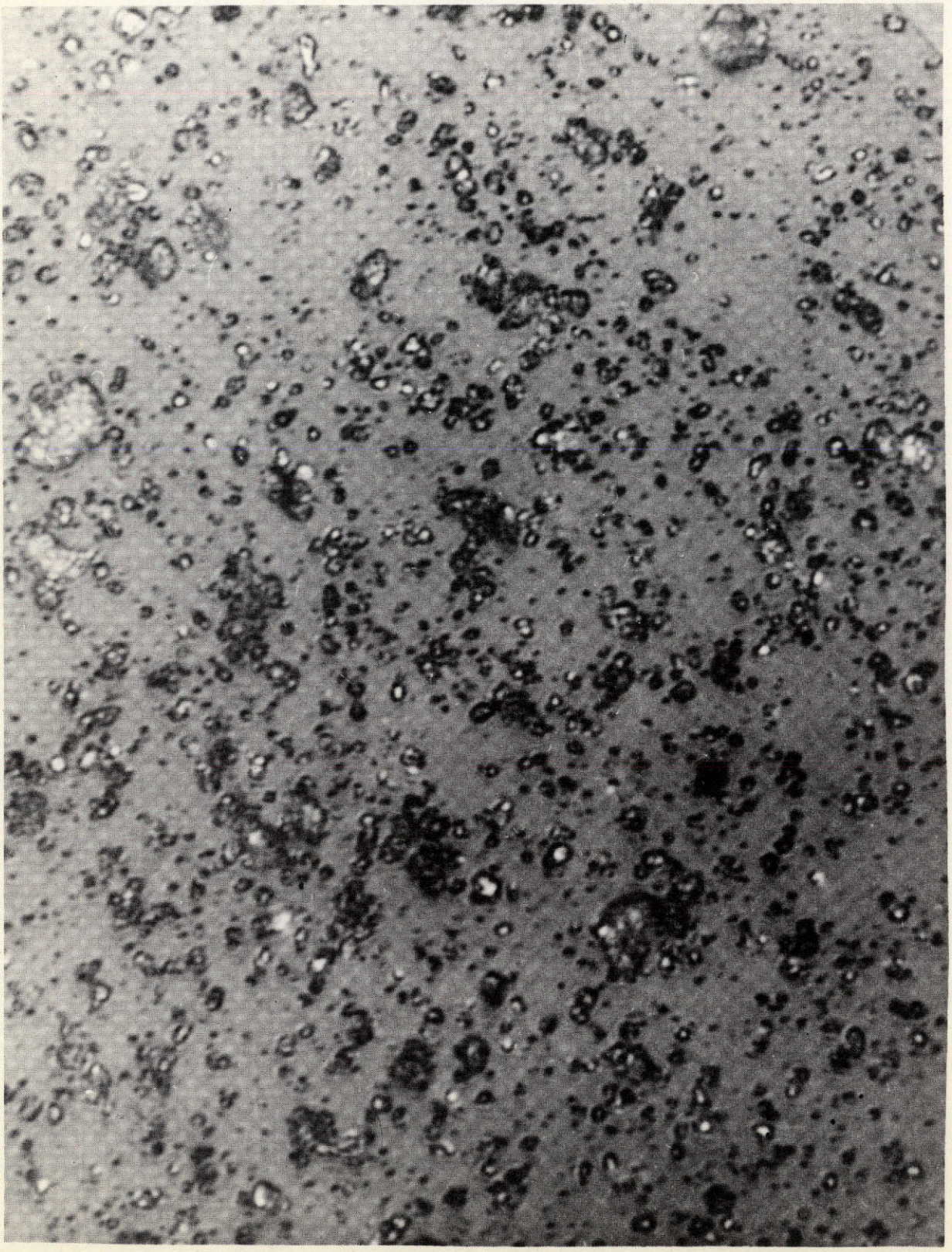

Figure V-1 AC "Coarse" Road Dust - 870X

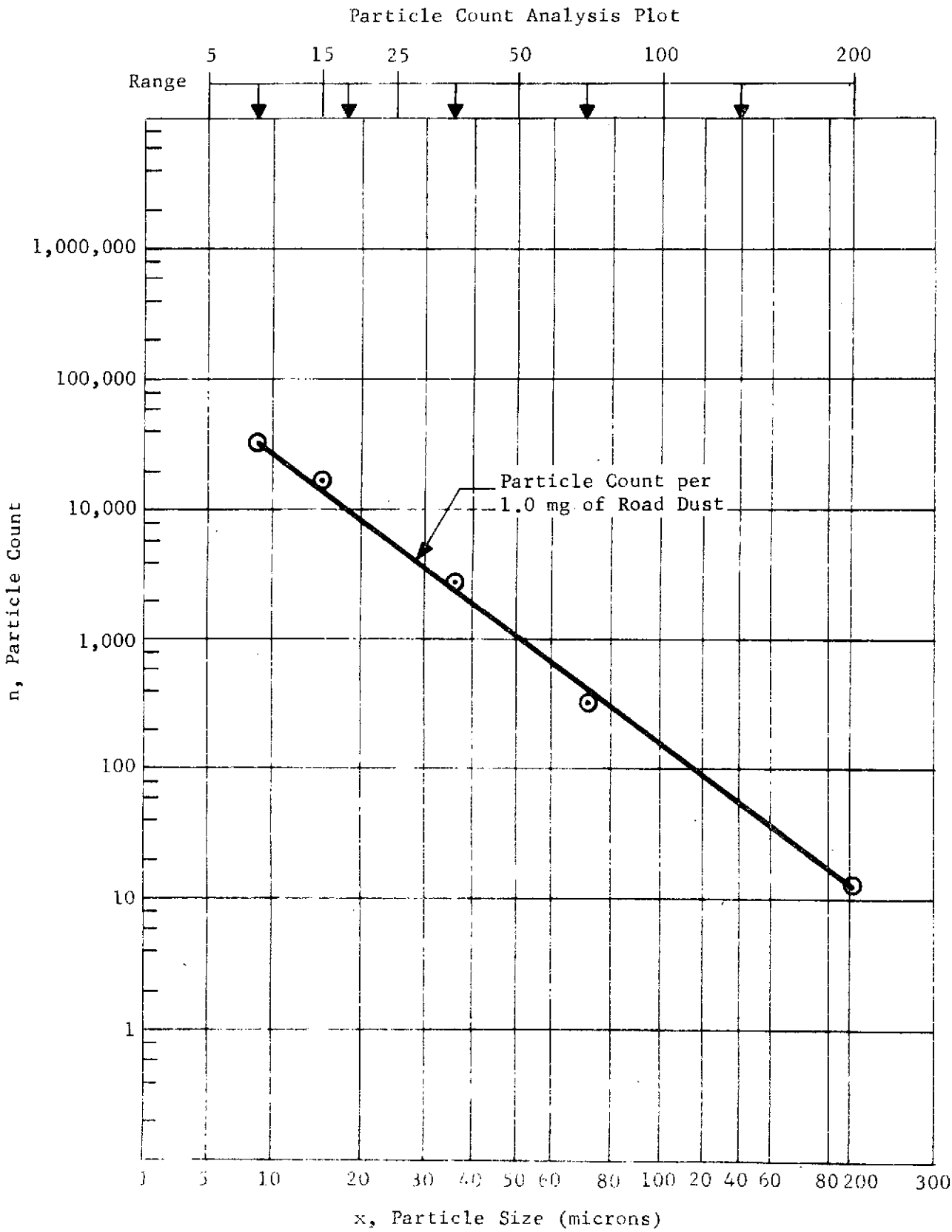

Figure V-2 Particle Count Composition AC "Coarse" Road Dust

of particles below the cutoff and the use of test filters with a rating of 20 micron nominal and 40 micron absolute would make the tests extremely conservative.

Because of the large percentage of particles below 40 microns, the road dust was sieved to separate the particles below 43 microns. The method used to separate the contaminant did not remove all of the less-than-43-micron contaminants. The separation process produced an indicated 53.4% of the contaminants greater than 43 micron as compared to 40%, which is the maximum possible. Thus, approximately 25% of the sieved contaminants were actually less than 43 microns. This fact has a significant effect on the indicated test efficiencies and if the contaminants actually were all greater than 43 microns, the test efficiencies would have increased.

Errors are inherent in contamination test programs and are attributed to the fact that the tests involve very small quantities of contamination. Any error in resolving quantity injected into the system versus output results in a large error in resultant efficiency. The test procedure required weighing the test contaminant in a pill capsule before injection and also afterward (pill capsule tare weight) to obtain the exact amount of contaminant added. To determine the efficiencies, it was necessary to recover the contaminant which passed through the filter or separator, was backflushed from the filter, or was contained in the filter bowl or separator trap. The contaminants were recovered on 0.45 to 3.0 micron millipore pads which requires a clean and contaminated weight determination to ascertain the weight of the contaminant recovered. The following errors were identified in the development program and the magnitude of their effect on the test program was taken into account.

- Humidity absorption and desorption on the millipore pads
- Weighing errors
- Particles trapped in the test system
- Particles below 0.45 microns
- Accumulation of small particles in the water supply in a size range of 0.45 microns to 2.0 microns

A. MOTOR/PUMP TESTS

The Hydro-Aire fluid pump (P/N SK64-077) acceptance tests were conducted at the vendors test facility in Burbank, California and were witnessed by Martin Marietta personnel. The performance of the pump during these tests verified all design and construction criteria, as well as all performance requirements specified by Martin Marietta Specification 849FRS00011.

The basic acceptance criteria for the pump were: 1) physical dimensions per the approved drawings, 2) pump performance to meet a minimum of 1034.1×10^3 N/m^2 (150 psi) pressure rise at 6.62×10^{-4} m^3/sec (10.5 GPM) using water with an inlet pressure of 137.9×10^3 N/m^2 (20 psig), 3) pump performance at 6.31×10^{-4} m^3/sec (10 GPM) shall require a maximum of 3000 watts total electrical power. The test sequence of the acceptance tests consisted of a break-in test, performance tests, and thermal tests. The data from the performance tests verified that the pump pressure rise was greater than the required minimum of 1034.1×10^3 N/m^2 (150 psig) at 6.62×10^{-4} m^3/sec (10.5 GPM) being approximately 1144×10^3 N/m^2 (166 psig). The power consumption (3040 watts) was slightly higher than the specified maximum of 3000 watts, but was considered acceptable since additional machining of the pump impeller would have been required to reduce the input power and was not considered worth the risk. The results of the thermal tests verified that the heat transferred by the pump assembly to the water in the closed loop test system over a period of 5 minutes at 6.31×10^{-4} m^3/sec (10 GPM) and at maximum flow was less than 2635 watts (2.5 Btu/sec).

Prior to testing, the pump assembly was visually checked for workmanship and conformance to the Hydro-Aire drawings SK64-076 and SK64-077. Particular attention was given to neatness and throughness of soldering, wiring, welding, plating, alignment of parts, identification and serialization, cleanliness, and freedom of parts from defects, burrs, and sharp edges.

1. Break-In Test - The break-in test was run prior to the performance and thermal acceptance tests. For this test, the motor/pump assembly was installed in the closed loop equipment test set-up, shown in Figure V-3. The water capacity of this system was 2.8×10^{-3} m^3 (0.74 gal). During this test, the motor/pump assembly was operated for 3 minutes with the flow rate adjusted to 6.31×10^{-4} m^3/sec (10 GPM). During this test, the current of each phase, total power consumption, and fluid temperature of the water was monitored. The phase currents measured were 10.6, 10.2, and 10.0 amperes. One phase, as indicated by 10.0 amps, showed poor response but the error was attributed to the test equipment used. It was determined that a malfunctioning shunt resistor was the cause of the low current level, because whichever phase terminal that the shunt resistor was connected to, the same low current level was obtained. The input power was measured at the start and end of the 3 minute test period. The power levels measured were 3056 watts at the start and 3040 watts at the end of the run period. These power levels were considered acceptable even though they were slightly higher than the maximum allowable power level (3000 watts) specified by Martin Marietta Specification 849FRS00011. In order to reduce the power level to the desired value, remachining of the pump impeller would have been required. Since the vendor had already cut down the diameter of the impeller in order to obtain the desired flow rate, pressure rise, and power consumption, the decision was made not to remachine the impeller. The major concern was that any further reduction of the impeller diameter could adversely affect the pump performance by decreasing the pump pressure rise. The temperature rise of the inlet water at the end of the 3 minute period was approximately 54.4°C (130°F).

2. Pump Performance Tests - The pump performance tests were conducted to verify that the pump performance was within the envelope shown by Figure V-4. Three separate tests were conducted with the pump assembly installed in the equipment test loop shown in Figure V-5. The capacity of this closed loop test system was 36.7×10^{-3} m^3 (9.7 gal) of water. The pump performance was determined by varying the inlet pump pressure and flow rate; and measuring the corresponding values of pump outlet pressure, power consumption, phase currents, and inlet/outlet water temperature levels.

During test No. 1, the motor/pump assembly was operated for 4 minutes. The inlet pump pressure was adjusted to 68.9×10^3 N/m^2 (10 psig) and the flow rate was varied from zero to

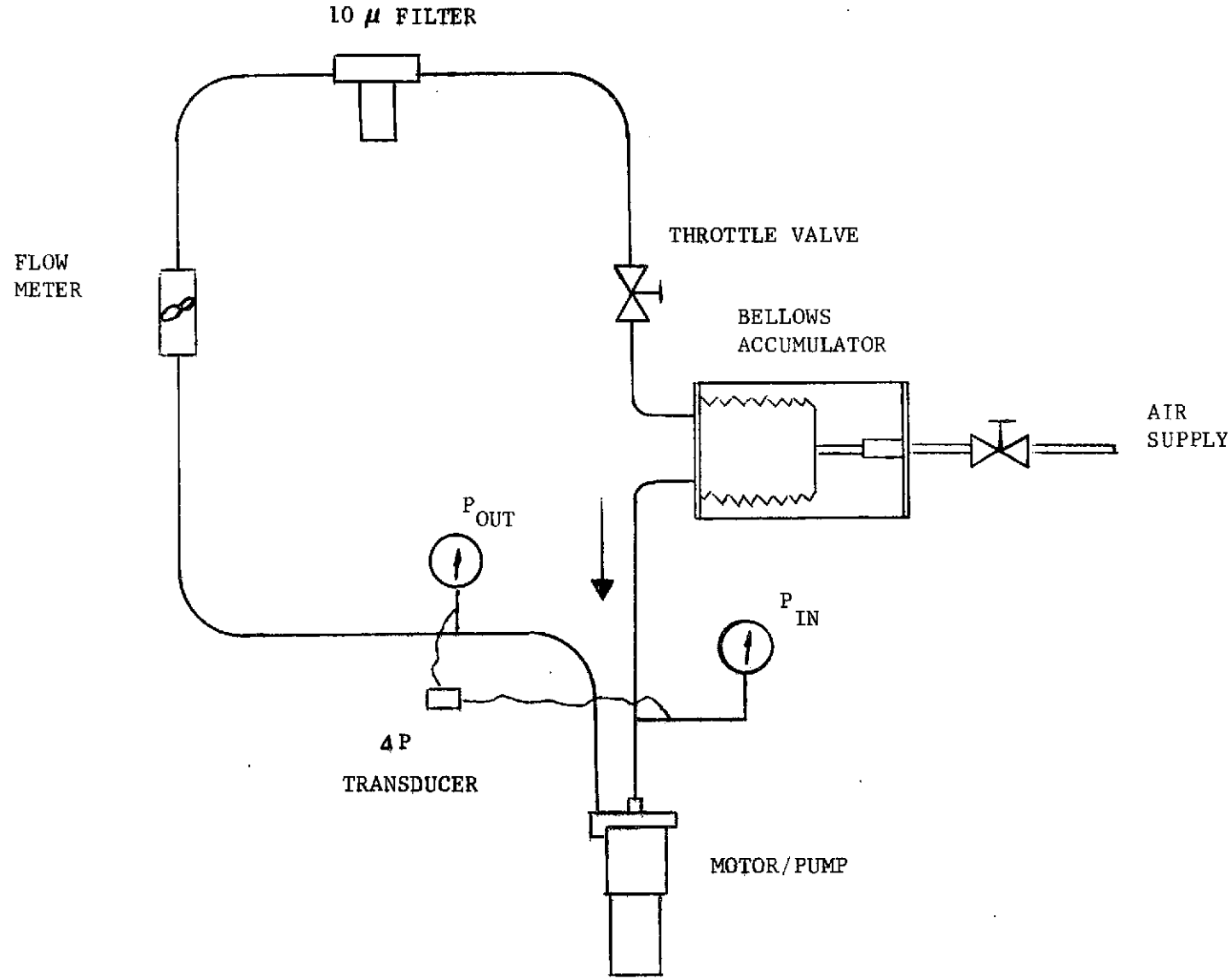

Figure V-3 Test Setup - 2.8 x 10^{-3} m^3 (0.74 gal) Capacity

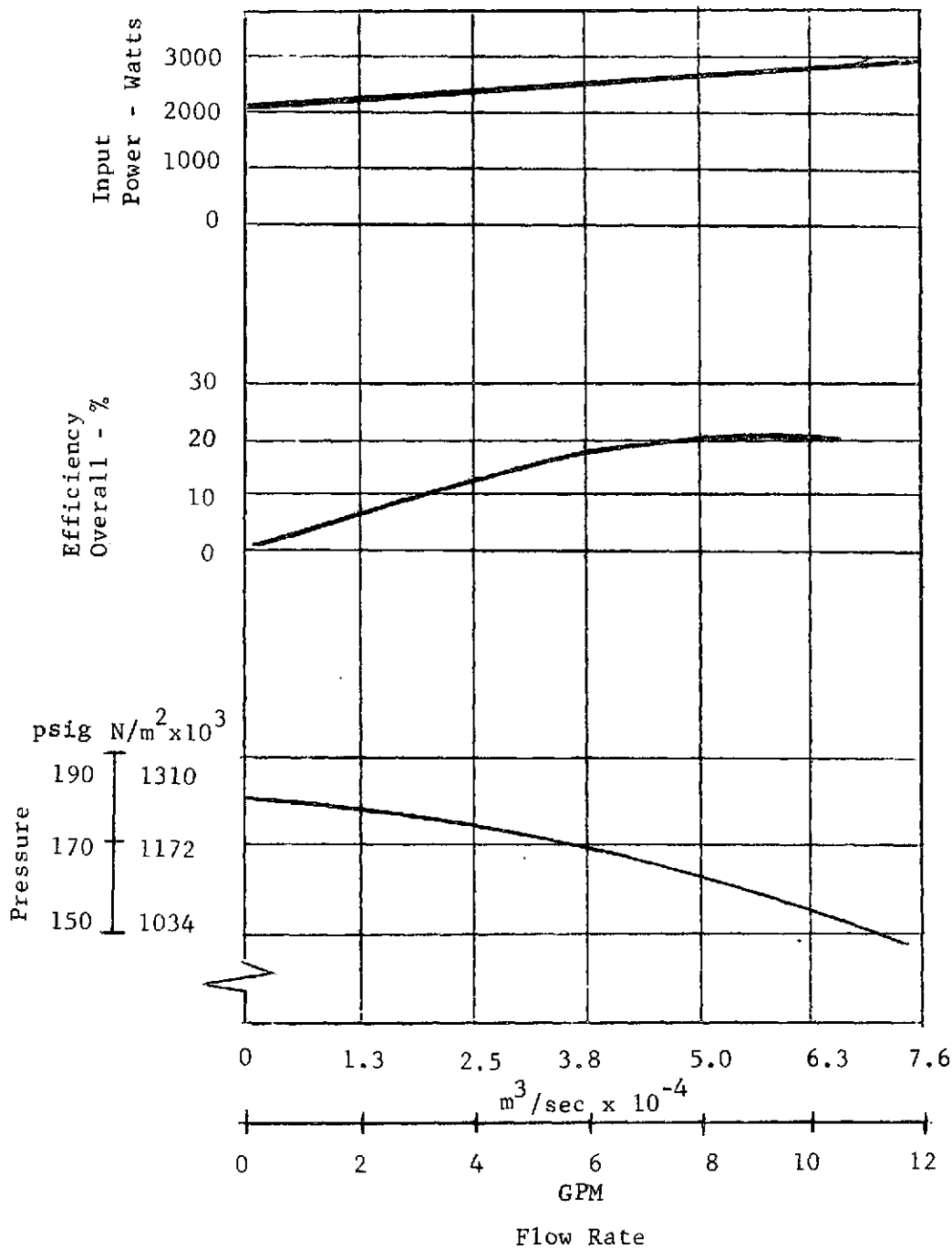

Figure V-4 Pump Performance Requirements

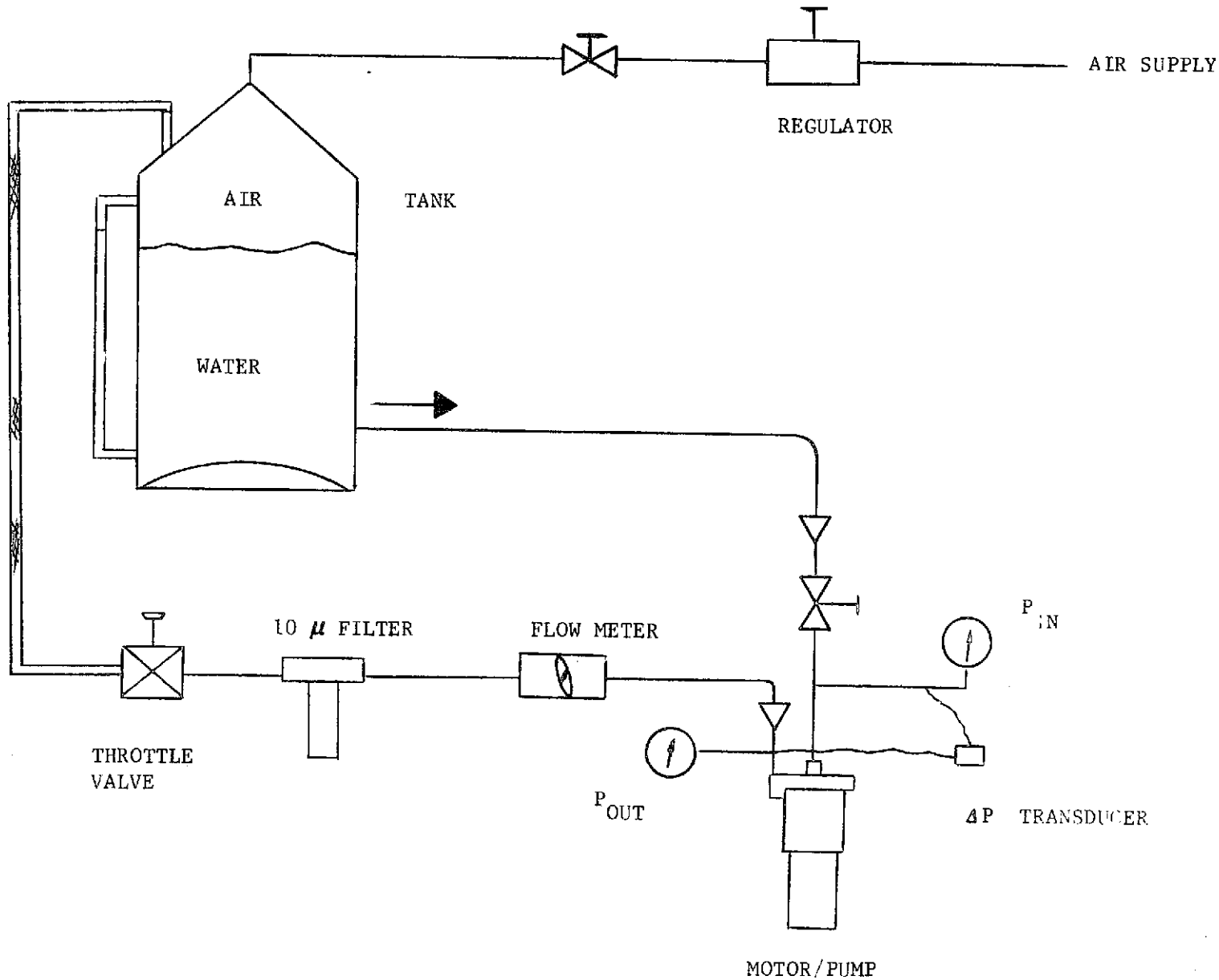

Figure V-5 Test Setup - 36.7 x 10^{-3} m^3 (9.7 gal) Capacity

8.07×10^{-4} m^3/sec (12.8 GPM). At each level of flow rate setting, the outlet pump pressure, power consumption, phase currents, and water temperature at the pump inlet and outlet were monitored. Table V-1 shows the measured performance values at the various flow rate settings and with a 68.9×10^3 N/m^2 (10 psig) pump inlet pressure.

Table V-1 Pump Performance with 68.9×10^3 N/m^2 (10 psig) Inlet Pressure

Flow Rate $m^3/sec \times 10^{-4}$ (GPM)	Outlet Pressure $N/m^2 \times 10^3$ (psig)	Power Consumption watts	Average Current amperes	Remarks
0 (0)	1351.2 (196)	2296	8.5	4 minute test
2.78 (4.4)	1289.2 (187)	2808	9.3	
5.68 (9.0)	1240.9 (180)	2976	10.2	
8.07 (12.8)	1151.3 (167)	3128	10.6	Maximum Flow

During this test, the input power varied from 2296 watts at system startup to a maximum of 3128 watts at full flow. The pump outlet pressure at full flow was 1151.3×10^3 N/m^2 (167 psig) which provided a good margin over the required minimum of 1034.1×10^3 N/m^2 (150 psi). The average current varied from 8.5 amperes soon after system startup to 10.6 amperes at maximum flow. The relationship between the phase currents and the system flow rate is given by Figure V-6. This curve shows that for a flow rate of 7.44×10^{-4} m^3/sec (11.8 GPM), which is the normal backflush rate of the regenerative unit, the current/phase is approximately 10.6 amperes. Upon system startup, an in-rush current of 53 amperes exists for a period of .09 seconds and then decreases to the normal operating range of 10.6 amperes at full flow within .14 seconds. Figure V-7 shows the current startup characteristics as a function of time.

Performance tests No. 2 and No. 3 were conducted in the same manner as test No. 1 except that in test No. 2, the inlet pump pressure was 137.9×10^3 N/m^2 (20 psig) with an operating time

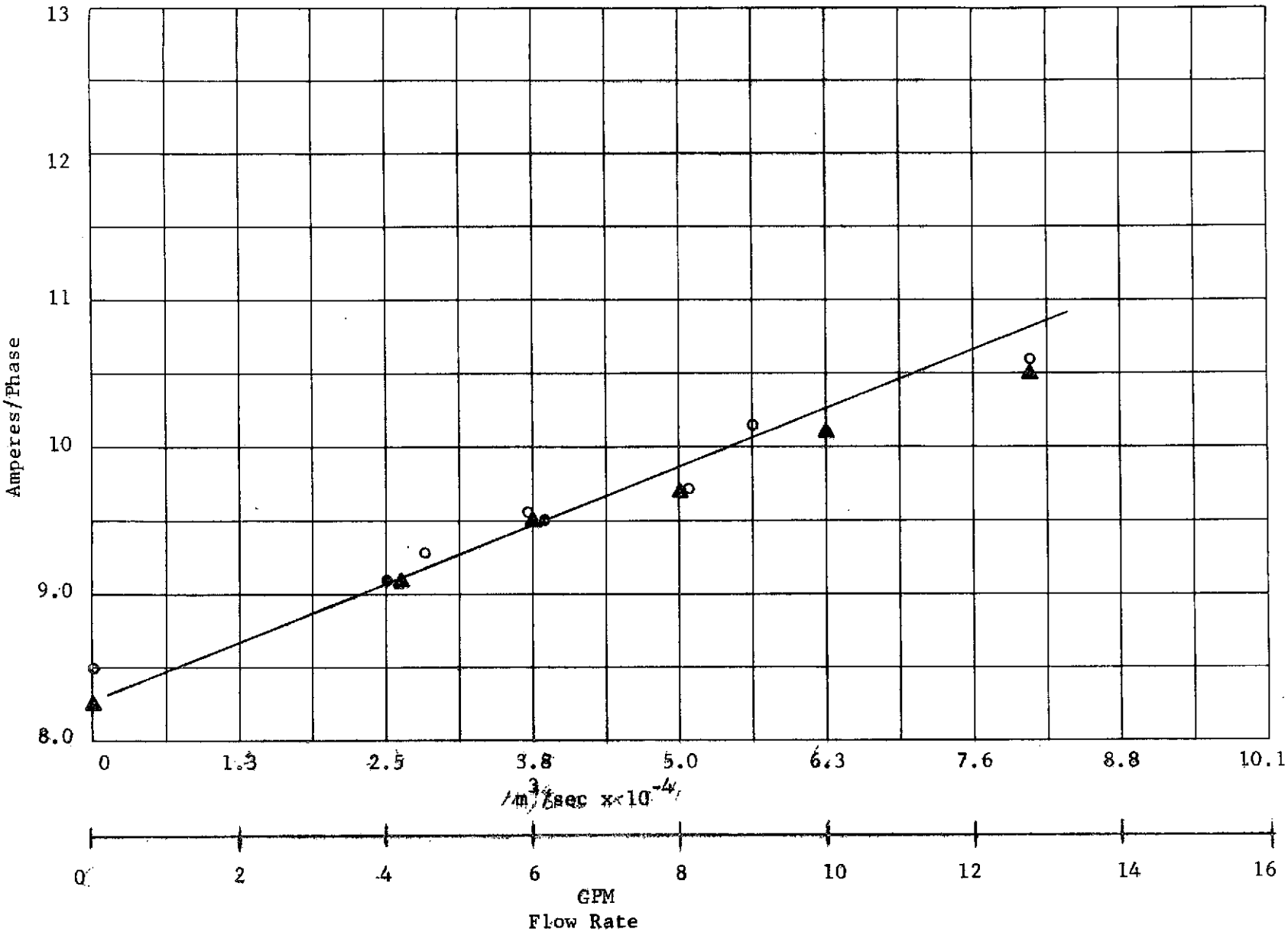

FIGURE V-6 MOTOR/PUMP CURRENT CHARACTERISTICS

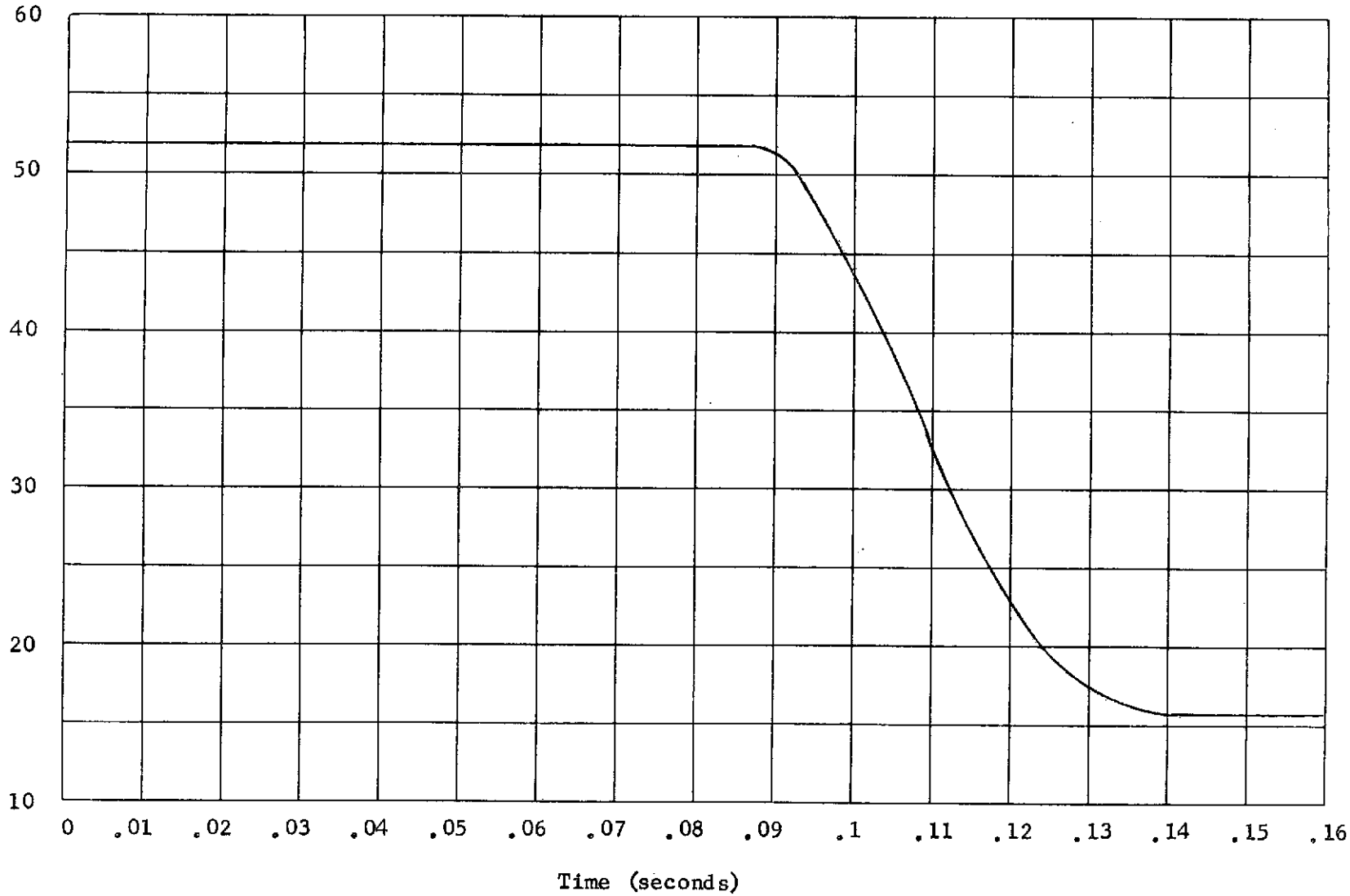

FIGURE V-7 MOTOR PUMP START-UP CURRENT

of 5 minutes, and in test No. 3, the inlet pump pressure was 206.8 x 10^3 N/m^2 (30 psig) and the operating time was 4 minutes. Again the flow rate was varied from zero to maximum flow and the corresponding values of outlet pump pressure, input power, current/phase, and inlet and outlet pump water temperatures were monitored. Table V-2 shows the results of performance tests Nos. 2 and 3.

Based on the pump performance tests, the overall pump performance is indicated by Figure V-8. It is important to note that at the normal backflush flow rate 7.44 x 10^{-4} m^3/sec (11.8 GPM), the pump pressure rise is about 1116.8 x 10^3 N/m^2 (162 psi) which provides some margin over the 1034.1 x 10^3 N/m^2 (150 psi) required. The efficiency curve shows that the overall pump efficiency at maximum flow rate 8.07 x 10^{-4} m^3/sec (12.8 GPM) is approximately 28%. The overall pump efficiency was determined from the following equation:

$$\text{Overall Efficiency } \% = \frac{\text{GPM x Pump } \Delta P \text{ x } 43.5}{\text{Input Watts}}$$

The primary factors contributing to pump inefficiency are impeller diameter, motor air gap, motor windings, and impeller convolute design. Additional machining of the pump in order to reduce the impeller diameter, reduce the motor air gap, or alter the motor windings or impeller convolute configuration, in order to increase efficiency, was considered economically unfeasible. Additional remachining also increased the possibility of permanent pump damage. To purchase another pump that would increase the efficiency to 30-35% was not considered to be worth the increased costs for the program.

3. Thermal Tests - The thermal tests were conducted with the pump assembly installed in the 2.8 x 10^{-3} m^3 (0.74 gal) capacity, closed loop water system shown in Figure V-9. Two tests were conducted in order to determine the heat transfer to the inlet/outlet water, the motor housing, and the pump housing and volute.

In the first test, the inlet pump pressure was set at 68.9 x 10^3 N/m^2 (10 psig) and the flow rate was adjusted to 6.31 x 10^{-4} m^3/sec (10 GPM). With an initial water temperature of approximately 24°C (75°F), the pump was operated for a period of 5 minutes and the circulating water, motor housing, and pump housing and volute temperatures were monitored. Figure V-10 shows the results of this test. The temperature of the pump surface, and inlet water after the 5 minute operating period was 73°C (163°F) and 68°C (154°F), respectively.

Table V-2 Pump Performance

	Flow Rate $m^3/sec \times 10^{-4}$ (GPM)	Outlet Pressure $N/m^2 \times 10^3$ (psig)	Input Power (watts)	Current/Phase (amperes)			Water Temp °C (°F)		Remarks
				T-1	T-2	T-3	In	Out	
Test No. 2 at 138 x 10^3 N/m^2 (20 psig) Inlet Pressure	8.07 (12.8)	1220 (177)	3120	10.8	10.5	10.2	32.1 (90)	33.3 (92)	Max flow
	6.31 (10.0)	1289 (187)	3008	10.5	10.1	9.8	33.9 (93)	35. (95)	
	5.02 (8.0)	1317 (191)	2888	10.2	9.8	9.6	34.5 (94)	35.5 (96)	
	3.79 (6.0)	1344 (195)	2752	9.8	9.5	9.2	35 (95)	36.6 (98)	
	2.52 (4.0)	1365 (198)	2600	9.5	9.1	8.8	35.5 (96)	38.5 (101)	
	0 (0)	1399 (203)	2288	8.7	8.2	7.9	36.1 (97)	40.5 (105)	5 min run
Test No. 3 at 207 x 10^3 N/m^2 (30 psig) Inlet Pressure	8.07 (12.8)	1289 (187)	3112	10.8	10.5	10.2	35 (95)	36.1 (97)	Max flow
	6.31 (10.0)	1344 (195)	3024	10.4	10.1	9.8	36.1 (97)	37.2 (99)	
	5.05 (8.0)	1379 (200)	2888	10.2	9.8	9.5	36.6 (98)	38.5 (101)	
	3.79 (6.0)	1406 (204)	2744	9.8	9.5	9.2	37.8 (100)	39.5 (103)	
	2.52 (4.0)	1427 (207)	2600	9.5	9.1	8.8	38.5 (101)	40.5 (105)	
	0 (0)	1462 (212)	2272	8.6	8.2	8.0	38.5 (101)	42.8 (109)	4 min run

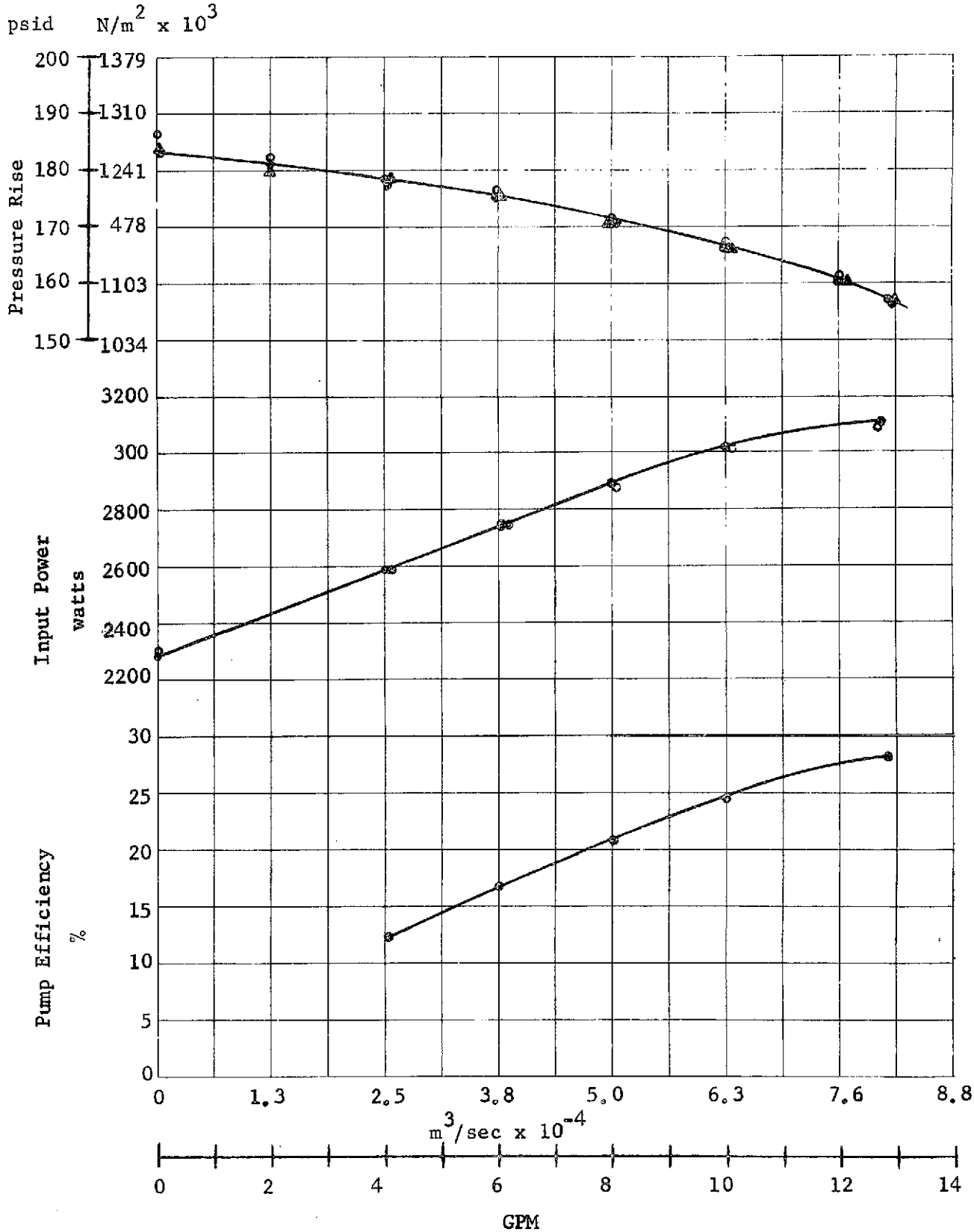

FIGURE V-8 PUMP PERFORMANCE

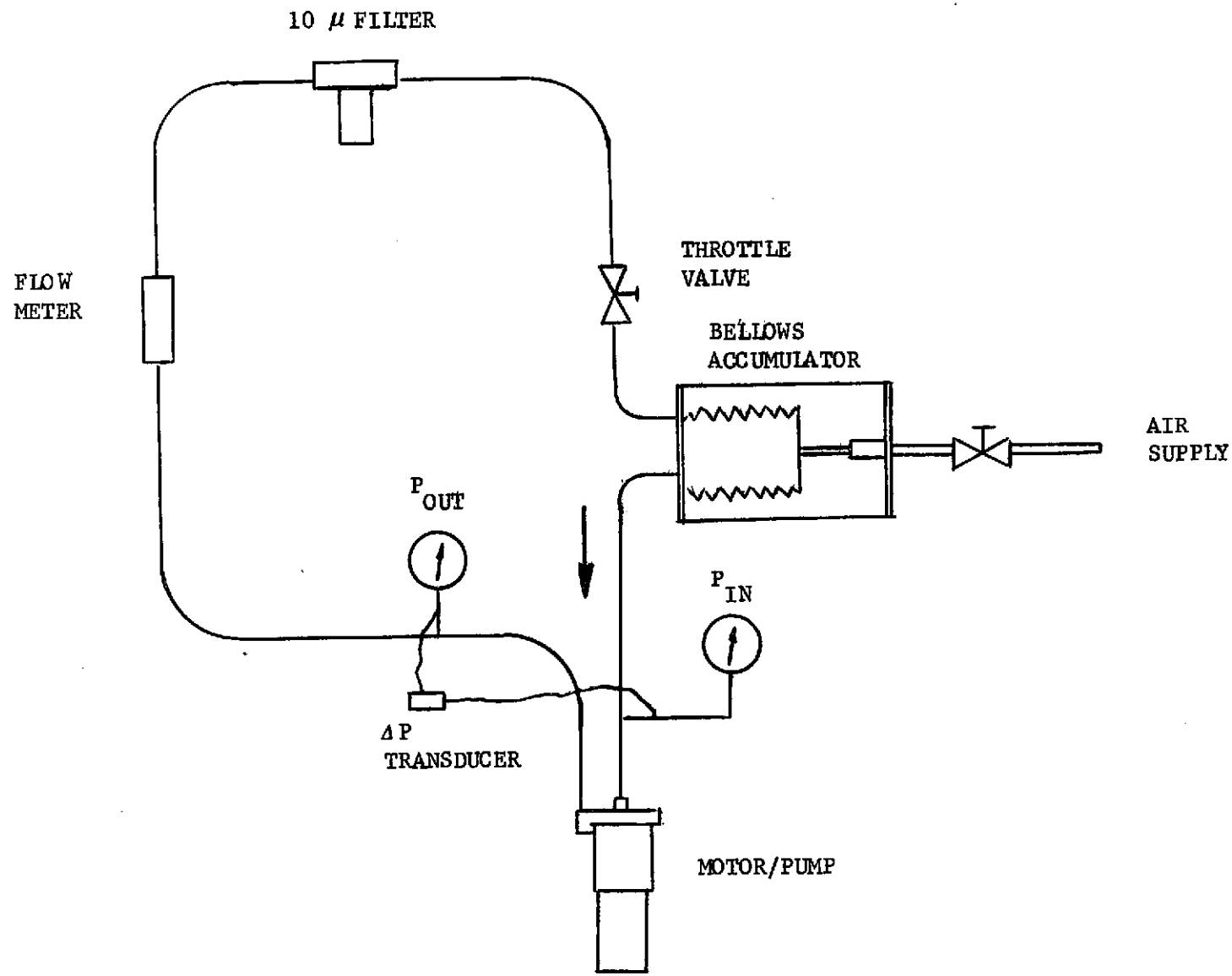

FIGURE V-9 TEST SET UP - $2.8 \times 10^{-3} m^3$ (0.74 gal) CAPACITY

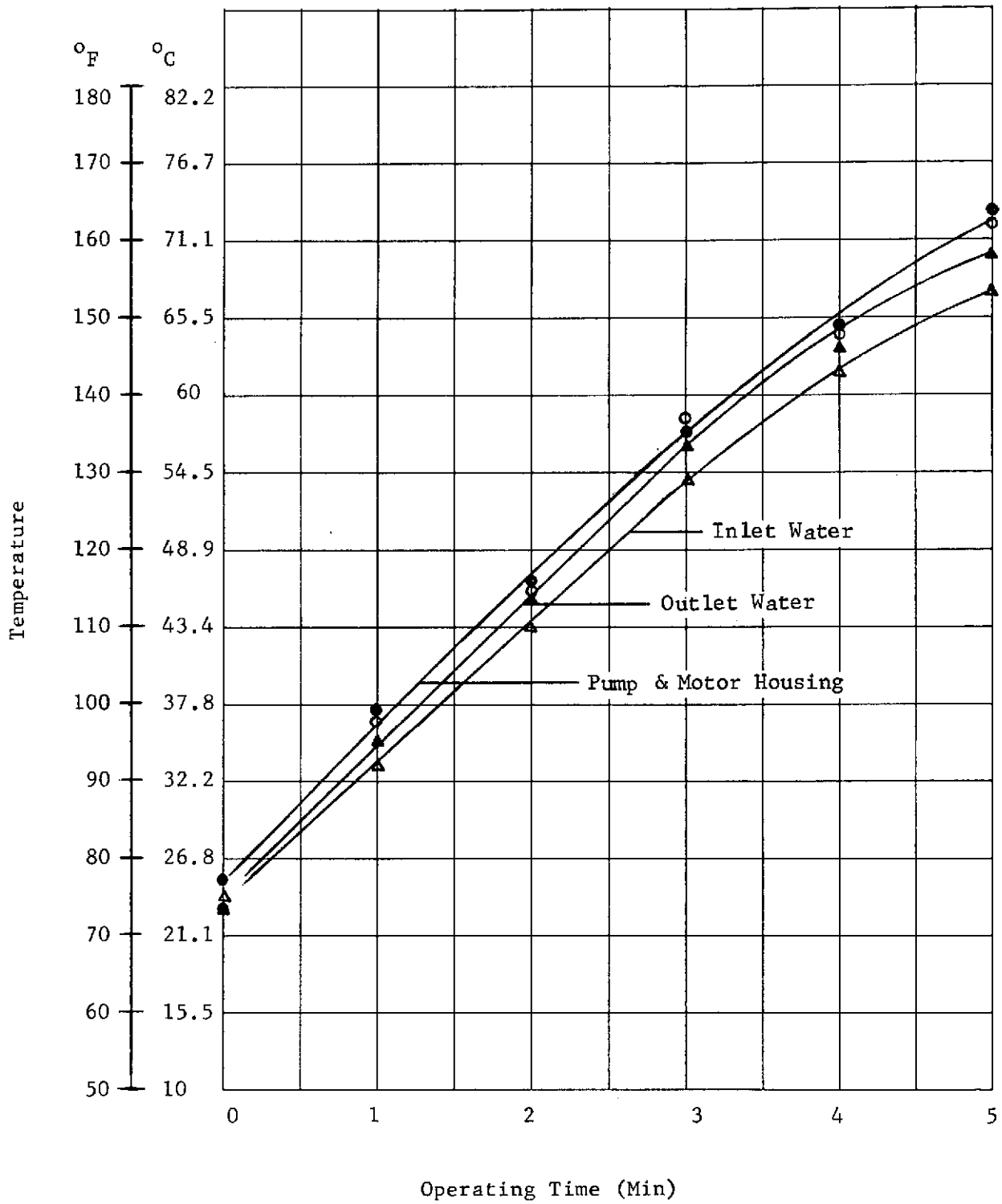

FIGURE V-10 TEMPERATURE RISE AT 6.31×10^{-4} m^3/sec (10 GPM)

The heat transfer to the water was determined by the equation:

$$Q = \dot{W} c_p \Delta T$$

where Q = Heat transfer (watts)

$\dot{W}$ = Flow Rate (lb/min)

c_p = Specific Heat (constant pressure)

ΔT = Temperature Differential

For the closed loop test system, the test volume was:

$$\text{Test Vol.} = (2815)\text{cc}\ (10^{-6}) = 2815 \times 10^{-6}\ \text{m}^3\ (0.74\ \text{gal})$$

The weight of this volume of water was therefore:

$$\text{Water Wt.} = (62.4)(16)\ \text{Kg/m}^3\ (2815 \times 10^{-6})\text{m}^3 = 2.8104\ \text{Kg}\ (6.2\ \text{lbs})$$

Therefore:

$$Q = (6.2)(1.0)\ \Delta T\ \text{Btu/min}$$

Transferring Q to watts gives:

$$Q = (6.2)(17.57)\ \Delta T = 109\ \Delta T\ \text{watts}$$

Table V-3 gives the net or effective heat transfer to the water in watts each minute at a flow rate of 6.31×10^{-4} m^3/sec (10 GPM). The table also shows the cumulative input watts for the 5 minute period. The average heat transfer to the water each minute was 1722 watts. The average cumulative heat transfer for the 5 minute period was 1821 watts.

The second thermal test was conducted to determine the temperature rise of the water, motor housing, and pump housing/volute at maximum flow, which was 8.07×10^{-4} m^3/sec (12.8 GPM), and with varying inlet pump pressures of 72.4×10^3 N/m^2 (10.5 psig) to 172.4×10^3 N/m^2 (25 psig). These temperatures were monitored with the pump operating at full flow for a period of 4 minutes. The initial water temperature was higher than that for the 6.31×10^{-4} m^3/sec (10 GPM) tests being about 34.5°C (94°F). Figure V-11 dipicts the inlet and outlet water temperature,

Table V-3 Heat Transfer to Water at 6.31×10^{-4} m^3/sec (10 GPM)

Time (min)	Inlet Water Temperature °C (°F)	ΔT Each Minute °C (°F)	ΔT Cumulative °C (°F)	Watts Input	Heat Transfer	
					Watts Each Min	Watts Cumulative
0	24 (75)	-	-	3048	-	-
1	32.8 (91)	-11.1 (16)	-11.1 (16)	3024	1744	1744
2	42.8 (109)	-12.2 (18)	1.1 (34)	3000	1962	1853
3	53.9 (129)	-13.5 (20)	10.2 (54)	2952	2180	1962
4	61.1 (142)	- 9.5 (13)	19.5 (67)	2952	1417	1826
5	67.8 (154)	- 8.9 (12)	26.1 (79)	2928	1308	1722

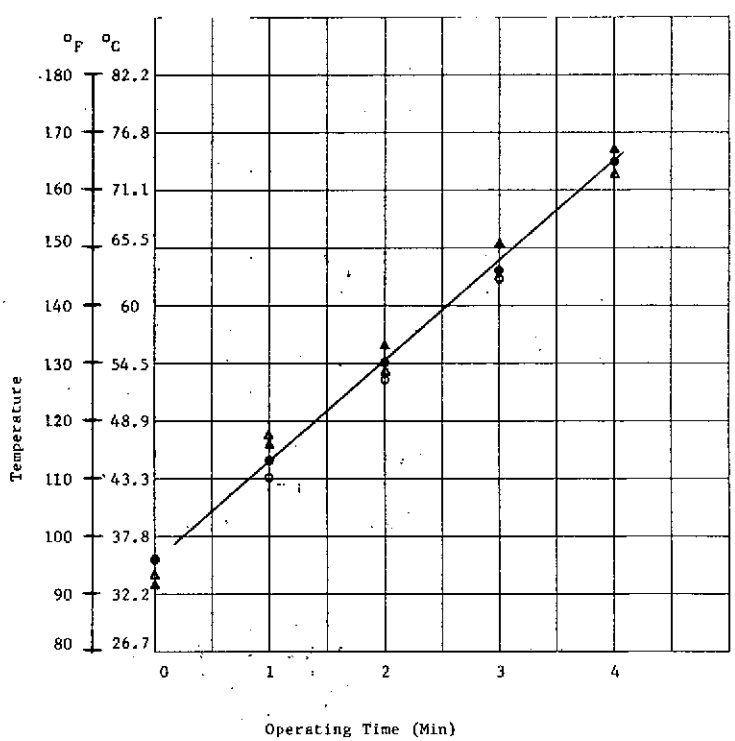

FIGURE V-11 TEMPERATURE RISE AT MAXIMUM FLOW

Table V-4 Temperature Rise at Maximum Flow

Time (Min)	Pressure $N/m^2 \times 10^3$ (psig)		Total Watts	Temperature °C (°F)			
	In	Out		Inlet Water	Outlet Water	Motor Housing	Pump Housing
0	131 (19)	1213 (176)	3128	34 (94)	34 (93)	36 (96)	36 (96)
1	172 (25)	1241 (180)	3104	48 (118)	47 (117)	43 (110)	45 (113)
2	90 (13)	1158 (168)	3092	54 (129)	56 (133)	53 (128)	54 (130)
3	114 (16.5)	1172 (170)	3056	62 (144)	66 (151)	62 (144)	63 (145)
4	72 (10.5)	1117 (162)	3024	72 (162)	74 (166)	73 (164)	73 (164)

motor housing temperature, and pump housing and volute temperature during the 4 minute operating period. Table V-4 shows the various temperature rises and the static inlet pump pressures used during the 4 minute test period.

A comparison of the 6.31×10^{-4} m^3/sec (10 GPM) flow and maximum flow, 8.07×10^{-4} m^3/sec (12.8 GPM), shows that there is an insignificant difference in the rate of temperature rise for the closed loop flow. Figure V-12 shows this comparison. Table V-5 shows the net heat transfer to the water each minute, as well as the cumulative heat transfer each minute for the 4 minute thermal test. The average heat transfer to the water each minute during the 5 minute 6.31×10^{-4} m^3/sec (10 GPM), thermal test was 1722 watts while the average heat transfer to the water during the 4 minute, maximum flow, test was 1853 watts each minute.

As part of the pump thermal tests, temperature decay for the pump motor and volute and for the inlet and outlet water were monitored after shutdown of the 6.31×10^{-4} m^3/sec (10 GPM), 5 minute test. With an ambient air temperature of 22.2°C (72°F)

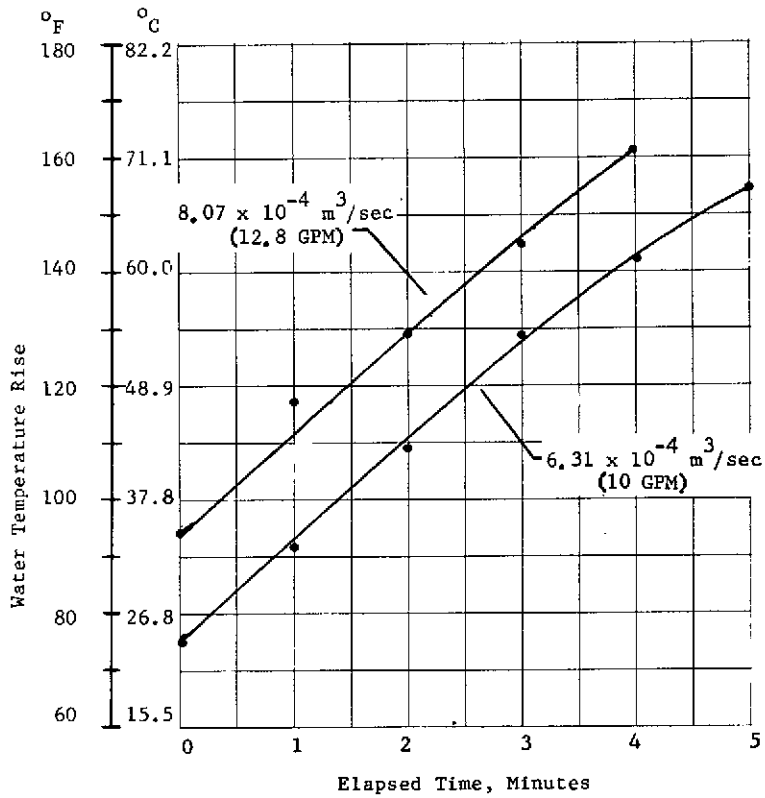

Figure V-12 Temperature Rise

Table V-5 Heat Transfer to Water at Maximum Flow

Time (min)	Inlet Water Temperature °C (°F)	ΔT Each Minute °C (°F)	ΔT Cumulative Each Minute °C (°F)	Watts Input	Heat Transfer to Water	
					Watts Each Minute	Watts Cumulative
0	34.5 (94)	-	-	3128	-	-
1	47.8 (118)	-4.5 (24)	-4.5 (24)	3104	2616	2616
2	53.9 (129)	-11.6 (11)	1.7 (35)	3092	1199	1908
3	62.2 (144)	- 9.5 (15)	10 (50)	3056	1635	1817
4	72.2 (162)	- 7.8 (18)	20 (68)	3024	1962	1853

and a ventilation air velocity of 2.54 m/sec (500 FPM) to 5.05 m/sec (1000 FPM), Figure V-13 shows the cooldown curves of the pump motor and volute and the inlet/outlet water as a function of time.

B. COMPONENT TESTS

Four major components of the regenerative prototype filter unit were tested to determine their individual performance data. These components are the filter (including element, impingement jets, and ΔP indicators), the vortex particle separator, the fluid accumulator, and the fluid disconnects. A total of 30 tests were run on these components. Each component and its accompanying tests are analyzed in the following sections.

1. Filter Component Tests - The filter testing procedure consisted of loading the filter with a known contaminant at an established flow rate and then backflushing the filter at an established flow rate. Figure V-14 shows a schematic of the test hardware. The basic procedure for the tests was to first load a known quantity of AC coarse road dust into the contaminant injection loop, establish a predetermined flow rate into the test filter, and then inject the contaminant. The injections were continued at one or one-half gram increments until a predetermined pressure differential was obtained across the filter. The .45 micron millipore pad was removed and weighed to determine the tare weight of the particles that went through the filter. After the contaminant was loaded, the test filter was backflushed for 5 minutes at a specified flow rate. The particles flushed from the filter element were trapped on the 293 mm diameter, 3.0 micron, millipore pad, thus providing a differential weight needed to determine the cleaning efficiency.

Four performance tests were conducted on the prototype regenerative filter to determine filter element regeneration efficiency. A 20 micron nominal filter element was used and the loading flow rate was 4.29×10^{-4} m^3/sec (6.8 GPM). Backflushing the filter at 7.29×10^{-4} m^3/sec (11.5 GPM) for 5 minutes obtained regeneration efficiencies ranging from 90.8 to 95.0%. The test results are summarized in Table V-6. The loading curves of the filter after each test are shown on Figure V-15. According to these curves the filter is being cleaned to very nearly its original condition or better each time.

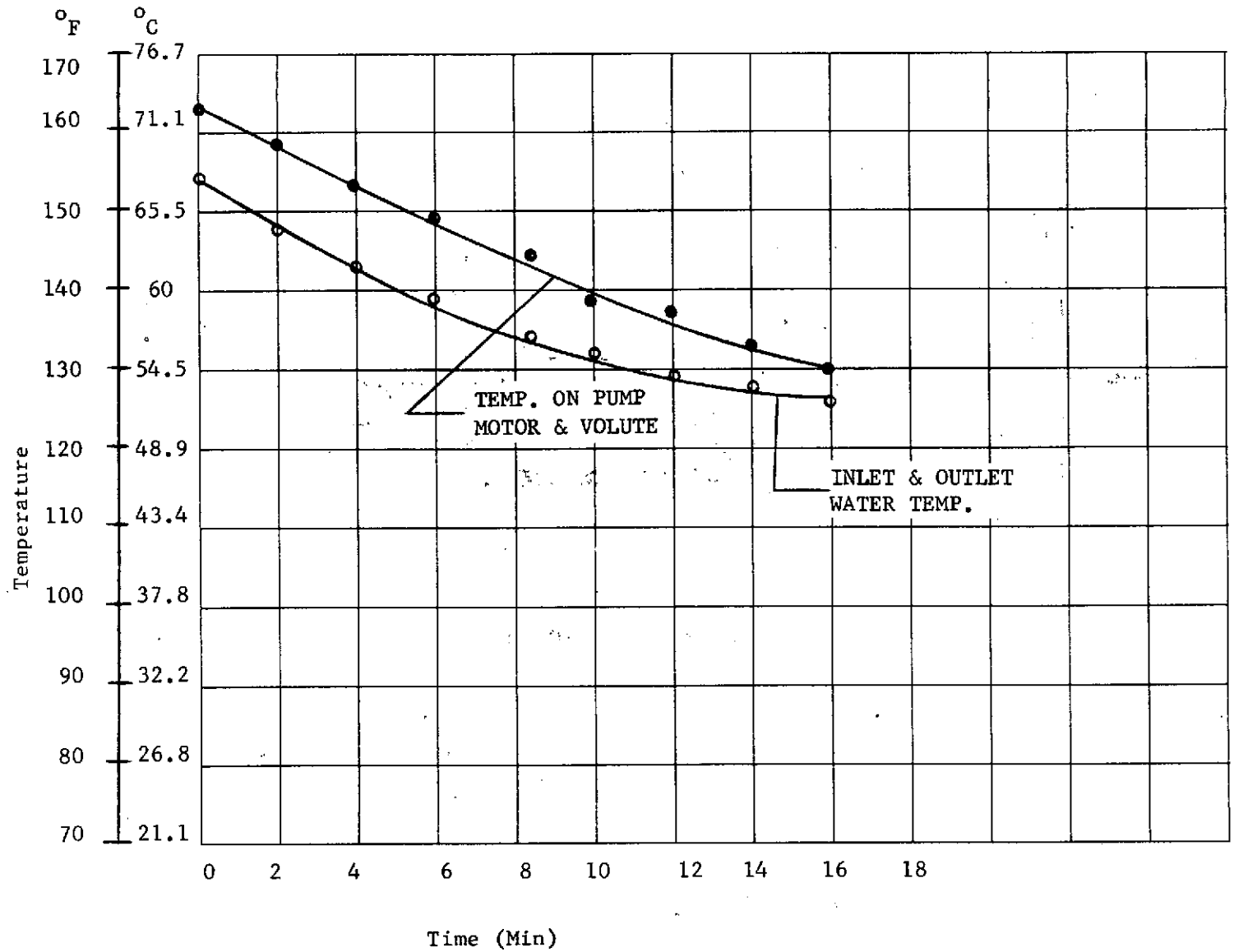

FIGURE V-13 TEMPERATURE COOLDOWN

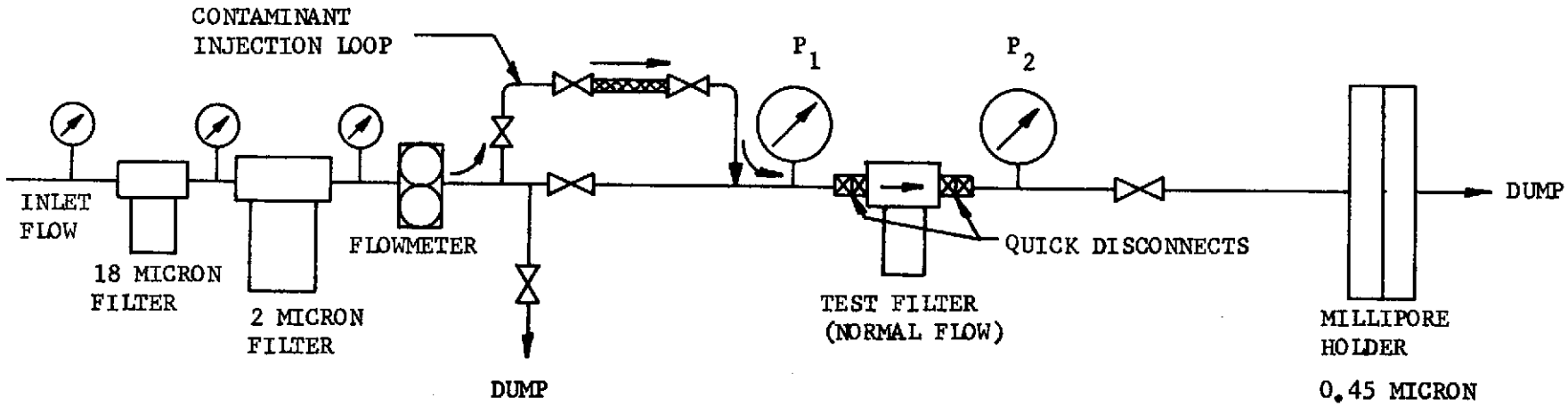

FILTER LOADING - NORMAL FLOW

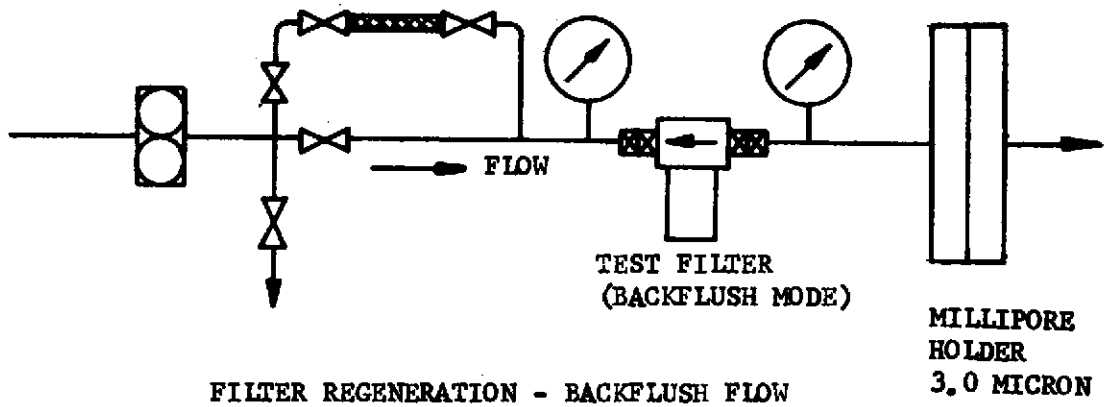

FILTER REGENERATION - BACKFLUSH FLOW

FIGURE V-14 FILTER TEST SYSTEM - SCHEMATIC

Table V-6 Filter Backflush Performance Test Results

Test Number	Total Added to System	Contaminant Added		Contaminant Removed			Regeneration Efficiency
		Recovered on Millipore	Retained on Filter Element	5-Minute Backflush on Millipore	Washed from Filter Bowl	Net Contaminant Removed	$EFF = \frac{F}{C}$
	A	B	C = A-B	D	E	F = D+E	
-023	5.6800	.3829	5.2971	3.3513	1.4590	4.8103	90.8%
-024	7.3720	.4607	6.9113	3.6850	2.8785	6.5635	95.0%
-025	6.3370	.3565	5.9805	2.7975	2.7886	5.5861	93.4%
-026	5.7502	.3202	5.4300	1.9249	3.1788	5.1037	94.0%

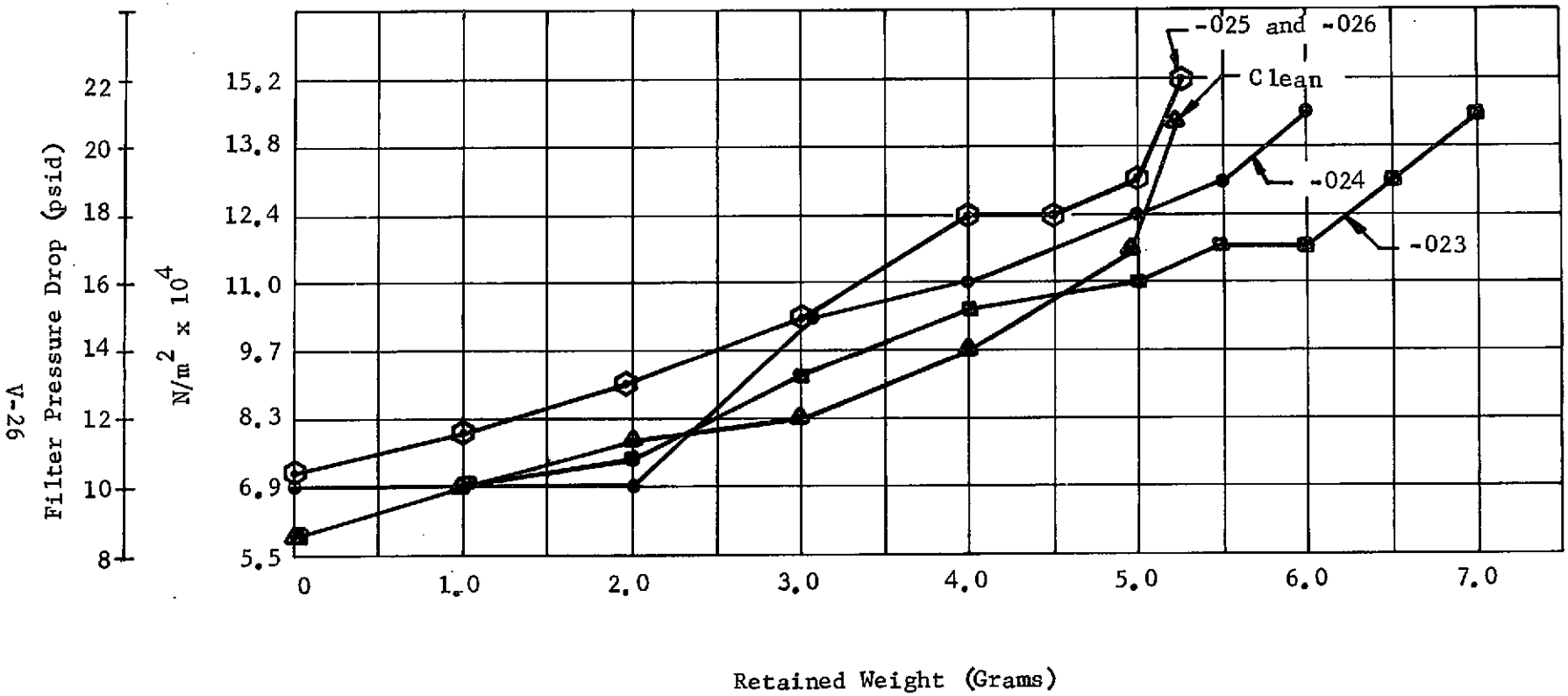

FIGURE V-15 DIRT CAPACITY - BACKFLUSH PERFORMANCE TESTS

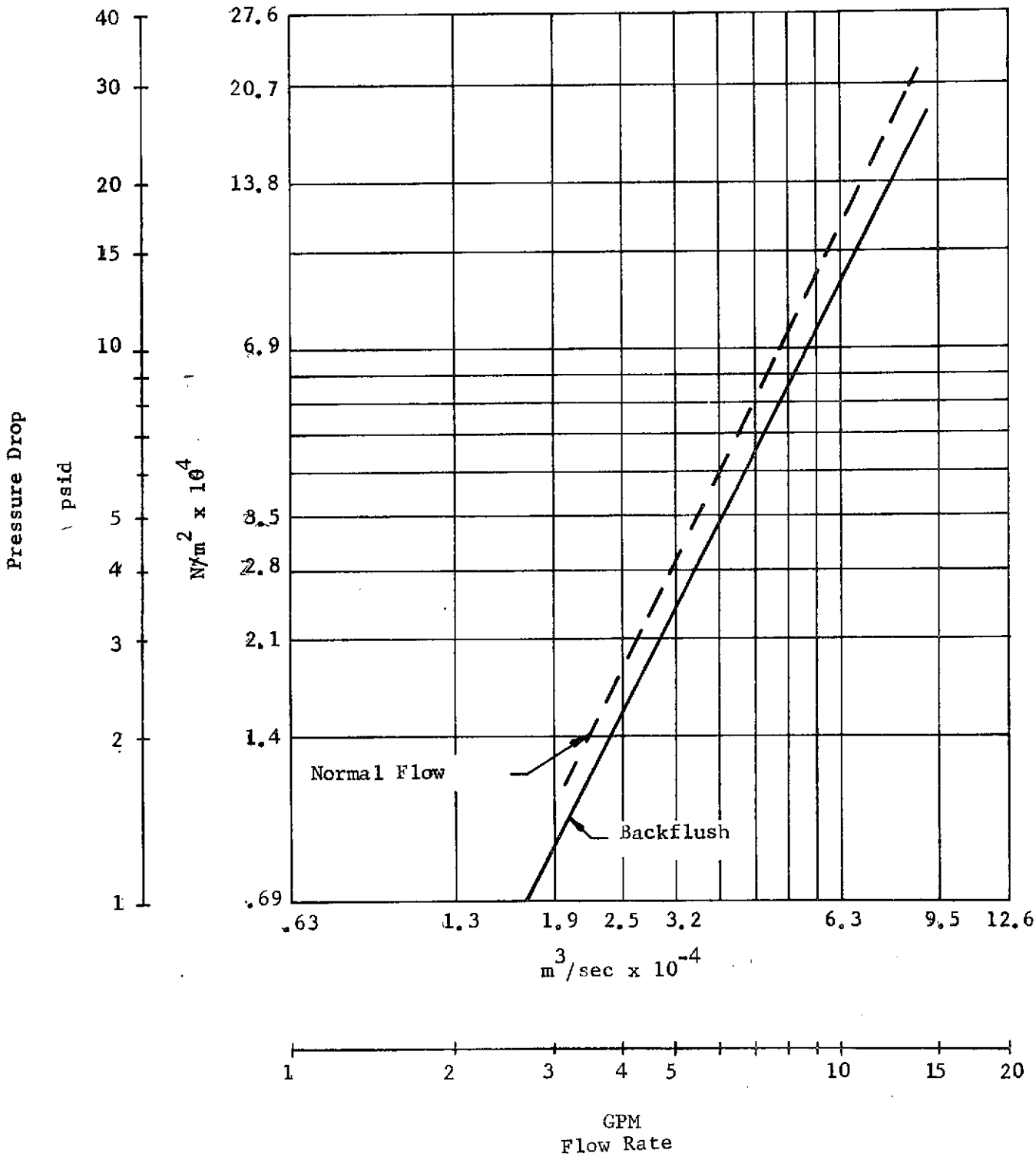

FIGURE V-16 FLIGHT PROTOTYPE FILTER PRESSURE DROP, WITH DISCONNECTS

The pressure drop for the flight prototype filter, with disconnects, is shown in Figure V-16 for the normal and backflush modes of flow. For comparison purposes, the pressure drop of the development regenerative filter is shown on Figure V-17. The development filter curve is for the filter without disconnects. The ΔP of the disconnects at 6.31×10^{-4} m^3/sec (10 GPM) are as follows:

Coupler to Nipple - 5.61×10^4 N/m^2 (8.0 psid)

Nipple to Coupler Flow - 4.27×10^4 N/m^2 (6.2 psid)

Therefore, by subtracting the pressure drop of the disconnects, it can be seen that the pressure drop of the flight prototype filter is 2.21×10^4 m^3/sec (3.2 psid) lower than that for the development regenerative filter. The reduction in ΔP of the prototype filter is a result of enlarging the inlet and outlet, and optimizing the flow design characteristics within the unit. Therefore, it is concluded the prototype is a cleaner, more efficient design than that used for the development tests.

2. Separator Component Tests - There were a total of six efficiency tests conducted on the prototype separator. The tests were conducted by injecting a known amount of contaminant through the separator and collecting the effluent that passed through it on a .45 micron millipore pad. Figure V-18 illustrates the test set-up.

The basic test procedure consisted of injecting AC coarse road dust in one gram increments, varying from 2 to 5 grams on each test. The injection was conducted at 7.29×10^{-4} m^3/sec (11.5 GPM) to simulate the backflush tests. The contaminant was recovered and weighed from the separator trap and the effluent millipore pad. Recovery and separator efficiencies were then calculated. The recorded data and efficiencies are shown in Table V-7.

Test number 032 shows a low efficiency (81.9%) as well as low recovery of contaminant (86.9%). The low recovery indicates that a test error had occurred which, in turn, caused the low separator efficiency. Therefore, discounting this particular test the overall average separator efficiency was 85.4% on the prototype unit. The prototype separator trap design is an extension of the development separator trap testing. There were several trap designs tested during the development tests, and the best design was selected for the prototype unit. The

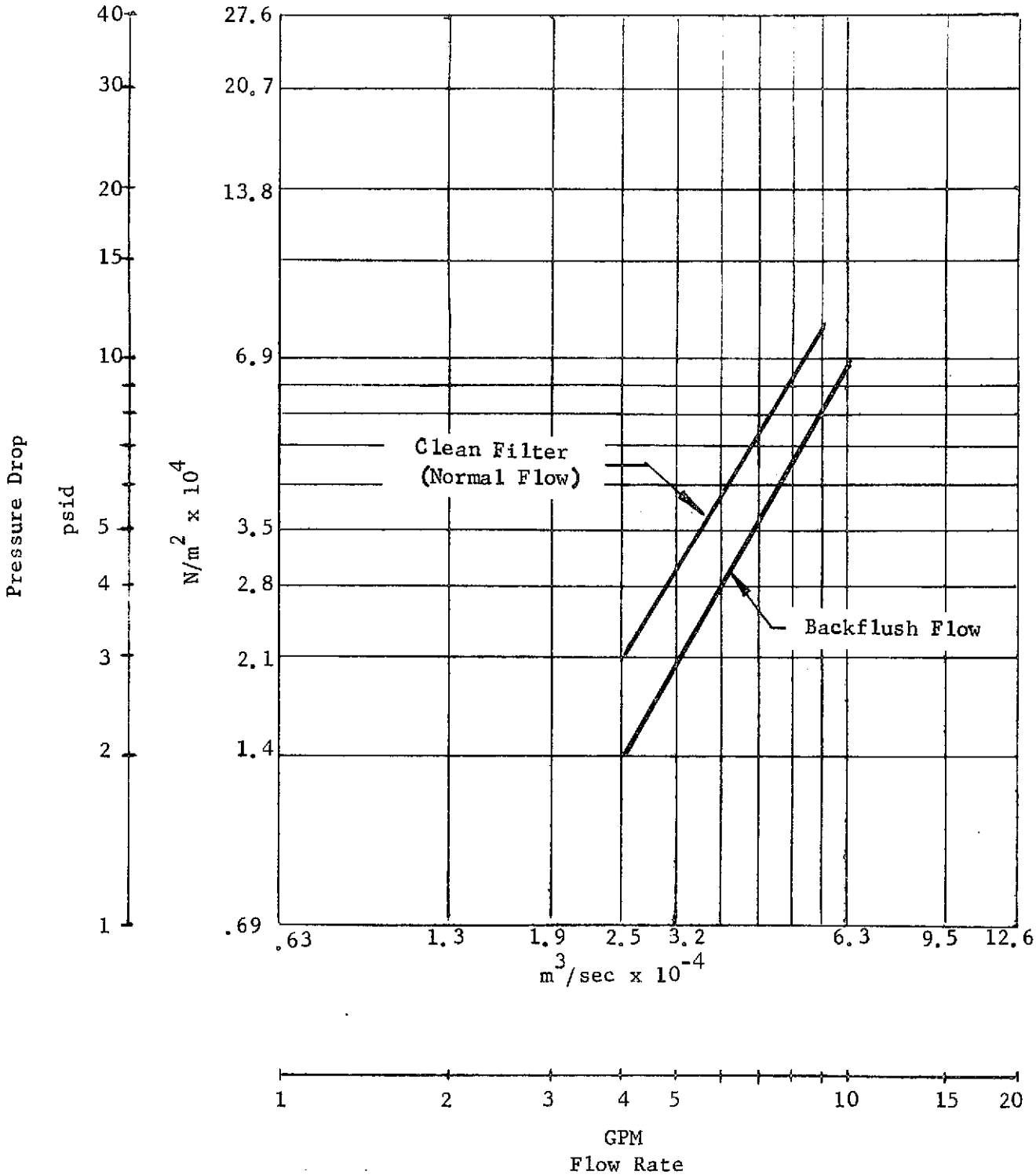

FIGURE V-17 DEVELOPMENT FILTER PRESSURE DROP WITHOUT DISCONNECTS

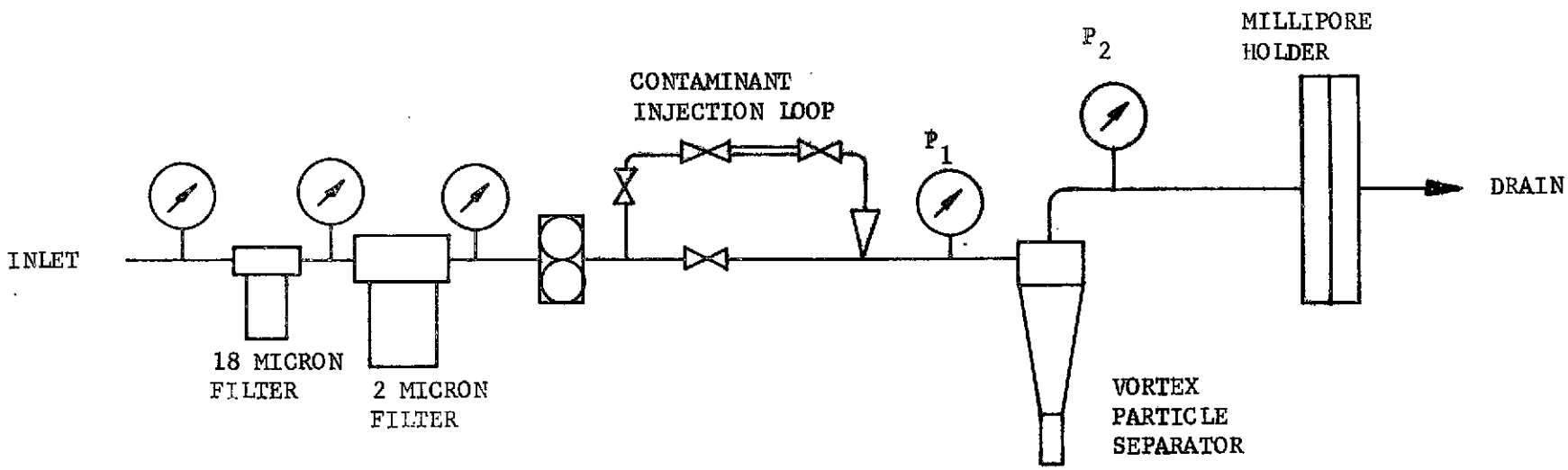

FIGURE V-18 VORTEX PARTICLE SEPARATOR TEST SCHEMATIC

Table V-7 Flight Prototype Particle Separator Performance Tests

Test Number	Flow Rate m^3/sec (GPM)	Total Contaminant Added	Passed Through Separator	Retained In Trap Bowl	Recovery Efficiency	Separator Efficiency
		A	B	C	(B+C)/A	Eff = C/A
032	7.29×10^{-4} (11.5)	5.0585	.2522	4.1454	86.9%	81.9%
033	7.29×10^{-4} (11.5)	2.0596	.3107	1.7384	99.5%	84.4%
034	7.29×10^{-4} (11.5)	2.0783	.3107	1.7585	99.6%	84.6%
036	7.29×10^{-4} (11.5)	4.1986	.5048	3.5600	96.8%	84.8%
037	7.29×10^{-4} (11.5)	4.2585	.5349	3.6892	99.3%	86.6%
038	7.29×10^{-4} (11.5)	4.1518	.4849	3.5984	98.4%	86.7%

development separator trap that was selected averaged 86.5% on a total of five tests. Comparing this to the 85.4% for the prototype indicates a consistency in the design. The flight prototype vortex particle separator is shown in Figure V-19 in the disassembled mode.

At the beginning of the vortex particle separator tests, tests were conducted to determine the pressure drop of the separator at various flow rates. Figure V-20 shows the pressure drop of the flight prototype vortex separator. For comparison, the pressure drop for the development vortex particle separator and is presented in Figure V-21. By comparing the two at a given flow rate of 6.31×10^{-3} m^3/sec (10 GPM) it can readily be seen that the prototype separator is a cleaner type design as far as ΔP is concerned. The development separator ΔP at 6.31×10^{-3} m^3/sec (10 GPM) was 30.33×10^4 N/m^2 (44 psid) whereas the flight prototype was 17.92×10^4 N/m^2 (26 psid) at the same flow rate. The decrease in pressure drop was achieved by increasing the port sizes of the inlet and outlet of the prototype separator. Straightener vanes were also added to the outlet to direct the flow more evenly thus reducing backflow type characteristics.

It was found that the separator trap bowl holds approximately 17 grams of contaminant before reaching the bottom of the injector. The length of the bowl was the determining factor in this case, and could be lengthened if necessary. The "O"-ring seal on the lexan bowl sealed perfectly under all testing, however, care must be taken to keep the "O"-ring groove free of contaminant.

3. Accumulator Component Tests - The regeneration unit develops a significant amount of heat during its operating cycle. It was therefore concluded that an accumulator was necessary as a heat sink to maintain thermal control during the operating cycle. In addition, the accumulator serves to maintain a positive pressure on the pump and make-up any fluid losses. The design of the accumulator was such as to allow sufficient mixing and passage of the water to accomplish this basic task. The testing that was conducted on the accumulator was to develop this design concept.

A plexiglass flow model of the accumulator, Figure V-22, was constructed and tested for its ΔP and flow mixing qualities. The accumulator flow model also provided a mockup to test the extended and nonextended positions of the bellows located in

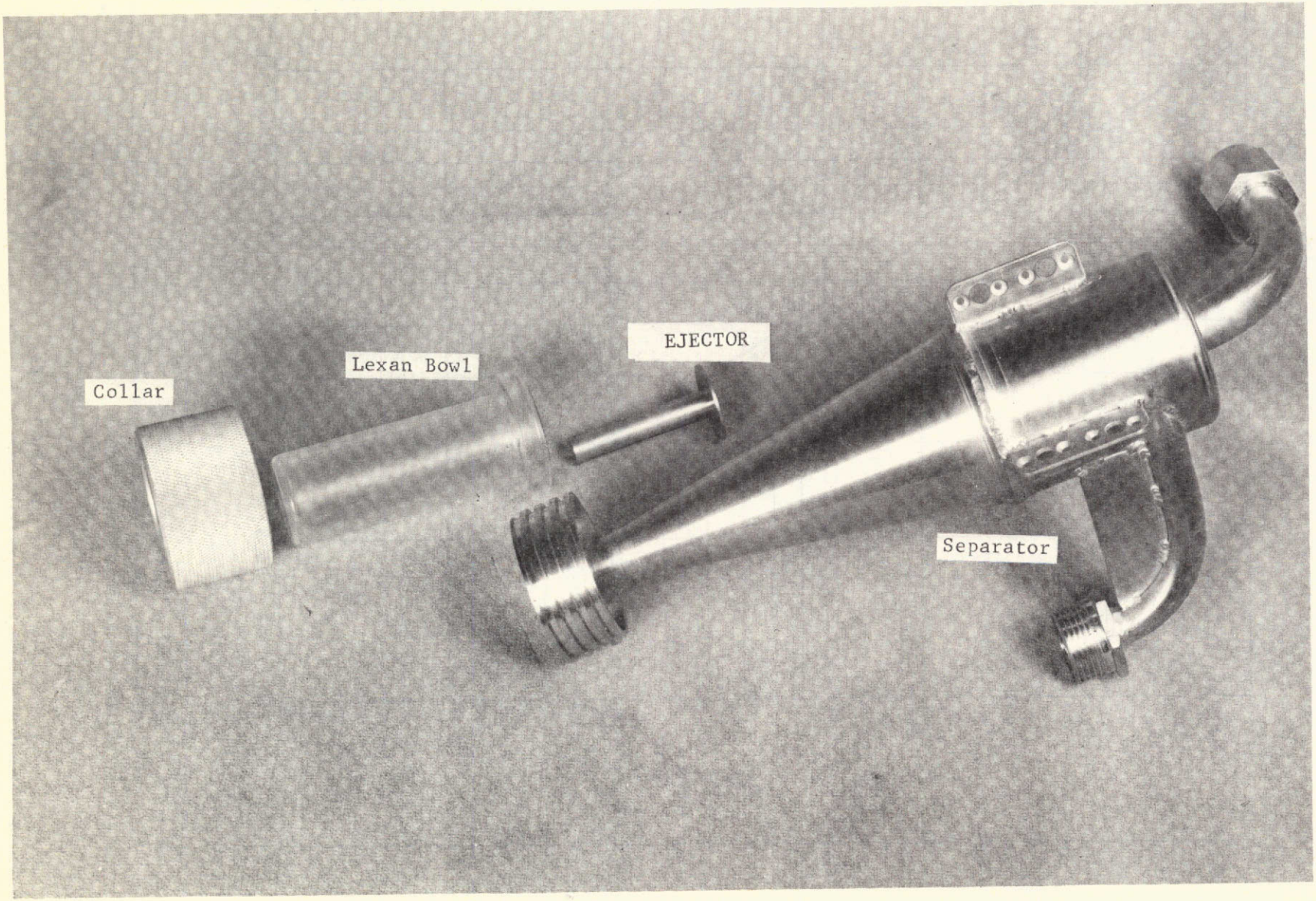

Figure V-19 Vortex Particle Separator - Disassembled

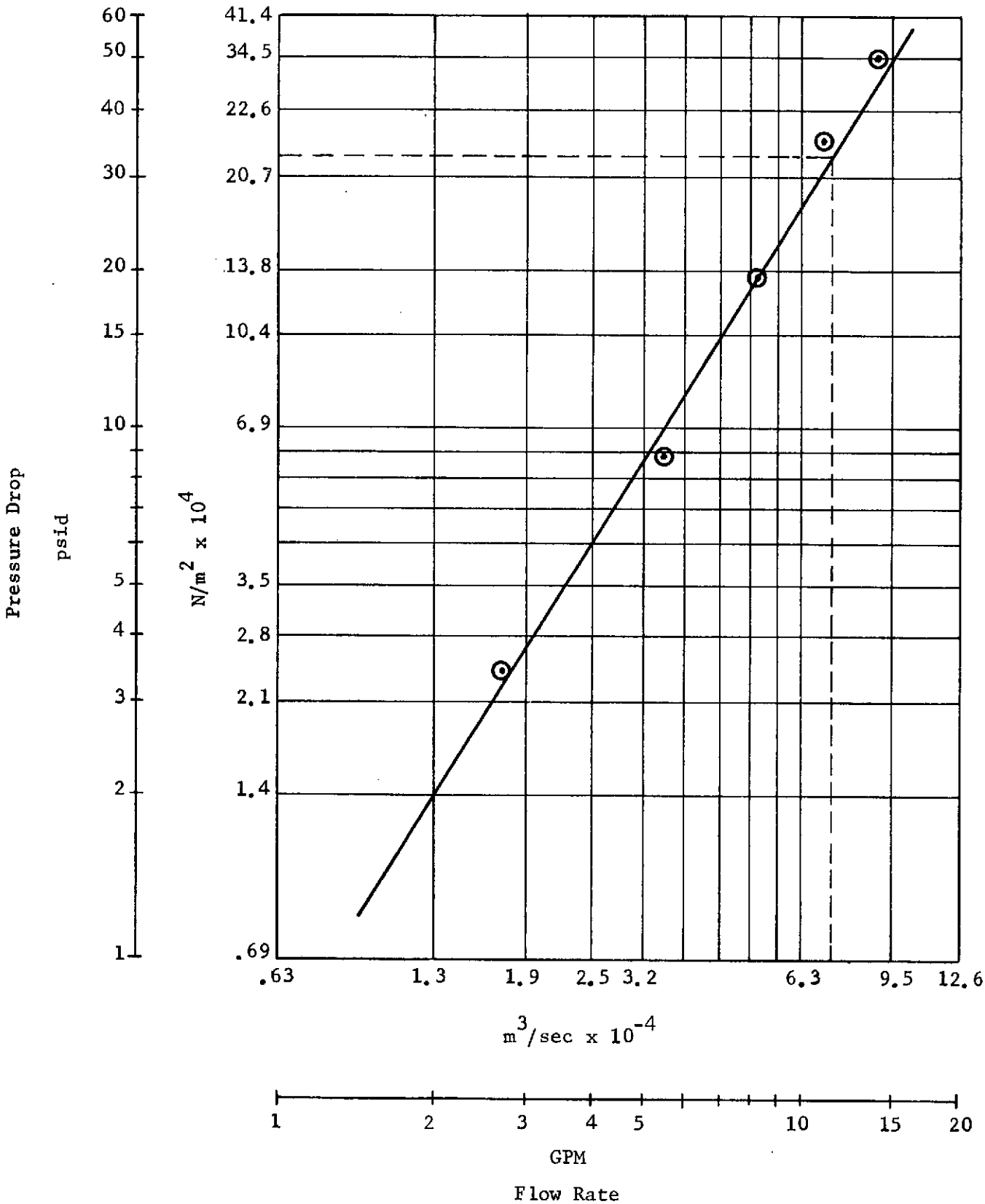

FIGURE V-20 FLIGHT PROTOTYPE SEPARATOR PRESSURE DROP

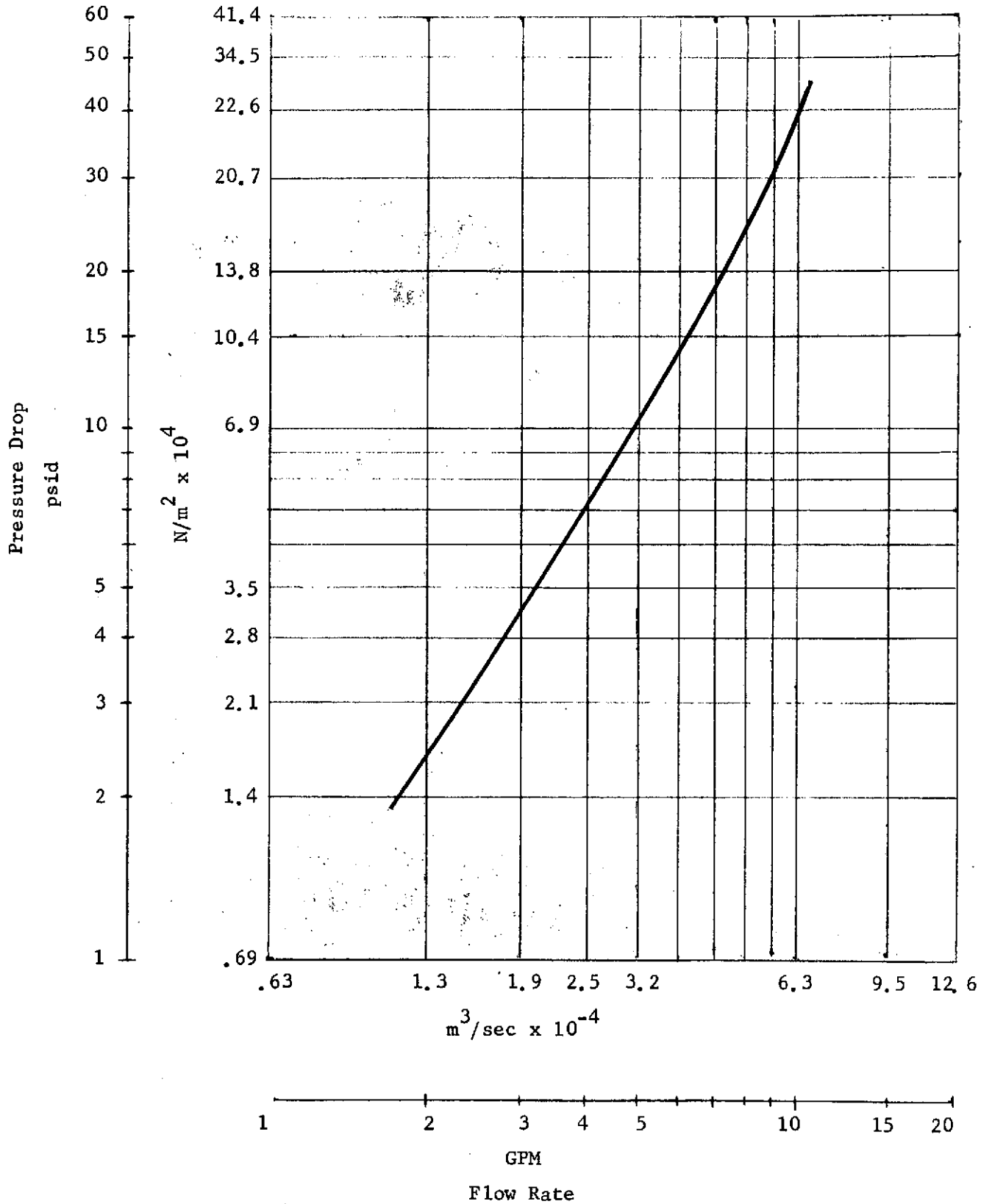

FIGURE V-21 DEVELOPMENT SEPARATOR PRESSURE DROP

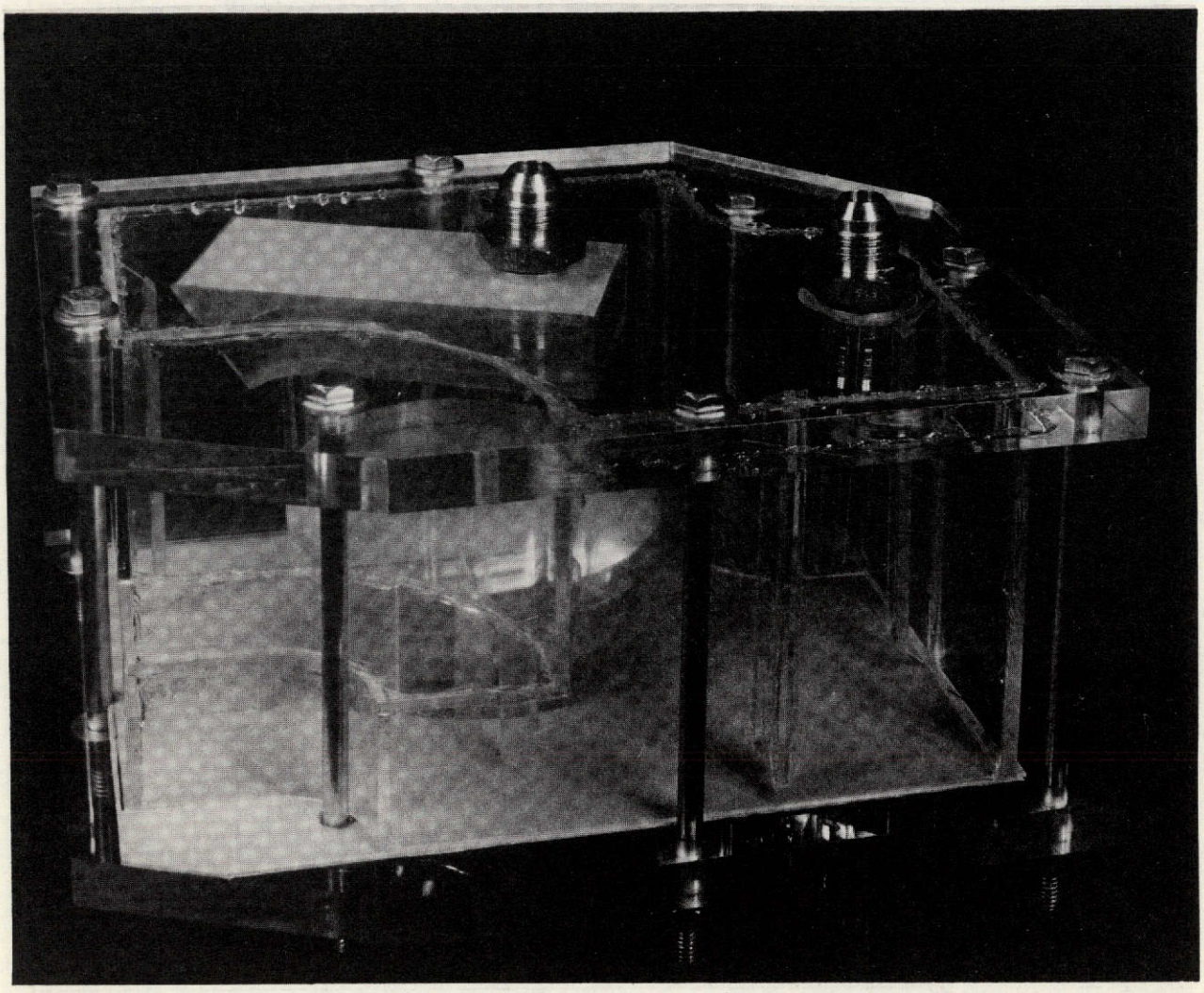

FIGURE V-22 PLEXIGLASS FLOW MODEL ACCUMULATOR

the accumulator. On the flight prototype unit this bellows is precharged to 10.34×10^4 N/m^2 (15 psig) and has an operating pressure of 24.13×10^4 N/m^2 (35 psig). The bellows is used to maintain constant unit pressure if small leakage occurs during connecting and disconnecting the filters to the unit.

The pressure drop for the plexiglass accumulator model is shown in Figure V-23 for both the normal position of the bellows and the fully extended bellows. At a flow rate of 6.31×10^{-4} m^3/sec (10 GPM) the pressure drop of the prototype accumulator was expected to be 5.51×10^4 N/m^2 (8.0 psid) for the bellows positioned in the normal configuration and 6.62×10^4 N/m^2 (9.6 psid) for the fully extended position.

Figure V-24 illustrates the pressure drops of the flight prototype accumulator for various flow rates. The tare ΔP was first taken of the system and then subtracted from actual ΔP readings to obtain the values reflected by the graph. As can be noted the ΔP at 6.31×10^{-4} m^3/sec (10 GPM) is 2.62×10^4 N/m^2 (3.8 psid) for the extended bellows and 2.41×10^4 N/m^2 (3.5) for the bellows in the normal position. These values are far below the expected values. It was concluded that the decrease in pressure drop was due to the clean design because of the flight prototype unit as compared to the plexiglass model. The amount of fluid change out versus time was checked on the accumulator model. Food dye, mixed in with the accumulator water, was used to visually record the time it took to completely change out the water in the accumulator. At a flow rate of 4.31×10^{-4} m^3/sec (6.8 GPM) the water was completely changed out in 20 seconds. Since this figure was very acceptable, and the prototype is of a better design, it was concluded the prototype unit accumulator would serve as a good heat sink. This conclusion was proven in the system tests and thermal tests.

4. Fluid Disconnect Tests - During development testing, several commercially available fluid quick disconnects were evaluated for both performance in one-g and crewman usage in zero-g. This evaluation benefited the design of the flight prototype unit which uses four such disconnects.

Evaluation testing was performed on five fluid quick disconnects: a Parker Corporation disconnect (SSH4-62), a Hansen Corporation disconnect (4-HK), a Aeroquip Corporation disconnect (P/N 3205-8/3202-8), a E. C. Wiggins, Inc. (EC 250B8/EC255B8), and a Seaton-Wilson disconnect (P/N 2-1452/1453-8). The following is an evaluation of each of these disconnects.

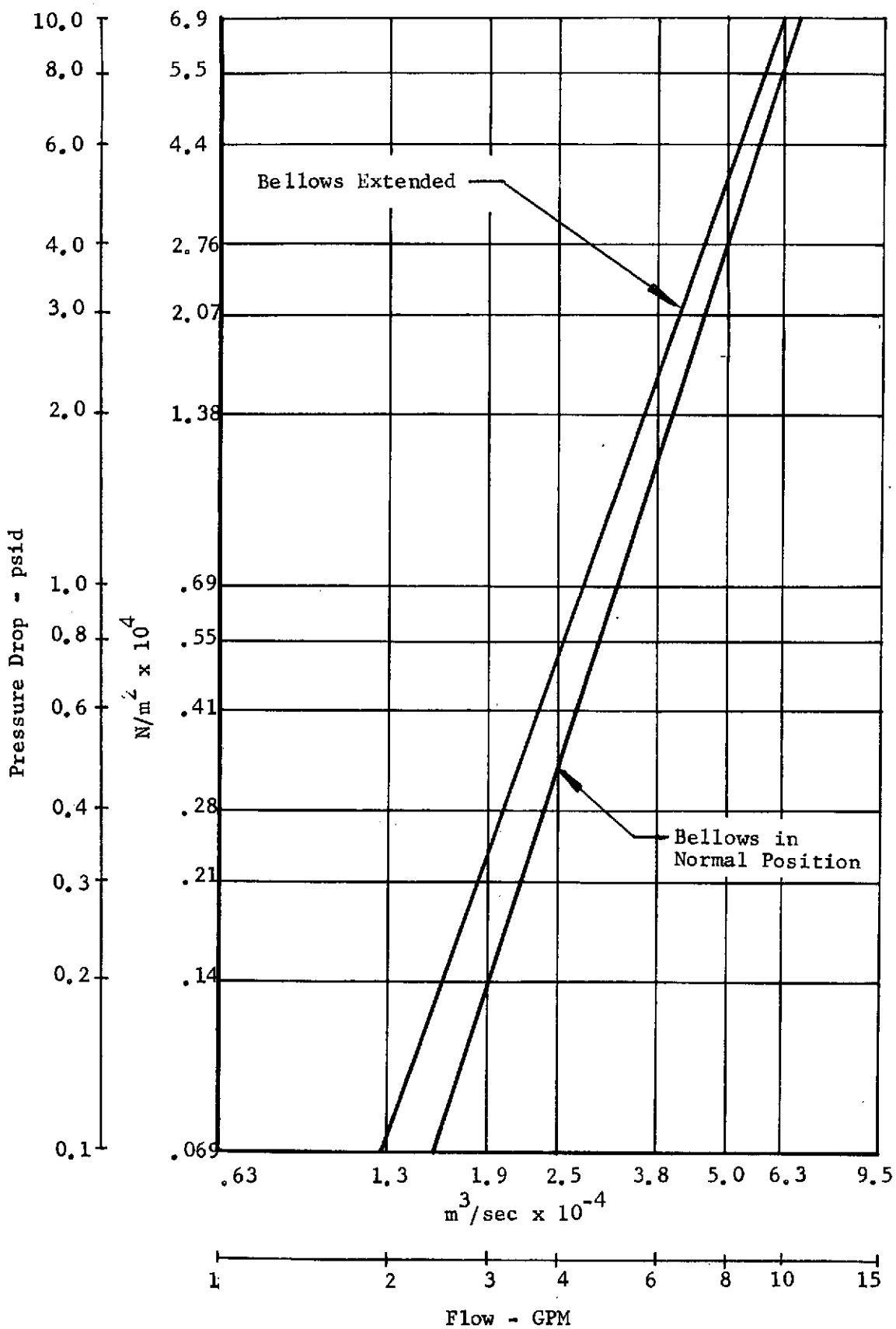

FIGURE V-23 ACCUMULATOR PRESSURE DROP - PLEXIGLASS MODEL

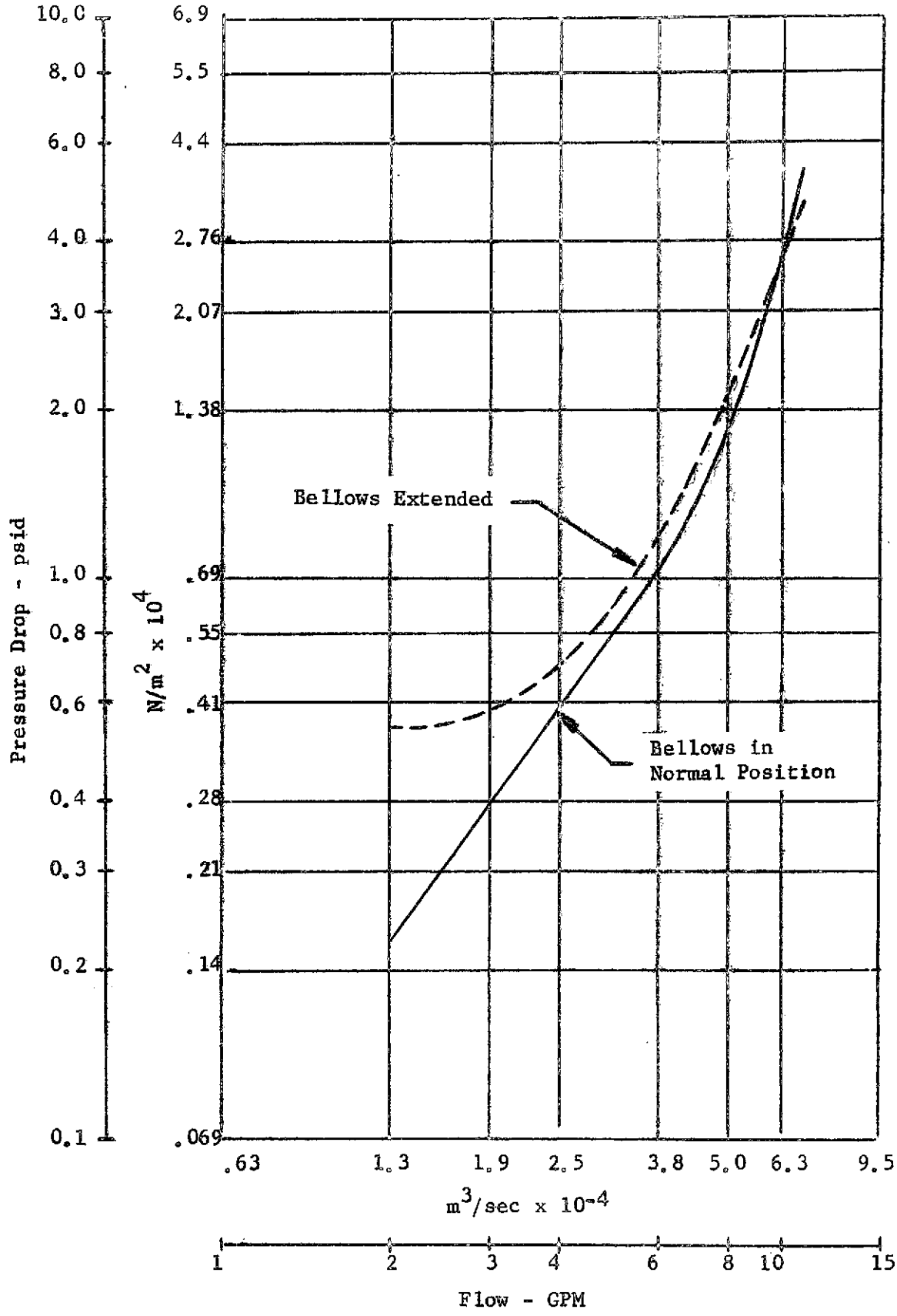

FIGURE V-24 ACCUMULATOR PRESSURE DROP - FLIGHT PROTOTYPE

The Parker disconnect had high rates of leakage during connection, high values for air inclusion, and was difficult to connect under pressure. This disconnect was not considered to be satisfactory for the application required in this program.

The Hansen disconnect did not exhibit any leakage during connection and had less spillage and air inclusion than did the Parker disconnect. Connection at 27.58×10^4 N/m^2 (40 psig) presents no real problems in terms of force application. At 34.47×10^4 N/m^2 (50 psig) it became more difficult to connect and the use of a 90 degree elbow (or tube tee) is recommended so that the force can be more efficiently applied to the connection operation. The pressure drop for the Hansen disconnect is quite high, 13.10×10^4 N/m^2 at 6.31×10^{-4} m^3/sec (19psid at 10 GPM), and is more than double that of the Parker disconnect.

The Wiggins disconnect exhibited considerable spillage (spraying) during connection and also during a disconnect test that was conducted at 68.94×10^4 N/m^2 (100 psi). The disconnect was relatively easy to connect, but required more force to disconnect. A two-handed operation was required for disconnect. The outside envelope of this disconnect was the smallest tested. The pressure drop at 6.31×10^{-4} m^3/sec is 18.61×10^4 N/m^2 (10 GPM is 27 psid) which was the highest pressure drop recorded for the five disconnects.

The Aeroquip disconnect uses a different technique for connection than the other disconnects tested. Connection is accomplished by a one-handed twisting action that drives the disconnect sleeve up an Acme thread arrangement. Disconnect is accomplished by pulling the sleeve back, as is common to other disconnects. Connect and disconnect forces were the lowest of any disconnect tested even at pressures of 68.94×10^4 N/m^2 (100 psig). It is expected that the twist-to-connect action would also be easier in a zero-g environment than a push-to-connect action. Leakage, spillage, and air inclusion were all zero. The pressure drop 11.03×10^4 N/m^2 at 6.31×10^{-4} m^3/sec (16 psi at 10 GPM) was relatively good and was the second lowest pressure drop of the five disconnects tested. This disconnect has the best characteristics of any of the disconnects tested.

The Seaton-Wilson disconnect requires a push-on and pull-off operation. It had a very smooth operation at zero pressure. However, as the pressure increased, the

push-on force became greater where at 27.58 to 41.36 x 10^4 N/m^2 (40 to 60 psig) two hands were required to easily connect it. At 68.94 x 10^4 N/m^2 (100 psig) the force required was excessive and some spraying occurred. The disconnect forces were very nominal, and uniform at a pressure of 68.94 x 10^4 N/m^2 (100 psig) the coupler could be removed with one hand by releasing the sleeve with the forefinger and middle finger. The envelope of the disconnect is smaller than the Aeroquip disconnect, but slightly larger than the Wiggins. There was no leakage or spillage except for wetted surfaces on the poppets. There was no measurable amount of air inclusion and the pressure drop was comparable to the Aeroquip disconnect.

A summary of test data for all five quick disconnects is given in Table V-8 and Figure V-25. The Aeroquip and Seaton-Wilson disconnects were selected for the zero-gravity tests because of their superior characteristics as compared to the other three. The Parker and Hansen disconnects were disregarded because of their excessive spillage and air inclusion. The Wiggins was eliminated because of spillage and excessive pressure drop.

Zero-g performance tests were conducted on the Aeroquip and Seaton-Wilson disconnects in order to determine the type most acceptable for use in the flight prototype filter regeneration system. During the zero-g test, both types were connected and disconnected at pressures of 34.47 to 37.92 x 10^4 N/m^2 (50 to 55 psig). It was observed that the Seaton-Wilson was difficult to connect at pressures approaching 41.36 x 10^4 N/m^2 (60 psig). The disconnect operation for both was a pull action. Due to the difficulty of connection of the Seaton-Wilson quick disconnect at higher pressures, the Aeroquip quick disconnect was considered most acceptable for use in the filter regeneration system.

The Aeroquip disconnects were used on the prototype filter regeneration unit, however the development tests used 1.27 cm (1/2 inch) disconnects while the prototype unit employed 1.59 cm (5/8 inch) disconnects. In order to see the gain in value of changing to the larger size disconnect, a ΔP curve for these disconnects is shown in Figure V-26. By comparing the two at

Table V-8 - Summary of Fluid Disconnect Test Data

	Parker SSH4-62/63		Hansen 4-HK		Wiggins EC250B8/EC255B8		Aeroquip 3205-8/3202-8		Seaton-Wilson 2-1452/1453-8	
	27.6×10^4 N/m^2 (40 psig)	41.4×10^4 N/m^2 (60 psig)	27.6×10^4 N/m^2 (40 psig)	41.4×10^4 N/m^2 (60 psig)	27.6×10^4 N/m^2 (40 psig)	41.4×10^4 N/m^2 (60 psig)	27.6×10^4 N/m^2 (40 psig)	41.4×10^4 N/m^2 (60 psig)	27.6×10^4 N/m^2 (40 psig)	41.4×10^4 N/m^2 (60 psig)
Leakage during connection	Excessive*	Excessive*	Zero	Zero	1.0-6.0*	1.0-6.0*	Zero	Zero	Zero	Zero
Air inclusion, ml	5.0	9.5	2.8	3.3	Negligible		Zero	Zero	Zero	Zero
Spillage during disconnect, ml	2.2	2.8	1.0	2.5	0.1	0.1	Zero	Zero	Zero	Zero
Leakage when connected	Zero	Zero	Zero	Zero	Zero	Zero	Zero	Zero	Zero	Zero
Force to connect	Max. limit of capability	Very difficult	Satisfactory	More difficult	Easy with one hand	Easy with one hand	Very easy with one hand	Very easy with one hand	Very easy	Easy
Force to disconnect	Easy	Easy	Easy	Easy	Easy	Easy	Easy	Easy	Very easy	Very easy
Pressure Drop @6.3×10^{-4} m^3/sec (10 GPM)	6.34×10^4 N/m^2 (9.2 psid)		18.61×10^4 N/m^2 (27.0 psid)		18.61×10^4 N/m^2 (27.0 psid)		11.03×10^4 N/m^2 (16.0 psid)		11.03×10^4 N/m^2 (16.0 psid)	

*Spraying occurred during connection.

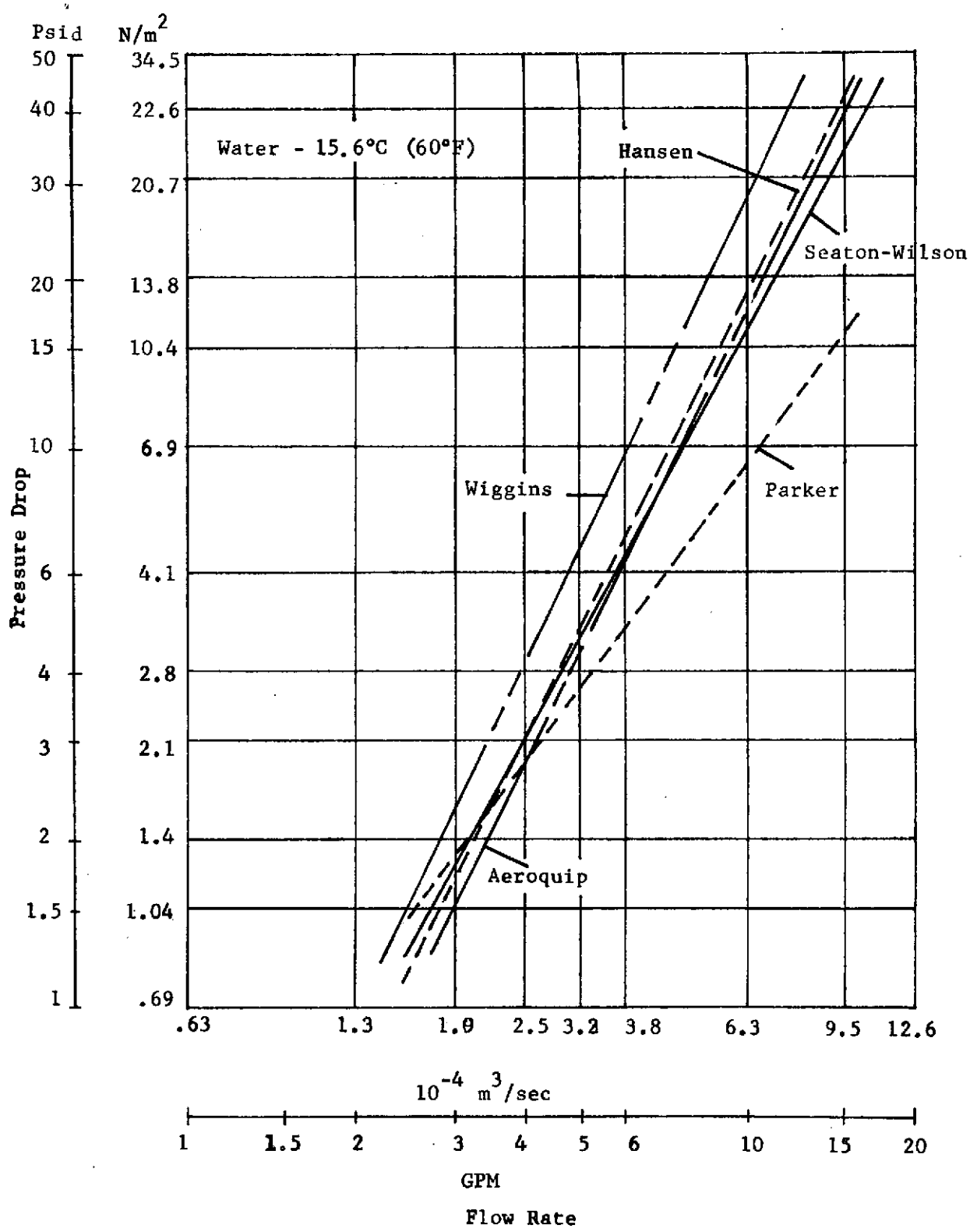

Figure V-25 Quick Disconnect Pressure Drop Data

6.31×10^{-4} m^3/sec (10 GPM) it can be seen that the 1.27 cm (1/2 inch) Aeroquip disconnect has a total pressure drop of 117.20×10^3 N/m^2 (17 psid) whereas the 1.59 cm (5/8 inch) Aeroquip has a 41.36×10^3 N/m^2 (6 psid) ΔP in the nipple to coupler flow direction and 51.15×10^3 N/m^2 (8 psid) ΔP in the coupler to nipple flow direction.

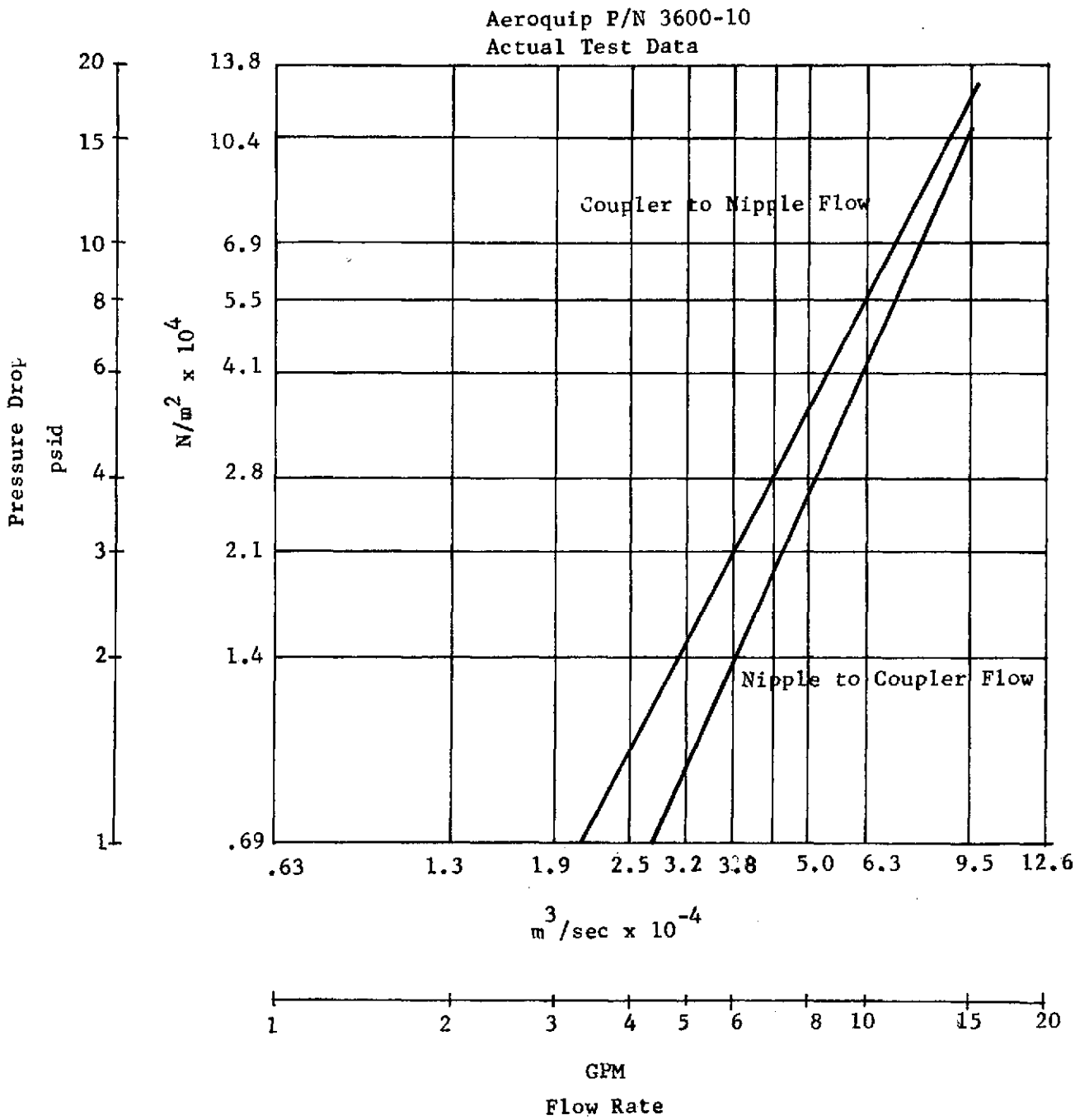

Figure V-26 Pressure Drop-Aeroquip Quick Disconnect

5. Filter Bubble-Point Tests - The bubble-point tests were used to monitor the deterioration, if any, of the individual filter elements used throughout the flight prototype regenerative filter testing program. Bubble-point tests as conducted during this program measure the pressure required to force a gas bubble through the largest pore of a filter element. Using conversion data the Standard Bubble-Point Pressure (P_s) in inches of water was obtained for each test filter element at various pertinent times throughout the testing program. By comparing the pressure of a clean filter to that same filter's pressure after loading and subsequent cleaning it can be subjectively determined if the pore size of that filter has enlarged, or in other words deteriorated. It must be realized, however, that bubble-point tests are only reproducible to within $\pm$ 0.254 cm (0.1 in) and accurate within $\pm$ 0.508 cm (0.2 in) water pressure.

Equipment used for the bubble-point tests and the schematic setup are shown in Figure V-27. Also used in conjunction with the test apparatus shown was a thermometer, range 0°C (32°F) to 37.8°C (100°F), and a 15.24 cm (6 in) steel scale graduated in .076 cm (.03 in) increments.

The procedure for the bubble-point tests was to insert the gas injector nozzle into the filter element immersed in the alcohol. The bleed valve was opened to allow complete filling of the element with the fluid. The element was then immersed approximately 1.27 cm (0.5 in) below the surface of the fluid.

The gas pressure was then slowly increased by means of the pressure adjusting valve, the regulator was set at 172.4×10^3 N/m^2 (25 psig) until the first continuous stream of bubbles appeared. Mechanical vibration or jarring of the test element was avoided to prevent upsetting bubble equilibrium which causes erroneous low pressure readings. The element was rotated to allow the pore to be at a point nearest the surface.

The gas pressure was then shut off and the bleed valve opened. The steps for gas pressurization to find the first bubble stream were repeated in order to check the first results. If the results were the same, the pressure was recorded to the nearest 0.254 cm (0.1 in) of water on the manometer. The distance from the pore to the surface of the fluid was measured to the nearest 0.15 cm (0.06 in) and recorded. The temperature of the fluid to the nearest °F was measured and recorded.

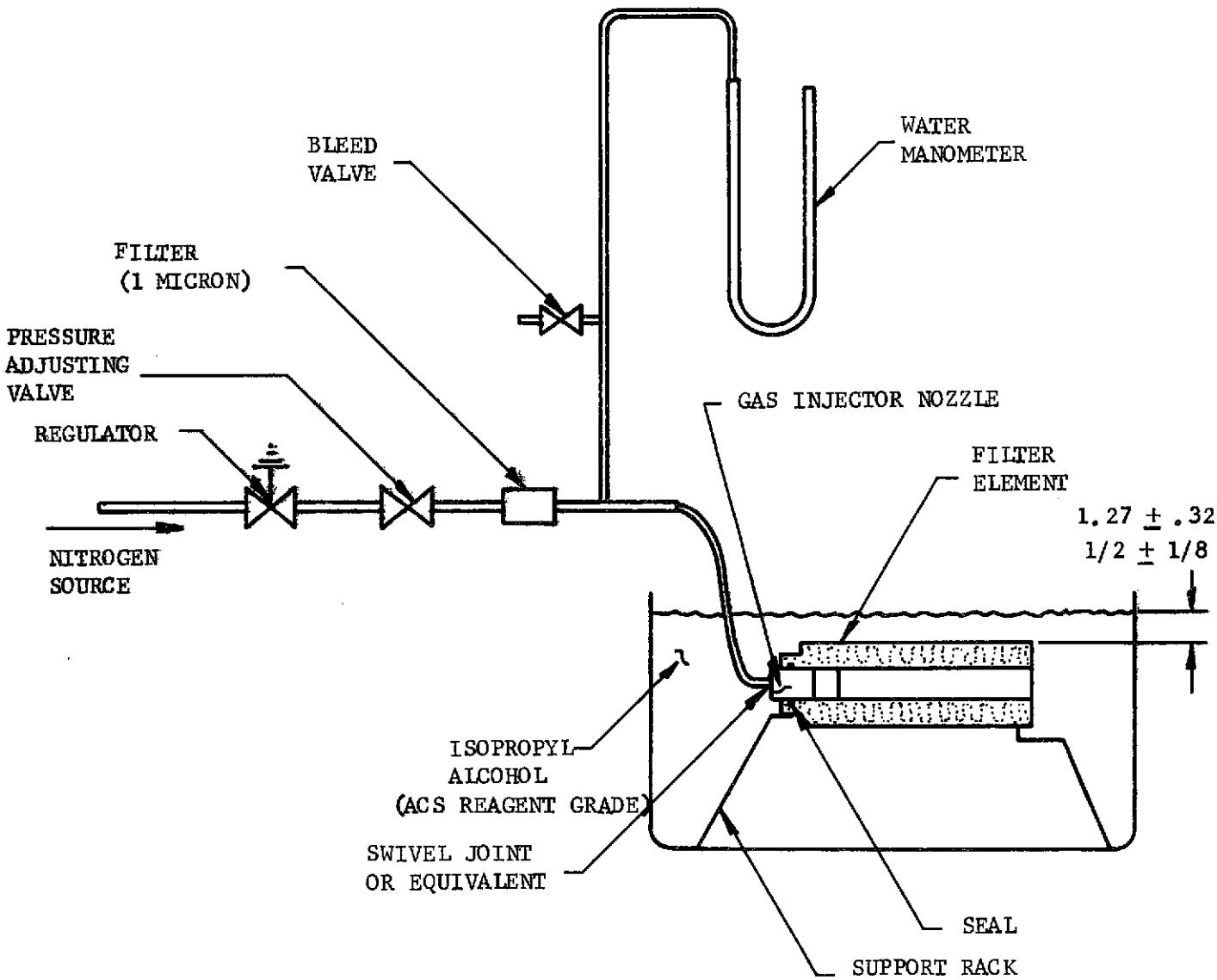

FIGURE V-27 BUBBLE-POINT TEST APPARATUS

Next the "boil-all-over" point was determined by the following procedure. After the preceding procedure data was recorded the gas pressure was slowly increased to a point where a general over-all-boiling point occurs. The pressure was recorded to the nearest 0.254 cm (0.1 in) of water and the depth of immersion and the temperature were recorded.

Also, the stabilization pressure was determined as follows. The pressure adjusting valve was closed after "boil-all-over". When the filter stopped bubbling the pressure was again recorded to the nearest 0.254 cm (0.1 in) of water. The depth of immersion and temperature were recorded. After this the bleed valve was opened and the next filter element was readied for the same procedure.

In order to convert the data taken into Standard - Bubble - Point Pressure it was necessary to correct for test liquid temperature variation and depth of immersion by the use of the following formula:

$$P_s = \frac{21.15\ (P-dh)}{S}$$

P_s = Standard Bubble - Point Pressure (inches of water)

P = Measured Pressure (in inches of water)

S = Surface Tension of Test Liquid (Refer to Figure V-28)

d = Density of Alcohol (Refer to Figure V-29)

h = Submersion Depth of Area from which first bubble eminated, in inches

Figure V-30 shows the data taken at various times throughout the testing program. Filters number 5 thru 10 have a rating of 20 microns nominal and 40 microns absolute. These filter elements were used for the regeneration tests. Filters 002 and 004 are secondary elements with a rating of 10 microns nominal and 25 microns absolute.

Filter number 5 was used most extensively in the one-g subsystem tests and for the primary filter component tests. A total of 9 tests were run on this filter element, all of which were of the continuous run cycle type. The physical appearance of the element remained unchanged throughout the testing program. As

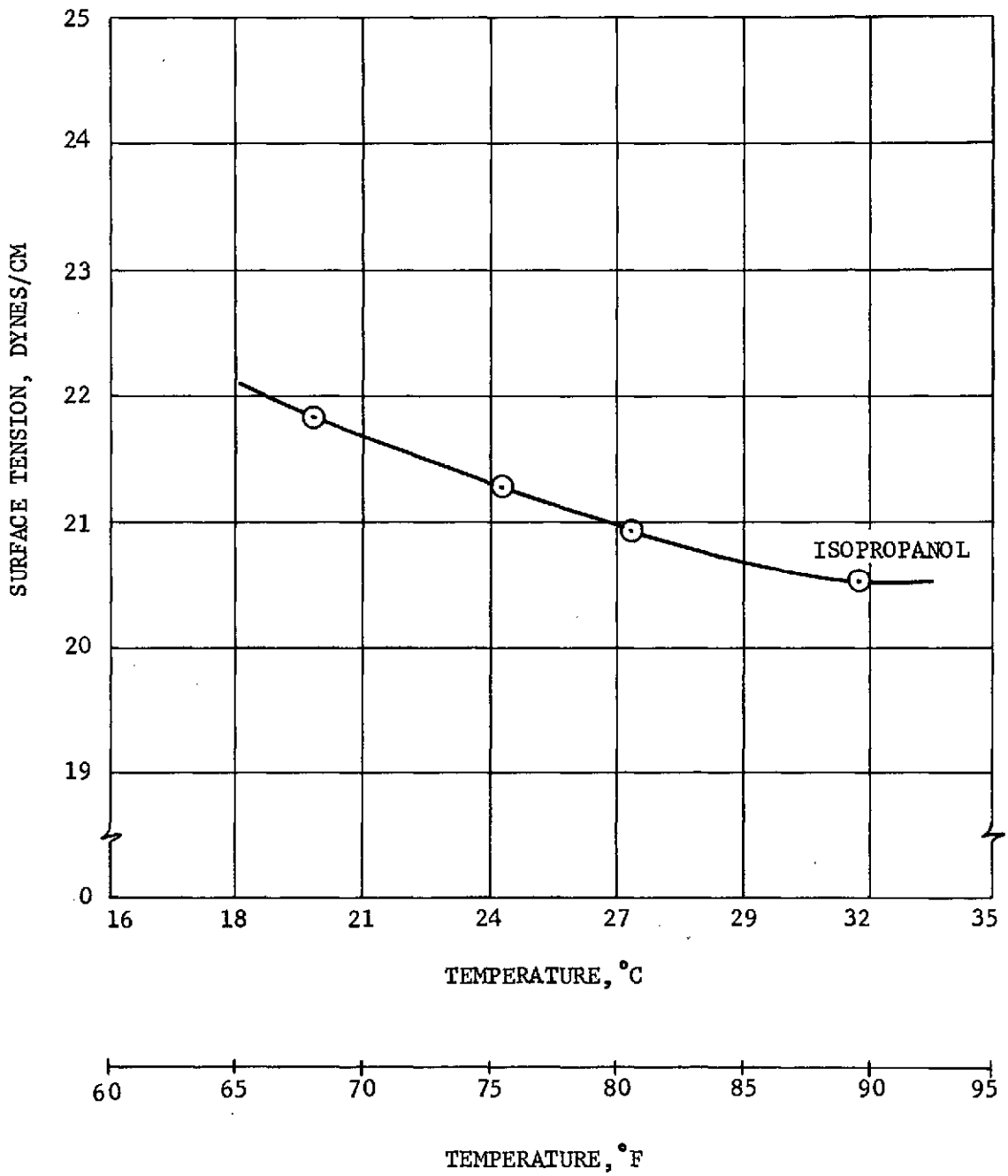

FIGURE V-28 TEST LIQUID SURFACE TENSION

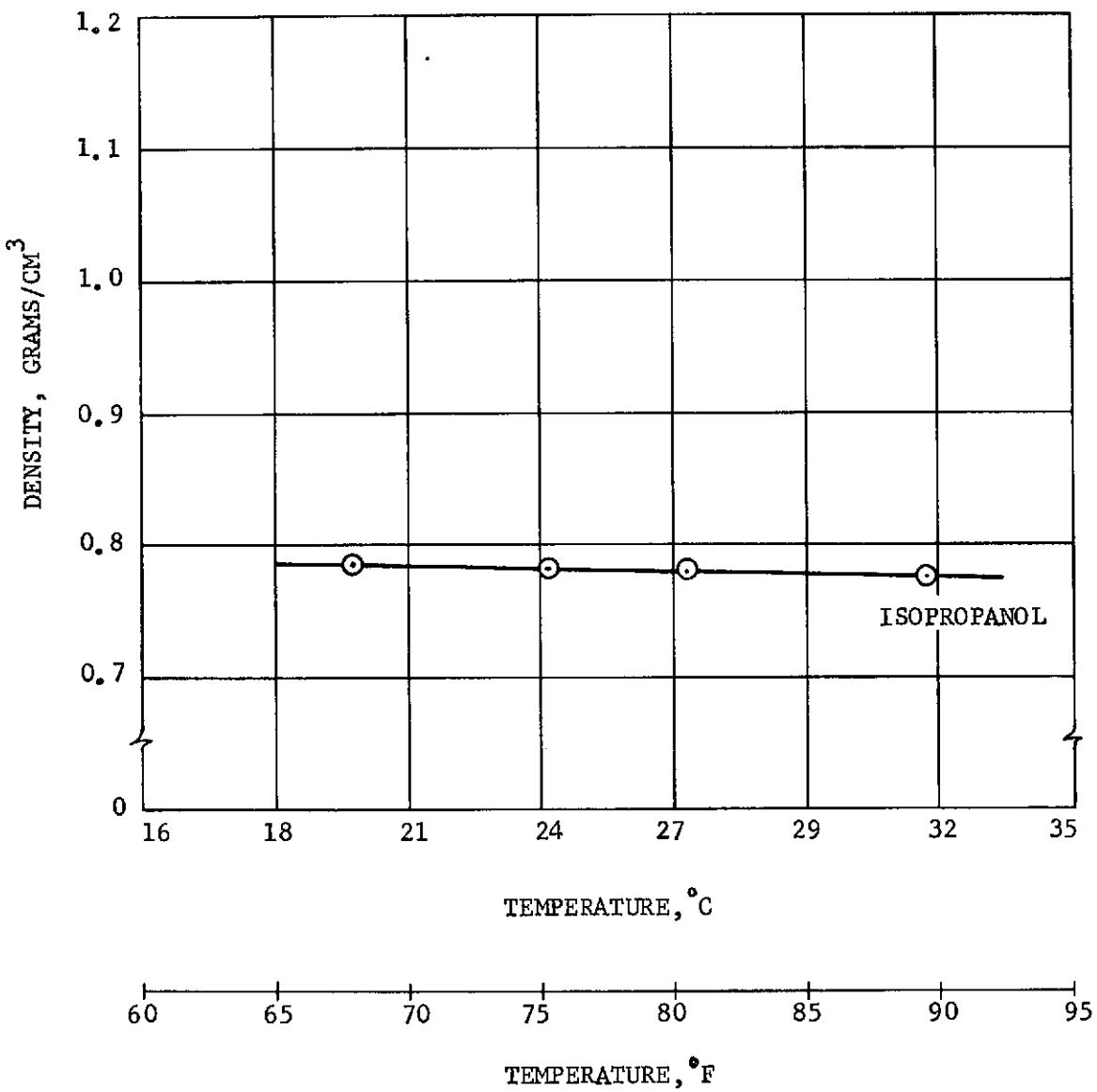

FIGURE V- 29 TEST LIQUID DENSITY

Filter Number	Date of Test	P_s, cm of H_2O, (in. of H_2O)								
		Clean (New)			After Regeneration, Before Cleaning			Clean (Ultrasonically)		
		1st Bubble	Boil All Over	Stable	1st Bubble	Boil All Over	Stable	1st Bubble	Boil All Over	Stable
5	5-30-73	8.6 (3.4)	12.7 (5.0)	6.6 (2.6)						
5	6-8-73				8.1 (3.2)	15.5 (6.1)	7.4 (2.9)			
5	6-8-73							9.4 (3.7)	15.7 (6.2)	6.6 (2.6)
6	5-30-73	8.9 (3.5)	11.9 (4.7)	7.9 (3.1)						
6	12-7-73							8.6 (3.4)	15.2 (6.0)	7.6 (3.0)
7	5-30-73	7.9 (3.1)	10.4 (4.1)	6.9 (2.7)						
7	12-7-73							7.6 (3.0)	14.7 (5.8)	6.1 (2.4)
8	5-30-73	9.1 (3.6)	11.4 (4.5)	7.9 (3.1)						
8	12-7-73							8.9 (3.5)	15.7 (6.2)	6.4 (2.5)
9	5-30-73	8.6 (3.4)	11.7 (4.6)	7.1 (2.8)						
9	12-7-73							9.7 (3.8)	9.4 (3.7)	7.4 (2.9)
10	5-30-73	8.6 (3.4)	11.9 (4.7)	7.6 (3.0)						
004	6-28-73	5.6 (2.2)	19.1 (7.5)	5.6 (2.2)						
004	12-10-73							7.6 (3.0)	20.1 (7.9)	3.0 (1.2)
002	12-10-73							19.6 (7.7)	25.1 (9.9)	8.9 (3.5)

FIGURE V-30 BUBBLE-POINT TESTS

can be seen from the data, the P_s for the first bubble varied from a new clean reading of 8.64 cm (3.4 in) of water down to 8.1 cm (3.2 in) and up again 9.4 cm (3.7 in) of water. This indicates that the filter after all testing did not suffer from pore size degradation. Also it can be noted the stable or static P_s was close to the same. The fluctuation of the "boil-all-over" point is expected because of the subjective nature of the test. It is, therefore, concluded that filter element number 5 suffered no degradation throughout its testing.

Filter element number 6 was used for the one-g system tests of which there were a total of 18, with three being voided because of a particle trap failure. The data again does not indicate any deterioration of the pores.

Filter elements 7, 8, 9, and 004 were used for the cyclic zero-g testing. Elements 7, 8, and 9 physically appear to be in good shape and the data shows no alarming change in the bubble-point pressure readings. However, the secondary filter element (004) which was used for all the zero-g tests and all of the system tests, a total of 27 tests, showed signs of twisting of the element. Figure V-31 is a picture of filter element 004 showing the distortion of the outside weave. The Hypro-pump used on the ground operations at Houston/JSC during the zero-g tests caused high peak pressures to be induced on the filter element. The secondary element -004 is of a 10 micron size thus extremely high pulse differential pressures were seen during backflush on the ground operation test set-up. The high pressure in element 004 caused fatiguing of the element housing thus lowering its column strength and resulting in a twist in the element weave. Figure V-32 is typical of a filter element over-pressure failure. The bubble-point pressure data for element 004 shows a slight change in P_s in the stable or static pressure area. This indicates that the pore size has opened up slightly, thus the lower pressure reading. If the proper graphs were available for this type filter element this P_s could be correlated to a micron rating that the degraded filter is equal too. Such a graph would be similar to the one shown in Figure V-33.

Test filter element 002, also a 10 μ element, shows the same characteristics as element 004 (see Figure V-31). This filter was used during the development tests (Contract NAS9-11984) with a Hypro-pump. It has been established that this particular pump was also inducing high peak differential pressures in the filter housing thus accounting for the dis-

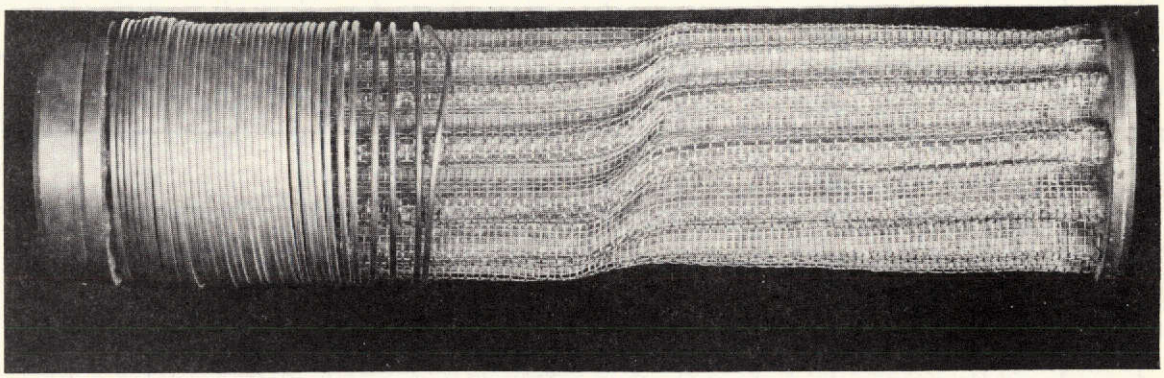

FIGURE V-31 SECONDARY FILTER ELEMENT 004

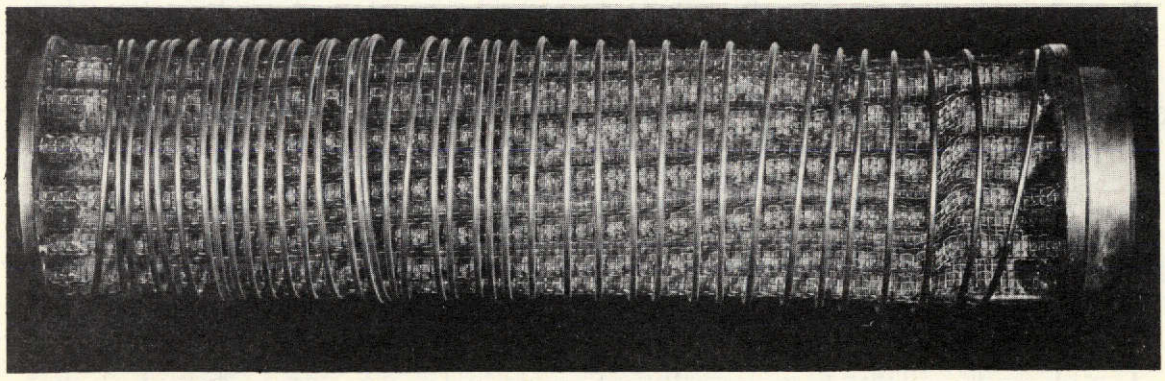

FIGURE V-32 DEVELOPMENT TEST FILTER ELEMENT 002

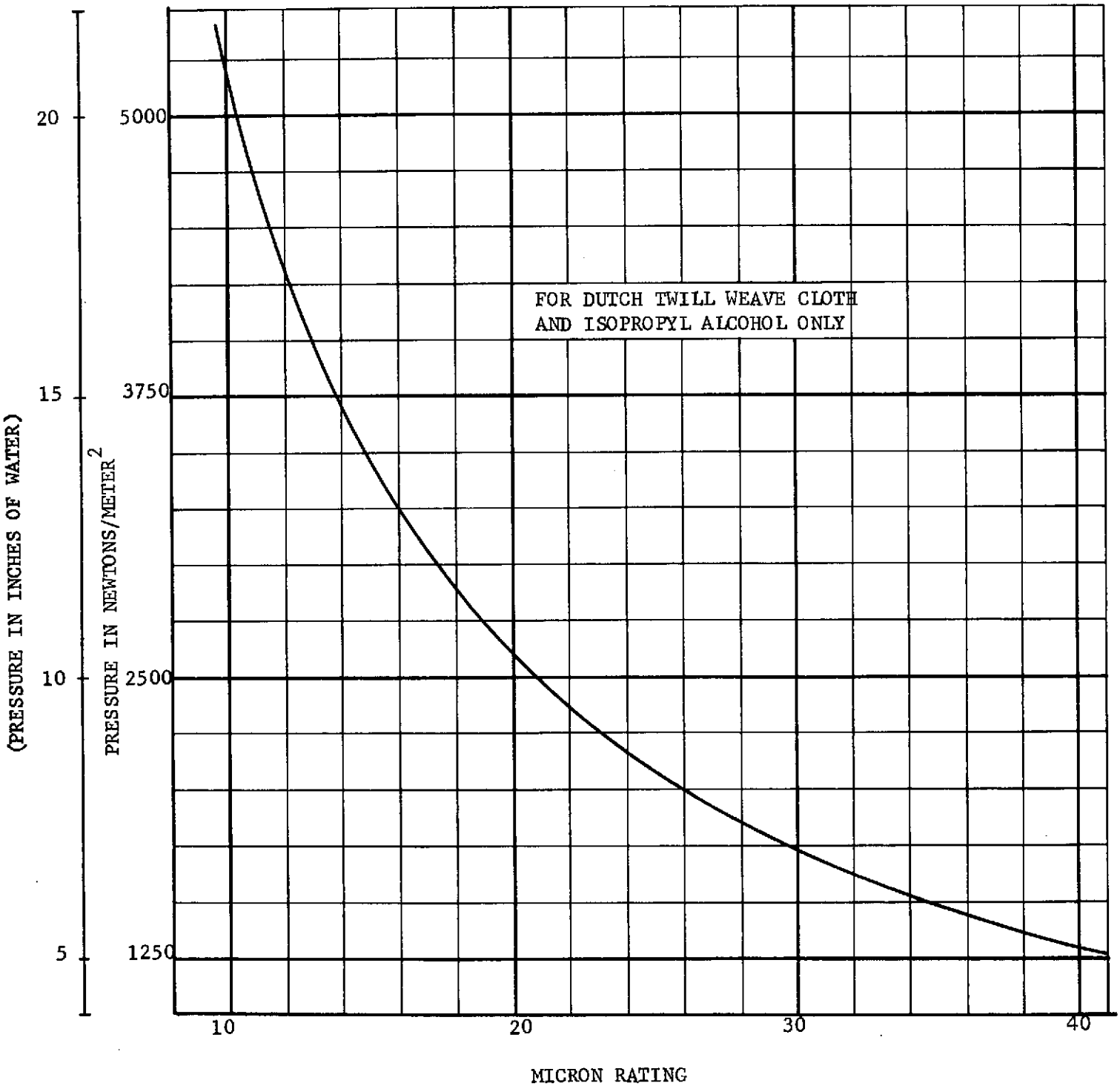

FIGURE V-33 MICRON RATING GRAPH

tortion of this element. No clean data was taken on element 002 as it was used during development testing; therefore, good conclusions cannot be drawn from this data without the use of a correct micron rating graph. These two filter failures were the only failures seen during all of the testing on the filter regeneration systems and were the result of the high peak pressures caused by the ground systems positive displacement piston pump. No failures have been attributed to the regeneration process.

C. SUBSYSTEM TESTS

Three tests were conducted using the filter and separator in combination. The filter was first loaded with AC road dust graded to 43 microns. The loading was done by the standard procedure with the filter in the "normal flow" direction. After loading the filter, it was connected upstream of the separator in the backflush direction. A millipore pad and holder were installed downstream of the separator, trapping all effluent. The schematic of this system is shown in Figure V-34.

Filter loading was conducted at 4.29×10^{-4} m^3/sec (6.8 GPM) and actual backflush subsystem tests were performed at 7.2×10^{-4} m^3/sec (11.5 GPM). The results of the subsystem tests are summarized in Table V-9.

Subsystem tests were operated for 5 minutes which was a reduction from the 30 minute regeneration cycle that was used during the development program. It was noted during the development testing that the cleaning of the filter appeared to be accomplished during the first few moments of operation. Development tests showed subsystem efficiencies of 87% with a 30 minute run cycle. The flight prototype subsystem tests showed an average of 89.7% efficiency with a 5 minute run cycle. Therefore, our assumption that cleaning takes place in the first few moments is correct. Therefore, a further reduction in time was indicated. Later in the System Tests the run cycle was reduced to 2 minutes, and the resultant data is itemized in section D.

Figure V-35 shows the ΔP vs. flow rate of the development subsystem versus the prototype subsystem. As can be seen at 6.31×10^{-4} m^3/sec (10 GPM) the development subsystem has a ΔP of 393×10^3 N/m^2 (57 psid) as compared to 248×10^3 N/m^2 (36 psid) for the prototype subsystem. Redesign of the flow pattern in the prototype filter and separator account for the majority of the difference. The redesign consisted of opening up the size of the outlet passage and adding straightener vanes in the prototype separator. The prototype filter passages were also opened up relative to the development filter.

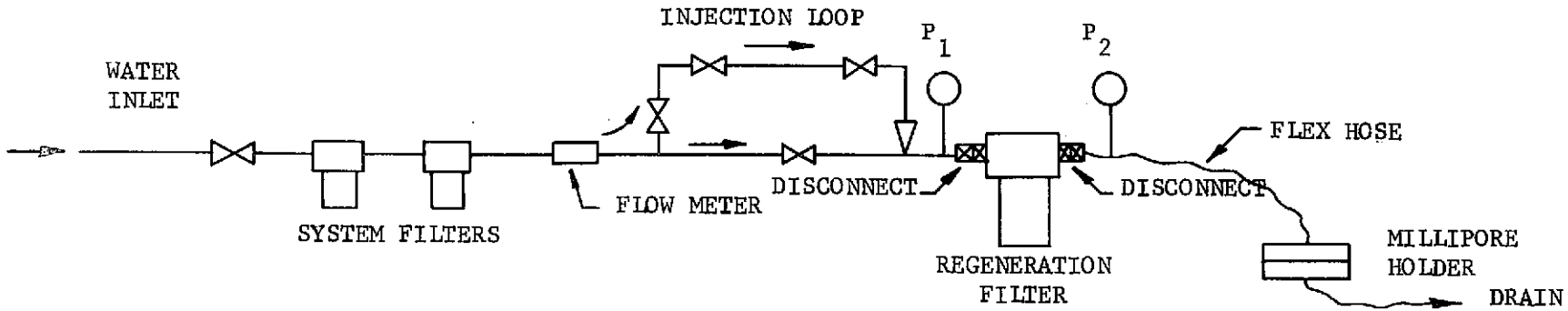

LOADING MODE

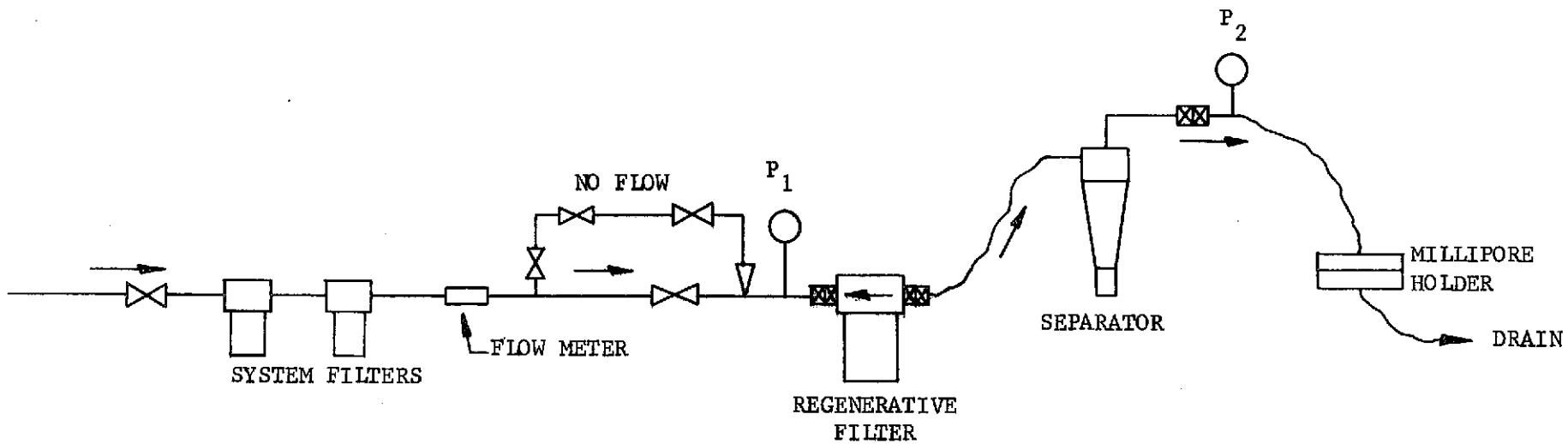

BACKFLUSH MODE

FIGURE V-34 FILTER-SEPARATOR SUBSYSTEM TEST SCHEMATIC

Table V-9 Filter-Separator Subsystem Performance Tests

(1) Test No.	Contaminant Added (grams)			Contaminant Recovered (grams)				Efficiency		
	Total Added to System	Recovered on Millipore	Retained on Filter Element (2)	Separator Trap	Wash from Filter Bowl	Millipore Pad	Net Contaminant Recovered	Separator	Regeneration	Subsystem
	A	B	C = A-B	D	E	F	G=D+E+F	Eff = $\frac{D}{D+F}$	Eff = $\frac{G}{C}$	Eff = $\frac{D+E}{C}$
-041	7.0054	.3742	6.6312	1.5510	4.3076	.3470	6.2056	81.7	93.6	88.4
-043	5.2242	.3069	4.9173	1.6918	2.6827	.2649	4.6394	86.5	94.4	89.0
-045	5.3601	.3140	5.0461	1.0442	3.5820	.2944	4.9206	78.0	97.5	91.7

(1) Backflush flow rate of 7.2×10^{-4} m^3/sec, (11.5 GPM) for 5 minutes

(2) Filter element type AN6235-2A, 20 micron nominal

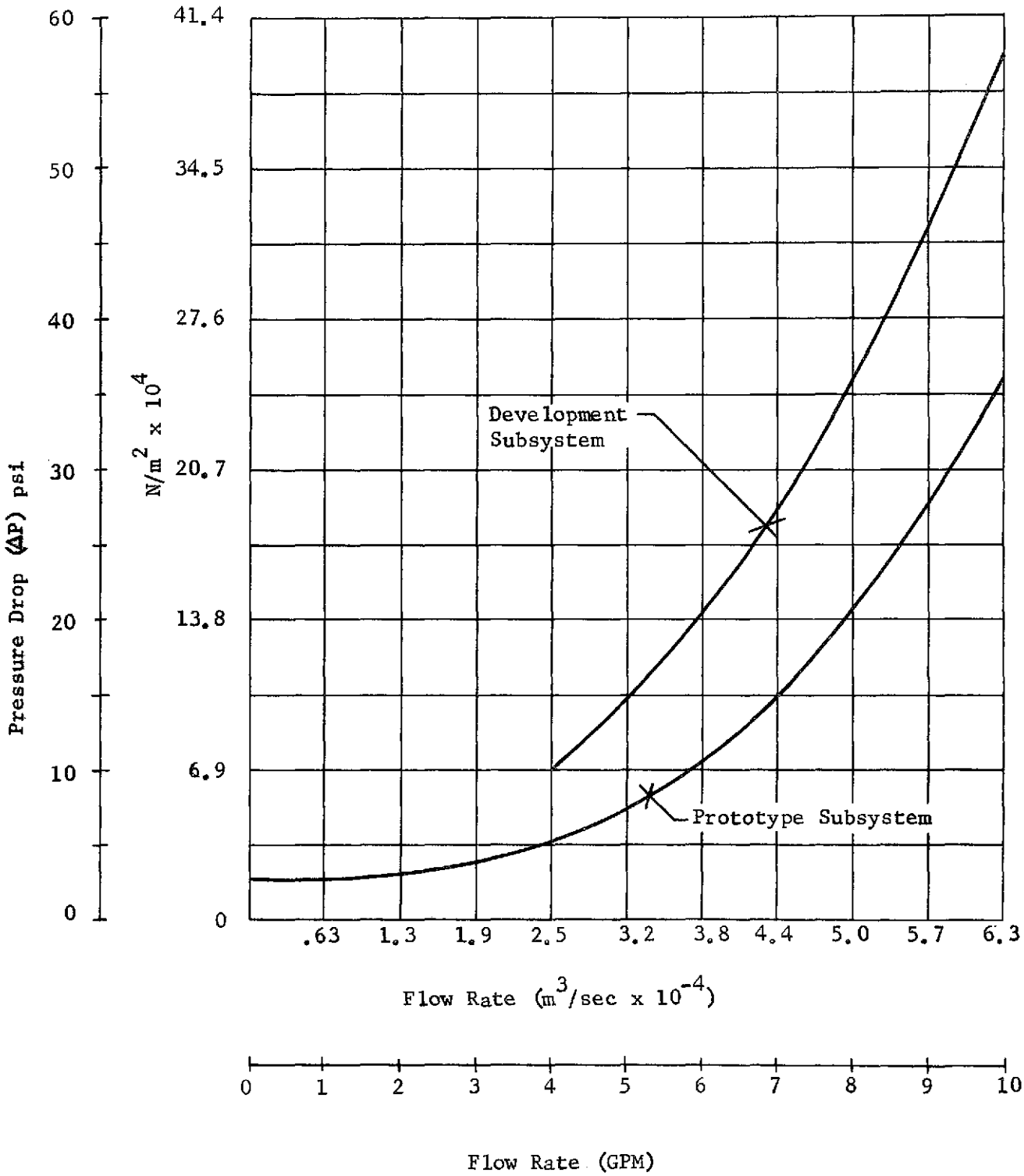

FIGURE V-35 SUBSYSTEM PRESSURE DROP

D. FILTER REGENERATION SYSTEM TESTS

A total of fifteen one-g performance tests were conducted on the filter regeneration unit to determine its overall efficiency, the optimum run cycle, and system integrity. Also, basic operating procedures were formulated, along with checking the leak integrity of each joint or component interface.

Table V-10 summarizes the efficiency test data as recorded for each system test. These tests were broken down into 5 minute, 2 minute, 1 minute, and 20 second cyclic tests. The 20 second cyclic tests were run 20 seconds on, and two minutes off for a total of 2 minutes of run time. These 20 second tests were conducted to simulate the upcoming KC-135 zero-g tests.

The average efficiency for the 2 minute runs was 92% as compared to 93.8% for the development unit, thus the two units exhibit almost the same efficiency rating.

Figure V-36 shows the schematic of the test system used for loading the filters with contaminant. The basic procedure for loading was to first load a known quantity of contaminant into the contaminant injection loop, establish a 4.31×10^{-4} m^3/sec (6.8 GPM) flow rate into the test filter, and then inject the contaminant. The injections were continued in one gram increments until a 137.9×10^3 N/m^2 (20 psid) pressure differential was obtained across the filter (readings P_1 and P_2). Figure V-37 depicts a average loading curve for a typical filter. The millipore pad was removed and weighed to determine the tare weight of the particles that went through the filter. After the filter was loaded it was then regenerated with the filter regeneration unit. Pads in the millipore holder were 293 mm diameter, .45 micron in size.

The basic procedure for checkout and running the pump was to first charge the unit with clean water to a pressure of 206.8×10^3 N/m^2 (30 psig) nominal plus or minus 68.9×10^2 N/m^2 (10 psig). Next, the loaded filter was connected to the unit. The cooling fan was then turned on to check out the electrical interface. The unit was then run for the particular run time prescribed by each test. Pump pressure and accumulator surface temperature were recorded during the test. At the end of the run cycle the unit was shut off, the separator trap removed and the tare weight

Table V-10 Filter Regeneration Unit Performance Tests

Test No.	Test Duration Minutes	Contaminant Added (grams)			Contaminant Recovered (grams)				Efficiency	
		Total Added to System	Recovered on Millipore	Retained on Filter Element	Separator Trap	Wash from Filter Backflush	Secondary Filter Backflush	Net Contaminant Recovered	Subsystem	System
		A	B	C = A-B	D	E	F	G = D+E+F	Eff = $\frac{D+E}{C}$	Eff = $\frac{G}{C}$
-048	5	7.1980	.5302	6.6678	5.5768	.0321	-	-	84.1	-
-050	5	7.3715	.5512	6.8203	5.0160	1.3580	-	-	93.5	
-052	5	4.3911	.3758	4.0153	3.0450	.7283	-	-	94.0	
-048 -050 -052	5	18.9606	1.4572	17.5034	13.6378	2.1184	.0959	15.8521	-	90.6
-057	2	4.3849	.3864	3.9985	2.7310	.9405	.0110*	3.6825	91.8	92.1
-060	2	4.2737	.2248	4.0489	1.4423	2.2305	.0117*	3.6845	90.7	91.0
-063	2	3.6905	.2128	3.4777	1.0081	2.1096	.0095*	3.1272	89.6	89.9
-066	2	3.7696	.2723	3.4973	2.4020	.8079	.0096*	3.2195	91.8	92.1
-068	2	3.2080	.2495	2.9585	1.0563	1.7947	.0082*	2.8592	96.4	96.6
-070	2	3.9991	.3260	3.6731	2.8836	.5583	.0101*	3.4520	93.7	94.0

* Secondary Filter Backflush Proportioned for Each Test

Table V-10 Filter Regeneration Unit Performance Tests (Cont'd)

Test No.	Test Duration Minutes	Contaminant Added (Grams)			Contaminant Recovered (Grams)				Efficiency	
		Total Added to System	Recovered on Millipore	Retained on Filter Element	Separator Trap	Wash from Filter Bowl	Secondary Filter Backflush	Net Contaminant Recovered	Subsystem	System
		A	B	C = A-B	D	E	F	G = D+E+F	Eff = $\frac{D+E}{C}$	Eff = $\frac{G}{C}$
-081	1	3.0212	.2146	2.8066	.9950	1.7456	-	2.7406	97.6	-
-084	1	2.2624	.1381	2.1243	.7954	1.2263	-	2.0217	95.2	-
-087	1	1.0067	.1136	.8931	.6112	.1255	-	.7367	82.5	-
-099	2*	3.1890	.3122	2.8768	-	-	-	-	-	-
-100	2*	2.1799	.2523	1.9276	-	-	-	-	-	-
-101	2*	3.0440	.3397	2.7043	-	-	-	-	-	-
Total				7.5087	4.9955	1.3103	.0580	6.3638	84.8	

* Test cycle was run with 20 seconds on, and 2 minutes off, to simulate zero-g parabolas.

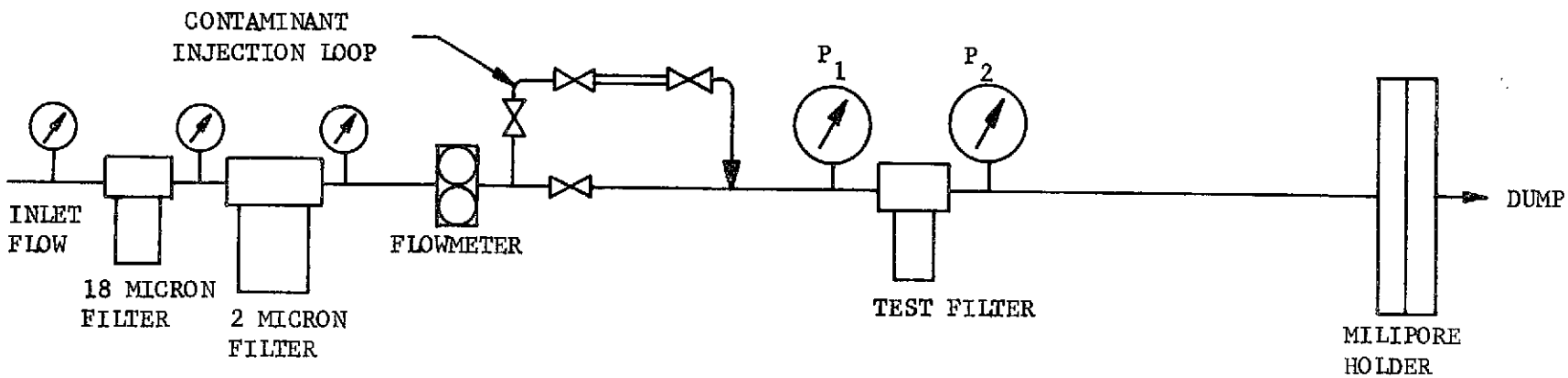

FIGURE V-36 FILTER LOADING SYSTEM

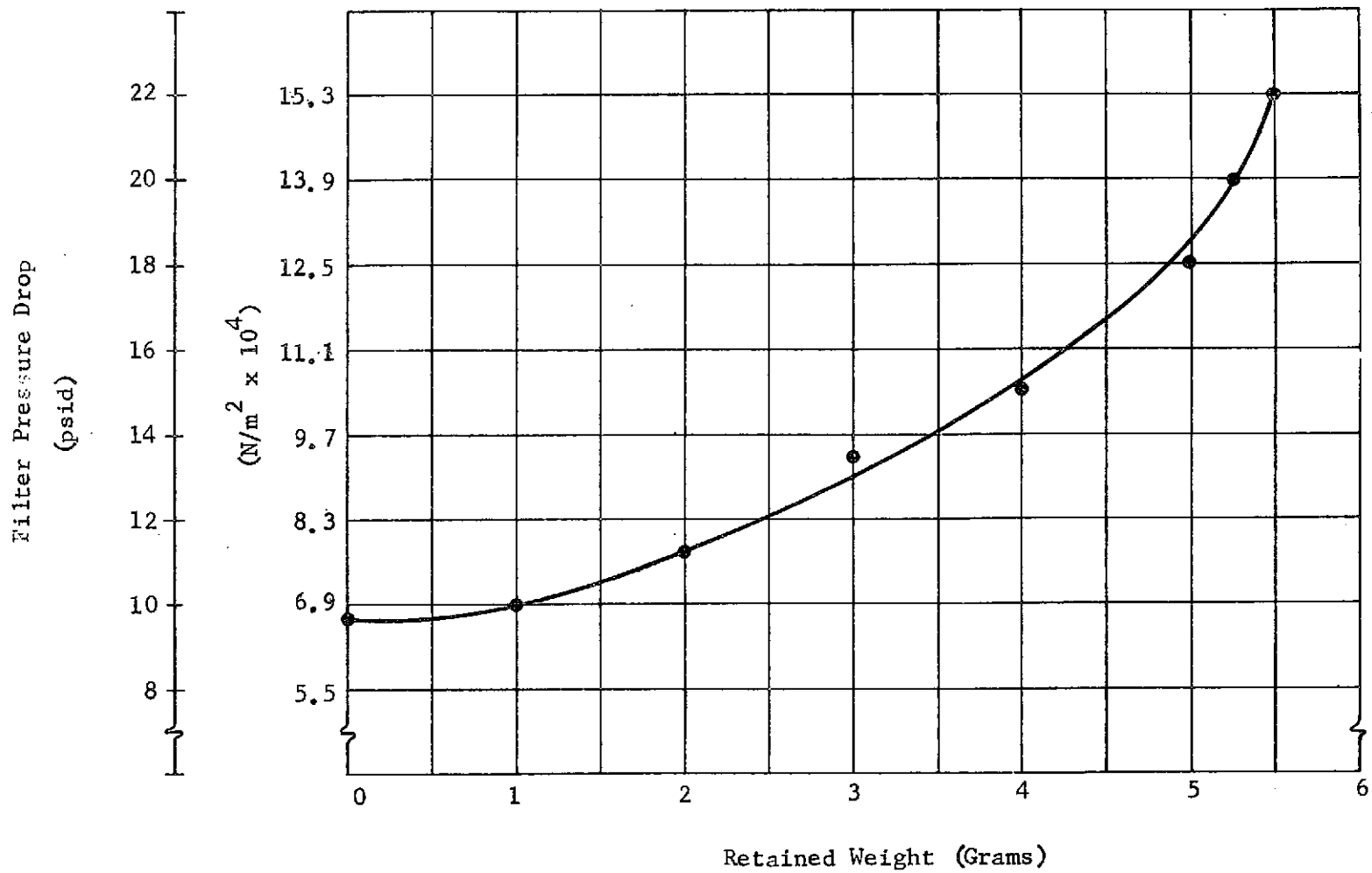

FIGURE V-37 FILTER LOADING CURVE

of the contaminant measured. Likewise, any contaminant in the secondary filter and any left in the bowl of the main filter being cleaned was weighed and recorded.

The filters that were used for testing were of the Hydraulic Research "421" type. This type of filter element is cleanable and is constructed from a pleated composite stainless steel material. The elements have a rating of 20 microns nominal and 40 microns absolute. The secondary filter element on the unit itself was also a Hydraulic Research "421" but of a 10 micron nominal and 25 micron absolute size.

The filter regeneration unit employs a 400 cycle, 10.6 amp motor which flows water thru the unit at 7.44×10^{-4} m^3/sec (11.8 GPM). All other parts in the unit are of the passive nature.

The unit motor depends upon the fluid passing through it in order to cool the motor. Therefore, the unit run time and the absence of all air pockets were of primary concern. In order to insure a minimum of air bubbles in the unit a pressurized bladder tank was used in charging the unit with fluid. A schematic of the loading tool is shown in Figure V-38. The bladder tank is filled with clean filtered water in such a manner as to eliminate bubbles in the water. The bladder is then pressurized to 275.8×10^3 N/m^2 (40 psi). Valve V_1 is opened and the pressure on the unit gage is noted. Valve V_2 is then opened and the unit is flushed until the dump water contains no bubbles. Then Valve V_2 is closed; Valve V_1 is then closed. The unit pressure is noted; if it is below 241.3×10^3 N/m^2 (35 psig) the bladder tank is pressurized to 379.2×10^3 N/m^2 (55 psig). Valve V_1 is then opened and then closed, thus leaving the unit at 241.3×10^3 N/m^2 (35 psi). The unit is now charged and is disconnected from the loading tool.

The filter prototype regeneration tests were performed using AC coarse road dust as the contaminant. The dust was sieved to remove particles greater than 43 microns. Testing started with a 5 minute continuous run. It was noted that the unit did heat up to a point where it was uncomfortable to hold your hand on it for a long period of time. Figure V-39 shows temperature profiles as measured on the top surface of the accumulator for 5 and 2 minute continuous run times. From these results it was decided to reduce run times to keep the temperature down. Also it may be noted from Table V-10 that the efficiency did not suffer from the reduced time.

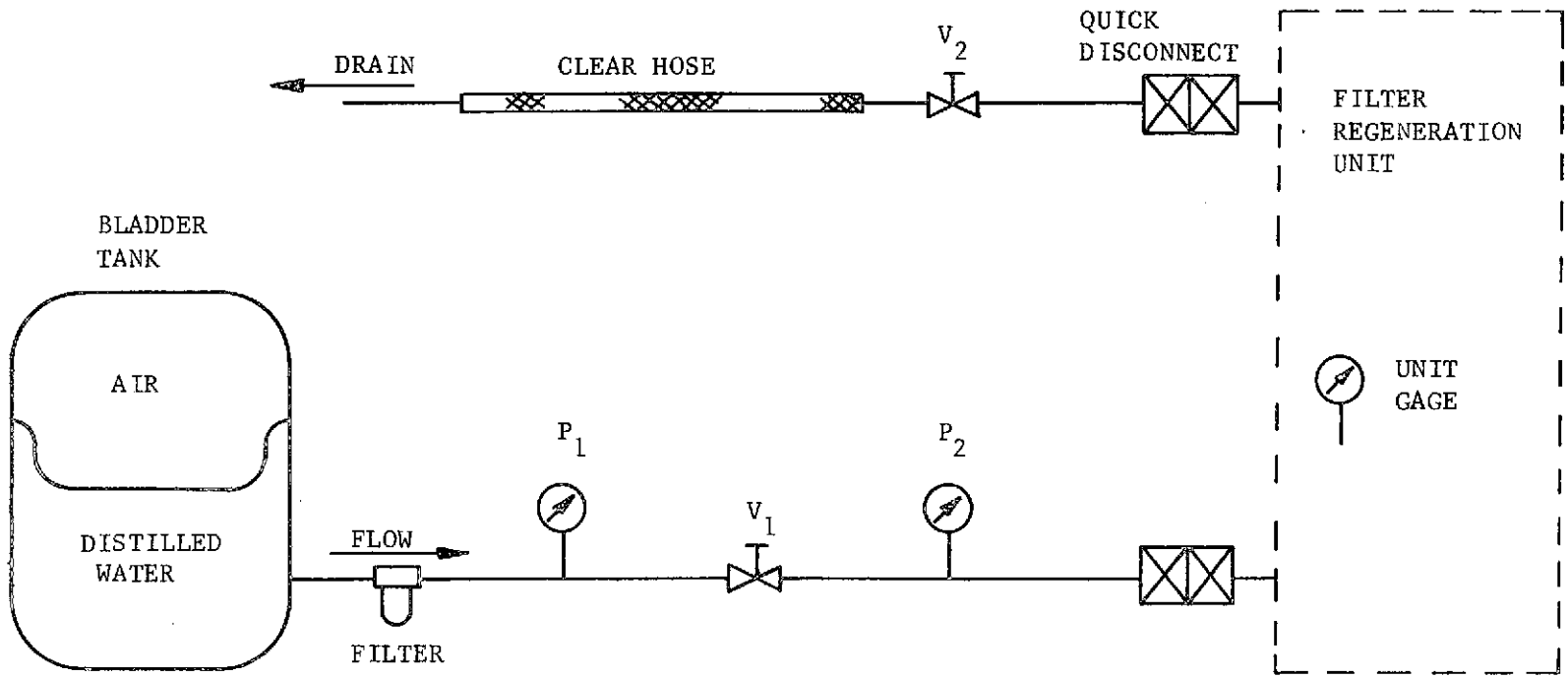

FIGURE V-38 CHARGING TOOL SCHEMATIC, FILTER REGENERATION UNIT

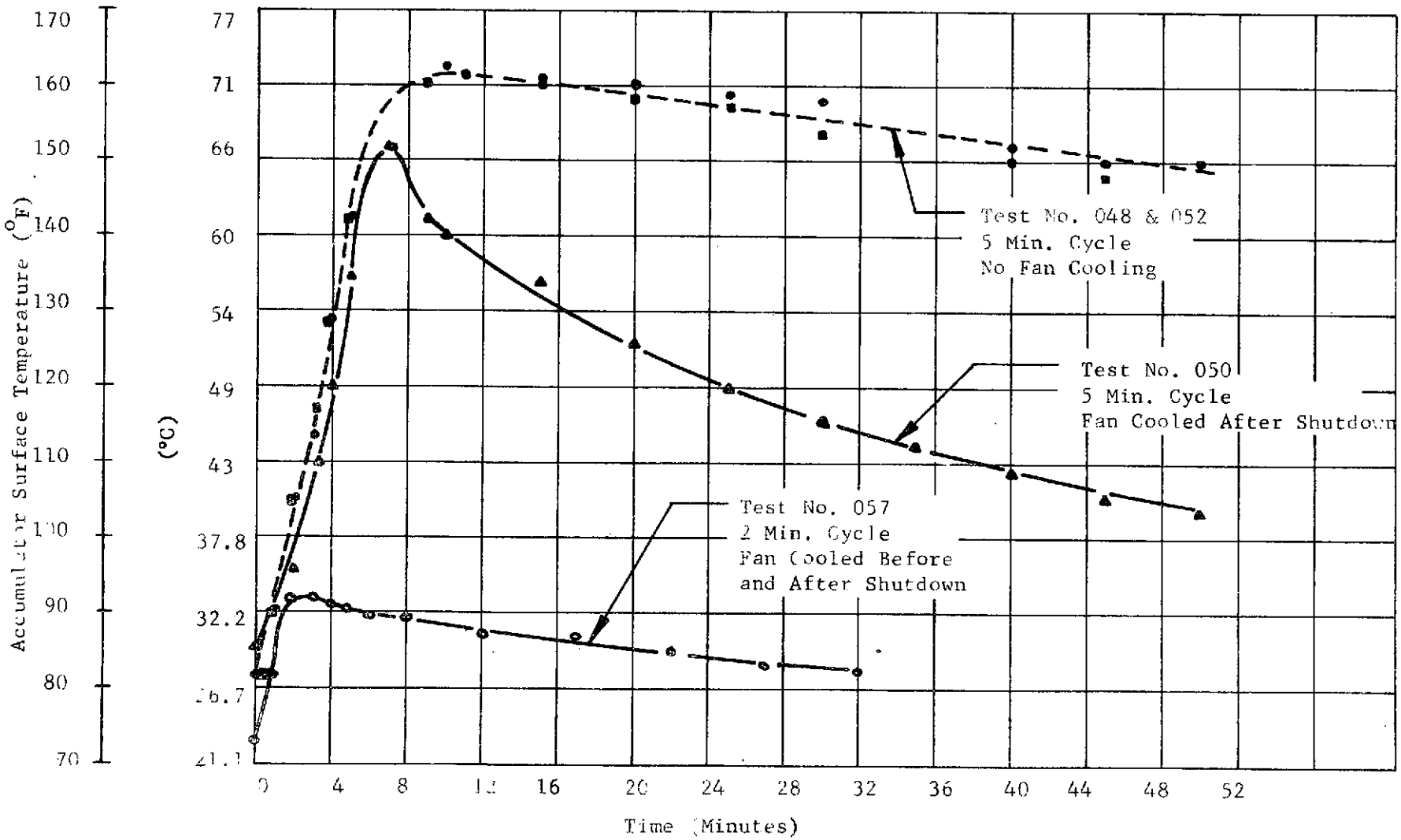

Figure V-39 Filter Regeneration Unit Surface Temperature Profile

One minute continuous runs were then tried with no appreciable loss in efficiency, however, when 20 second cyclic tests were tried with 2 minute total run times the efficiency dropped on the average of 7%. The cyclic tests were conducted to simulate the upcoming zero-g tests which also reflected this loss in efficiency.

Cyclic combined tests -091, -093, and -095 were voided because of a fracture in the separator bowl. The plexiglass bowl was redesigned and a new one built with more material and a full radius at the bottom of the trap.

It was noted the unit ran very smoothly with negligible vibration. The motor pump was quiet and was not objectionable even during the 5 minute runs. The fan has a slight whine, although not objectionable for 2 minute runs, it did become objectionable for the five minute runs. A baffling system could be employed to eliminate this problem.

The CPV fittings used were very good in allowing little if any leaks. The inlet disconnect was cleaned to correct a slight leak. It should be noted that disconnects should be kept clean and well lubricated as binding will occur if they are not.

The one-g testing of the flight prototype regenerative unit indicated that it could be flown in the NASA, KC-135 test aircraft. Through this ground testing it was possible to formulate procedures for the zero-g tests. The tests also gave a sound basis for comparison of efficiencies versus run cycle time.

In order to keep the unit at a safe operating temperature it was concluded that a 2 minute run cycle, with fan cooling before and after shutdown, was the optimum run time. This run time should also be a continuous run cycle as the efficiency decreased in the cyclic test. The 2 minute duration was chosen in order to give adequate time for the impacted contaminant to exit the filter element. This type of run cycle should yield 93.6 to 97.5% cleaning efficiency of the filter element.

E. ZERO-GRAVITY TESTS

Zero-gravity tests were conducted on both the Development Unit and the Flight Prototype Filter Regeneration Unit. The Development Unit was designed and fabricated under Contract NAS9-11984 to evaluate and test concepts whereby contaminated fluid filters are regenerated (cleaned) by utilizing a special backflush/jet impingement technique. The Flight Prototype Filter Regeneration Unit was designed, fabricated, and performance tested under Contract NAS9-12685 to verify the applicability of the filter regeneration process to typical Space Station/ Shuttle zero-gravity fluid systems.

The primary objectives of the two sets of zero-g tests conducted were twofold: 1) to determine the fluid dynamic characteristics and the system performance of the Filter Regeneration Unit and the Regenerative Filter in a zero-gravity environment; 2) Evaluate the aspects of human factors in the design and operation of the Filter Regeneration Unit when used in a zero-g environment. Zero-gravity conditions were simulated in a specially modified KC-135A jet transport which flew parabolic arcs to provide approximately 20 seconds of zero-gravity environment for each parabola. A total of 158 parabolas were flown during the two tests with 13 regenerative filters cleaned. All zero-g filter regeneration tests were conducted with filter elements that had been preloaded with a known quantity of AC coarse road dust.

1. Development Unit Zero-G Tests - A description of the test hardware and the results and conclusions of the zero-g filter regeneration tests are summarized below. For a more detailed description, refer to "Final Report, Regenerative Particulate Filter Development", May 1972, Martin Marietta Corporation, Report No. MCR-72-40, and "Test Report, Filter Regeneration Unit Zero-Gravity Test, October 1972, Martin Marietta Corporation, Report No. MCR-72-252. For detail drawings, refer to "Prototype Design Drawings, Regenerative Particulate Filter Development", Report No. MCR-72-65.

The Development Unit, Figure V-40, is a self-contained unit that utilizes a backflush/impingement jet technique to clean water system filters. The unit contains a pump, motor and other equipment, Figure V-41, which provide the flow rate and pressure required for the backflush operation. The working fluid within the unit is water. Flow from the pump is directed through the regenerative filter in the reverse direction.

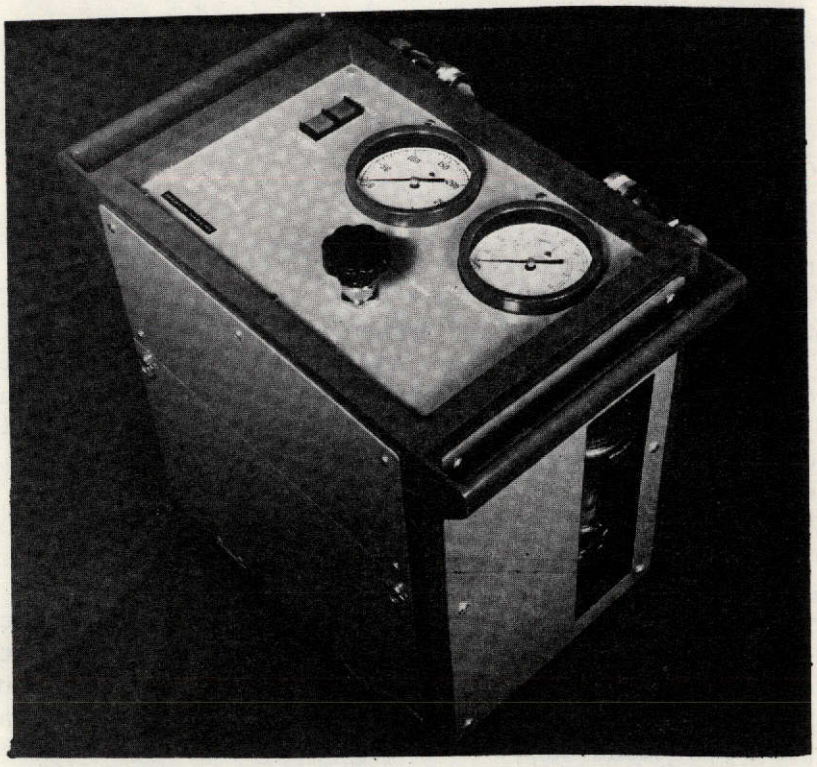

FIGURE V-40 FILTER REGENERATION DEVELOPMENT UNIT

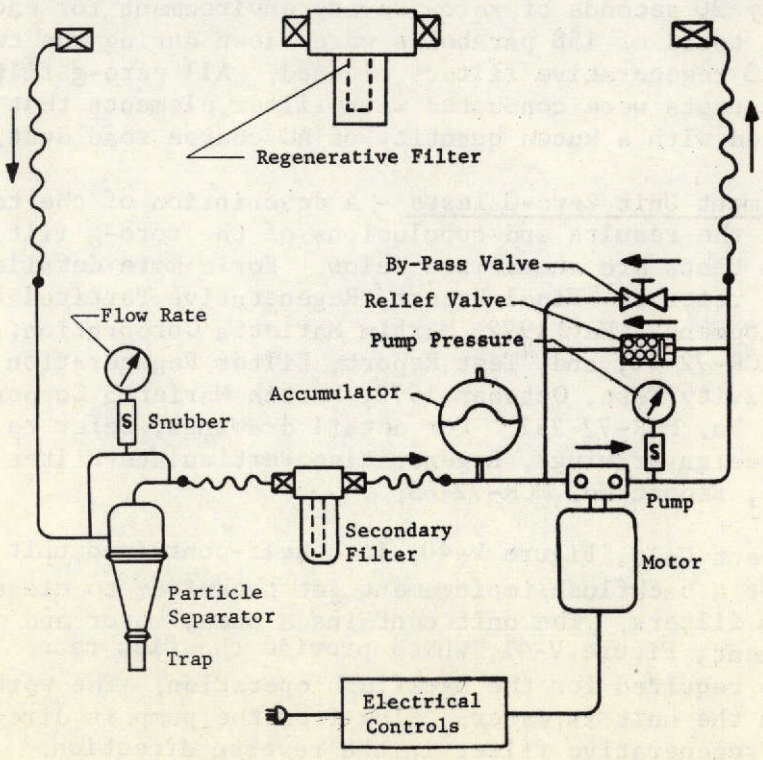

FIGURE V-41 DEVELOPMENT UNIT SCHEMATIC

Particulate is washed from the filter element with the aid of an impingement jet. The particulate is then carried to the transparent vortex particle separator where the majority (88 to 93%) of the particles are separated from the water and collected in the particle separator trap. The remainder of the particulate passes through the separator and into the secondary filter (10 micron) where it is collected.

A relief valve and bypass loop provide protection for the piston pump and motor in the event the operational procedures are not followed. A FLOW CONTROL valve and bypass loop are available to regulate the BACKFLUSH FLOW RATE. The PUMP PRESSURE GAGE provides an indication of unit pressure while operating and the residual pressure when not operating. The accumulator provides a positive pressure on the pump inlet, maintains a hard fluid system in the event of fluid loss, and dampens the pulsations created by the piston pump.

The equipment in the unit is enclosed within a paneled aluminum framework approximately 38.1 cm (15 inches) x 58.4 cm (23 inches) x 50.8 cm (20 inches) high. When loaded with water, the unit weighs 68 kg (150 lbs). Handles are provided on the unit for carrying.

The unit is operated from a 2 HP electric motor which runs off a 200 volt, 400 Hz, 3 ϕ power source. All electrical wiring and components comply with applicable government specifications.

The regenerative filter consists of a filter body, a 10 micron nominal/25 micron absolute filter element, a backflush impingement jet, and two quick disconnect nipples. Two regenerative filter bodies were used. One was a conventional aluminum body and the other was constructed of plexiglass to provide visual observation of the backflush cleaning action.

The zero-g tests were conducted during the period September 11, 1972 - September 13, 1972 with an accumulation of 82 zero-gravity parabolas. Four regenerative filters were "cleaned" using the filter regeneration unit. These filter elements had a rating of 20 microns nominal and 40 microns absolute. Prior to the zero-g tests, a series of three tests were conducted in one-g on the test equipment to verify the test procedure and to obtain baseline data for comparison with the zero-g tests results. These tests were conducted at Martin Marietta-Denver just prior to shipment of the test equipment to Wright-Patterson Air Force Base. The filter regenerations performed during these tests were intermittent in nature so as to duplicate the characteristics of

zero-g flight on the KC-135 aircraft. The regeneration of the filters was conducted in 20-second increments to a total time of 5 minutes. The interval between these runs was 1.5 minutes for tests 1G-1 and 1G-3 and 1.0 minute for test 1G-2. The effects of an intermittent regeneration cycle had not been tested previously in the initial development program and its effect on performance was not known. For the one-g tests four filter elements were cleaned in accordance with the test procedure. Two more filter elements were loaded and cleaned during the third test series in order to gain additional test data. All filters were loaded with AC coarse road dust as in the previous development and performance efficiency tests.

The results of the one-g tests are shown in Tables V-11 and V-12. Table V-11 provides loading and regeneration data and Table V-12 provides the total contaminant recovery data. The contaminant retained in the filter element was found by subtracting the tare quantity found on the downstream millipore pad from the total amount injected into the filter body. When the filter elements were loaded, the water flow was maintained at 4.29×10^{-4} m^3/sec (6.8 GPM). The millipore pad was located downstream from the filter and was used to recover the AC road dust that was not retained on the filter element or in the filter bowl.

The regeneration efficiency was based on the sum quantity of contaminant recovered in the separator trap and the filter bowl. Comparing this quantity with the quantity retained or loaded on the filter provides the regeneration efficiency. The contaminant recovered in the filter bowl is included because it theoretically will not settle in a zero-gravity environment and should easily be removed and retained in the separator trap during regeneration.

The efficiency of test 1G-1 was 97.1% which was comparable to data obtained during development tests of the Filter Regeneration Unit using a 5-minute continuous regeneration cycle. Test 1G-2 resulted in a much lower regeneration efficiency of 61.9%. This low efficiency was attributed to a testing error due to loss of contaminant during handling, weighing and transferring. A third test was conducted using the same filter elements. They were loaded with AC coarse road dust and then stored in bottles, as was done for Test 1G-2. The efficiency of Test 1G-3 improved significantly supporting the theory that a testing error occurred during Test 1G-2. The 82.4% efficiency of Test 1G-3 was still lower than the first test but the fact that

Table V-11 One-Gravity Performance Test Data

	Contaminant Added (grams)			Regeneration	
	Total Added to System	Recovered on Millipore	Retained on Filter Element	Contaminant Recovered (Filter Bowl & Trap)	Efficiency
Test 1G-1	X	Y	A = X-Y	B	Eff = B/A
Filter Element 2	3.0803	.1938	2.8865	2.0874	
Filter Element 4	1.1057	.1107	.9950	.1653	
Separator Trap				1.5171	
Total			3.8815	3.7698	97.1%
Test 1G-2					
Filter Element 1	4.4874	.3935	4.0939	1.3702	
Filter Element 3	1.0093	.1348	.8745	.2874	
Separator Trap				1.4158	
Total			4.9684	3.0734	61.9%
Test 1G-3					
Filter Element 1	4.7248	.3670	4.3578	2.2556	
Filter Element 3	1.0102	.0875	.9227	.2098	
Separator Trap				1.8857	
Total			5.2805	4.3511	82.4%

Table V-12 One-Gravity Contaminant Recovery Data

	Contaminant Retained on Filter Element (Grams)	Regeneration		Total Test Contaminant Recovery		
		Contaminant Recovered (Grams in Filter Bowl & Trap)	Efficiency	Post-Test Backflush (Grams)	Total (Grams)	Efficiency
Test 1G-1	A	B	Eff = B/A	C	D = B+C	Eff = D/A
Filter Element 2	2.8865	2.0874		.0269	2.1143	
Filter Element 4	.9950	.1653		.0000	.1653	
Separator Trap		1.5171			1.5171	
Secondary Filter*				.1152	.1152	
Total	3.8815	3.7698	97.1%	.1421	3.9119	100.8%
Test 1G-2						
Filter Element 1	4.0939	1.3702		.1943	1.5644	
Filter Element 3	.8745	.2874		.3013	.5887	
Separator Trap		1.4158			1.4158	
Secondary Filter*				.1472	.1472	
Total	4.9684	3.0734	61.9%	.6428	3.7161	74.8%
TOTAL	8.8499	6.8432	77.3%	1.4277	7.6280	86.2%
SECONDARY FILTER TOTAL				.2624		
Test 1G-3						
Filter Element 1	4.3578	2.2556		.1944	2.4500	
Filter Element 3	.9227	.2098		.0191	.2289	
Separator Trap		1.8857			1.8857	
Secondary Filter				.1320	.1320	
Total	5.2805	4.3511	82.4%	.3455	4.6966	88.9%

*Approximate apportionment of Secondary Filter Total based on Total Contaminant Retained on Filter Element.

both Tests 1G-2 and 1G-3 were lower than Test 1G-1 indicated that the filter elements removed from the filter body after being loaded had a lower efficiency than those that were not removed before regeneration. The reason again was due to loss of contaminant during the transferring process. This action was necessitated by the requirement to regenerate four filters with only two regenerative filter housings being available for the test.

The possibility of contaminant loss is supported by the "Total Test Contaminant Recovery Efficiency" given in Table V-12. There is a significant decrease in recovery for Tests 1G-2 and 1G-3 were a 100.8% efficiency was obtained for Test 1G-1 and efficiencies of 74.8% and 88.9% were obtained for Test 1G-2 and 1G-3, respectively.

The total test contaminant recovery was based on the quantity of contaminant recovered in the separator trap plus the quantity recovered from backflushing the filter elements and the secondary filter. The filter elements were backflushed into a millipore pad for a period of 10 minutes with the flow rate ranging between 5.8 and 8.8 x 10^{-4} m^3/sec (9.2 and 14.1 GPM). The secondary filter was regenerated and the total contaminant recovered was proportioned back into the individual tests in direct proportion to the load capacity of the filters. For the one-gravity tests only one secondary filter was used. A small amount of unrecovered contaminant can be attributed to the contaminant particles that are smaller than 10 microns that become suspended in the water during the regeneration process.

The results of the three one-g tests were somewhat inconsistent. However, the purpose of the tests, to verify the zero-g procedure and obtain baseline data, was successfully accomplished.

The test data obtained from the zero-gravity tests is shown in Tables V-13 and V-14. The efficiency of the first test, Test ZG-1, was low because of a failure in the separator trap, and the subsequent loss of contaminant. The 90.4% regeneration efficiency for Test ZG-2 is very good and gives the best data point because two filters were regenerated. The only other data point for efficiency is for Test ZG-3 which regenerated only one filter and resulted in a low but comparable efficiency. The 72.9% efficiency is higher than that obtained for the second one-g tests, 1G-2, but is lower than the other two efficiencies obtained during one-g tests. When combining Tests

Table V-13 Zero-Gravity Performance Test Data

	Contaminant Added (Grams)			Regeneration	
	Total Added to Load System	Recovered on Millipore	Retained on Filter Element	Contaminant Recovered (Filter Bowl & Trap)	Efficiency
Test ZG-1	X	Y	A = X-Y	B	Eff = B/A
Filter Element 4	1.0256	.0082	1.0174	.0107	
Separator Trap				.4236	
Total	1.0256	.0082	1.0174	.4343	*42.7%
Test ZG-2					
Filter Element 2	2.1538	.1286	2.0252	.0532	
Filter Element 3	1.0690	.1905	.8785	.1358	
Separator Trap				2.4360	
Total	3.2228	.3191	2.9037	2.6250	90.4%
Test ZG-3					
Filter Element 1	4.1840	.2042	3.9798	.0842	
Separator Trap				2.8165	
Total	4.1840	.2042	3.9798	2.9007	72.9%
TOTAL	8.4324	.5315	7.9009	5.9600	

Table V-14 Zero-Gravity Performance Test Data

	Contaminant Retained on Filter Element (Grams)	Regeneration		Total Test Contaminant Recovery		
		Contaminant Recovered (Grams in Filter Bowl & Trap)	Efficiency	Post-Test Backflush (Grams)	Total (Grams)	Efficiency
Test ZG-1	A	B	Eff = B/A	C	D = B+C	Eff = D/A
Filter Element 4	1.0174	.0107		.0565	.0672	
Separator Trap		.4236			.4236	
Secondary Filter*				*.0655	.0655	
Total	1.0174	.4343	42.7%	.1220	.05563	54.7%
Test ZG-2						
Filter Element 2	2.0252	.0532		.1669	.2201	
Filter Element 3	.8785	.1358		.0260	.1618	
Separator Trap		2.4360			2.4360	
Secondary Filter*				*.1864	.1864	
Total	2.9037	2.6250	90.4%	.3793	3.0043	103.5%
Test ZG-3						
Filter Element 1	3.9798	.0842		.1375	.2217	
Separator Trap		2.8165			2.8165	
Secondary Filter*				*.2561	.2561	
Total	3.9798	2.9007	72.9%	.3936	3.2943	82.8%
TOTAL	7.9009	5.9600		.8949	6.8549	86.8%
TOTAL SECONDARY FILTER				.5080		

* Approximate apportionment of Secondary Filter Total based on Total Contaminant Retained on Filter Element.

ZG-2 and ZG-3, the average efficiency comes out to 80.3% which is comparable to the one-g tests for an overall value. More data points would have been desirable, but due to limitations on flight time and the high costs involved, the existing data was considered sufficient.

The total test contaminant recovery shown in Table V-14 shows good efficiencies for Tests ZG-2 and ZG-3. Since only one secondary filter was used for all three tests, the total quantity obtained after it was backflushed was proportioned out to the individual tests based on a direct ratio of the loaded contaminant for each test. The 54.7% efficiency of Test ZG-1 verifies that there was a considerable loss of contaminant due to the failure of the separator trap. The efficiencies for Test ZG-2 and ZG-3 are 103.5% and 82.8%, respectively and when combining them, an overall efficiency of 91.5% is obtained, which is good.

Two of the three filters regenerated during Test ZG-2 and ZG-3 were removed from the filter body that they were loaded in and then replaced for regeneration. This was necessary because there were only two filter bowls available for the tests. This creates the possibility for contaminant loss and can adversely affect the test data.

When comparing the residue that settles out in the regenerative filter bowl for the one-g and zero-g tests, there is a considerable decrease for the zero-g tests. The one-g tests show a 16% to 72% residual contaminant left in the filter bowl (see Table V-11). The percentage is based on the total contaminant loaded on the filter. The zero-g test data in Table V-13 shows a 1%, 2%, 3% and 15% residual left in the filter bowl. Aside from the 15% value, the quantities are essentially zero which has been the basic assumption during development testing. The contaminant recovered from the filter bowl has been assumed to be removed and retained in the separator trap when in a zero-g environment. The low quantities left in the filter bowl for the zero-g tests would be even less if the system were operated continuously in a zero-g environment. For the tests, the period of zero-g was only for 20 seconds and between each period there was a period of a two-g downward force acting on the equipment. This caused the loose particles to be compacted down to the bottom of the filter bowl between each cyclic operation of the system.

The efficiencies of the zero-g tests are comparable to those obtained for the one-g tests which concludes that the Filter Regeneration System operates as well in a zero-g environment as in a one-g environment. The average regeneration efficiency for the zero-g tests, excluding the 42.7% test due to the separator trap failure, was 81.65% as compared to the 80.47% average regeneration efficiency of the one-g intermittent, 5 minute tests. The regeneration efficiency of 90.4%, obtained for Test ZG-2, is comparable to those obtained during the initial one-g, continuous cycle, 5 minute development tests which averaged 93.88%. However, the average zero-g regeneration efficiency is 12.23% lower than the average one-g, continuous cycle, 5 minute tests. The reason for the lower zero-g regeneration efficiencies is believed to be caused primarily by two factors. The first factor is the 20-second cyclic mode of operation that is inherent in the KC-135 parabolas. The cyclic operation causes a loss of inertia in the particles during each cleaning cycle. This does not occur during a continuous regeneration process and it is believed that the efficiencies of the system would increase if operated continuously in a real zero-gravity system. The second factor that produced a lower efficiency was the two-g downward force which acted on the equipment between parabolas. This caused the loose particles to be compacted down to the bottom of the filter bowl between each cyclic operation of the system. The zero-g environment does facilitate, however, the removal of residual contaminant from the filter bowl as can be seen by comparing the contaminant recovery data of Table V-11 with that of Table V-13.

The performance data from the zero-g tests verified the successful operation of the particle separator, but high speed movie coverage (400 frames/second) provided excellent additional information. The majority of the contaminant can be seen entering the separator within 2 seconds after initiation of the cleaning cycle. The contaminant appears in the form of a cloud and immediately goes into the trap passing through the separator in a helix pattern. The trap starts to retain the particles immediately and becomes clouded with contaminant rotating around the trap.

After the main portion of the contaminant enters the trap, there is nothing to observe in the separator except a whispy cloud rotating just above the apex of the separator and a column of air up through the center of the separator. The whispy cloud was only apparent when there was flow through the separator. The cloud appeared to be very, very small particles that became

suspended in the rotating fluid but were so small that they became suspended after the flow ceased. The column of air through the center of the separator extends from the vortex up to the outlet tube. It pulsates in a rhythmic cycle that coincides with the piston pump stroke. The center of the core in a vortex separator is an area of low pressure. An explanation for the air column may be that the low pressure area causes desaturation of the air in the water, or possibly vaporization (cavitation). As the flow progresses past the separator, the pressure profile across the flow area becomes more uniform, therefore, re-entraining the air. The suction phase of the piston pump stroke causes the low pressure required to do this.

Between the zero-gravity parabolas the equipment encountered a two-gravity force downward which tended to compact the contaminant onto the trap vane and trap bottom. The separator trap became clouded with contaminant within 1 to 2 seconds of the system start-up even with the contaminant compacted. There was no migration of particles into the separator at any time during or after the operation of the system. When the system was shut down just prior to zero-g, the cloud continued to rotate around the trap for the full twenty seconds of zero-g decelerating very slowly. The test subject theorized that the cloud would eventually stop rotating but would stay in a dispersed phase. After the contaminant settled on the trap vane and trap bottom, there was no activity at all when subjected to zero-g with no flow in the system.

When the system was operating, the cloud of contaminant in the separator trap indicated that the density of contaminant above the trap vane was slightly less than below the vane. Previous zero-g tests performed on the trap, without the separator, indicated that the vane forced the contaminant below the vane causing a significantly higher density below the vane. However, during the zero-g system tests, there was not a significant difference between the amounts of contaminant above and below the vane. Subsequent design and development activities, in an attempt to obtain a better trap with the smallest probability of particle migration, produced a trap with a tangential slot on the inside diameter of the vortex chamber and no vane. It was determined that this tangential slot trap design was sufficient to prevent the re-entrainment of particles and was tested during the zero-gravity tests of the Flight Prototype Filter Regeneration Unit.

The trap was removed from the separator in zero-g with negli-

gible water loss or air inclusion. It was removed during three parabolas and each time it was removed, a small air bubble, approximately 0.3 mm (.12 inches) in diameter, entered the separator. The trap was turned upside down and was moved about with no apparent fluid loss.

The existing design, with a small exposed fluid surface, was therefore an acceptable design for zero-g usage.

The high speed movie coverage also provided excellent coverage of the transparent filter bowl. The backflush flow was apparent as the contaminant was flushed off the filter element surface. Contaminant came off in the form of a cloud straight off the filter element surface and was directed upward. There was obvious turbulent action throughout the bowl. The visible residue on the bottom of the bowl was moved around by the turbulent action and most of it was removed by the end of the first zero-g parabola (20 seconds). The visible contaminant coming off the filter element was also gone by the end of the first parabola. It appeared therefore that the majority of the contaminant had been removed from the filter element and bowl within a 20-second period. The small residual contaminant left on the bottom of the bowl appeared to remain, even with the turbulent action. One factor that does not provide a true representation of zero-g usage is the two-gravity downward force encountered by the KC-135 aircraft between parabolas. This causes the residual to settle to the bottom of the filter bowl and may have been the reason that residual contaminant was found in the filter bowl after regeneration. This induced a slight reduction of the regeneration efficiencies.

Zero-g performance tests were also conducted on two different sets of quick disconnects in order to determine the type most acceptable for use in the flight prototype filter regeneration system. These two sets, shown below, were selected from a group of five different types after extensive evaluation tests considering pressure drop, air inclusion, spillage and human factors had been conducted.

Supplier	P/N	Size
Aeroquip Corp. Jackson, Michigan	3205-8 3202-8	1.27 cm (1/2 inch)
Seaton-Wilson, Inc. Burbank, California	2-1452-8 2-1453-8	1.27 cm (1/2 inch)

They both have similar pressure drops and both can be connected and disconnected under pressure. Both also have essentially zero fluid loss and air inclusion during the connect and disconnect operations. Their connect and disconnect operations are not the same. The Aeroquip requires a torquing motion to connect and has a relatively large body as compared to the Seaton-Wilson. The Seaton-Wilson has a push-to-connect operation.

During the zero-g tests, both types were connected and disconnected at pressures of 345×10^3 to 379×10^3 N/m^2 (50 to 55 psig). It was observed that the Seaton-Wilson was difficult to connect at pressures approaching 414×10^3 N/m^2 (60 psi). The disconnect operation for both was a pull action. Due to the difficulty of connection of the Seaton-Wilson quick disconnect at higher pressures, the Aeroquip quick disconnect was considered most acceptable for use in the filter regeneration system.

The maintainable filter was disconnected and connected a number of times in zero-g. There was no fluid pressure on the filter. Both the connect and disconnect operations were performed easily. A counterclockwise torquing action is required to disconnect the filter canister and a clockwise torquing action is required to connect. With this torquing action using one hand, the other hand had to be used to restrain the test subject. The test subject concluded that any torque that can be accomplished by a person in one-g could be accomplished in zero-g as long as one hand can be used for restraining.

F. ZERO-G TESTS, FLIGHT PROTOTYPE UNIT

The zero-g tests for the flight prototype filter regeneration unit was conducted on November 8-9, 1973 at Ellington Air Force Base, Texas. The zero-g tests were flown on a KC-135A aircraft. A total of 76 parabolas were flown during these two days of testing.

The hardware that was tested included the Filter Regeneration Unit (P/N 849FRS00001-009), a flight prototype filter (P/N 849FRS00007-010), and two regenerative filters (P/N RES31704-009).

Two different filter body designs were used during the tests. One was a Flight Prototype regenerative filter and the other two were

the same as those used during the development tests. The filter element micron rating for this test were 10 microns nominal/25 microns absolute. The backflush/impingement jet was the same as that used during the Development tests.

The zero-gravity environment tests were conducted in four separate tests over two days with two zero-gravity flights per day. A total of eight filters were regenerated in the zero-gravity environment with five filters regenerated with a total cumulative regeneration cycle of two minutes each, and three filters regenerated with a cumulative regeneration cycle of one minute each. One filter was installed upside down on the interface panel by the test subject and was not regenerated. In this position, no backflushing of the filter element occurs since the flow from the regeneration unit is merely pushed through the element in the normal flow direction. This error could not occur in a spacecraft system where the filter and the interface panel for the fluid subsystem would be fixed. This testing error was attributed to the test subjects' unfamiliarity with the operation of the filter regeneration system even though he was briefed on the proper filter connection procedure. The human factors aspects of the filter regeneration system were evaluated during both days of testing. The evaluation procedure consisted of the test subject removing and reattaching the particle separator trap, and removing and reattaching the Filter Regeneration Unit to the interface panel on the test skid. Figure V-42 shows the Flight Prototype Unit and the test skid as installed in the KC-135.

During the first day of testing, two tests were conducted with a total of 18 parabolas flown. For test No. 1, three regenerative filters were preloaded with AC coarse road dust using the filter loading and test support system shown in Figure V-43. Before the zero-g test flight, the test subject was briefed on the proper procedure of connecting and disconnecting the filters to the regeneration unit.

During test No. 1, only one of the three filters was regenerated properly. Upon completion of the regeneration cycle for the first filter, the test subject removed it from the regeneration unit and connected the second filter improperly as described above.

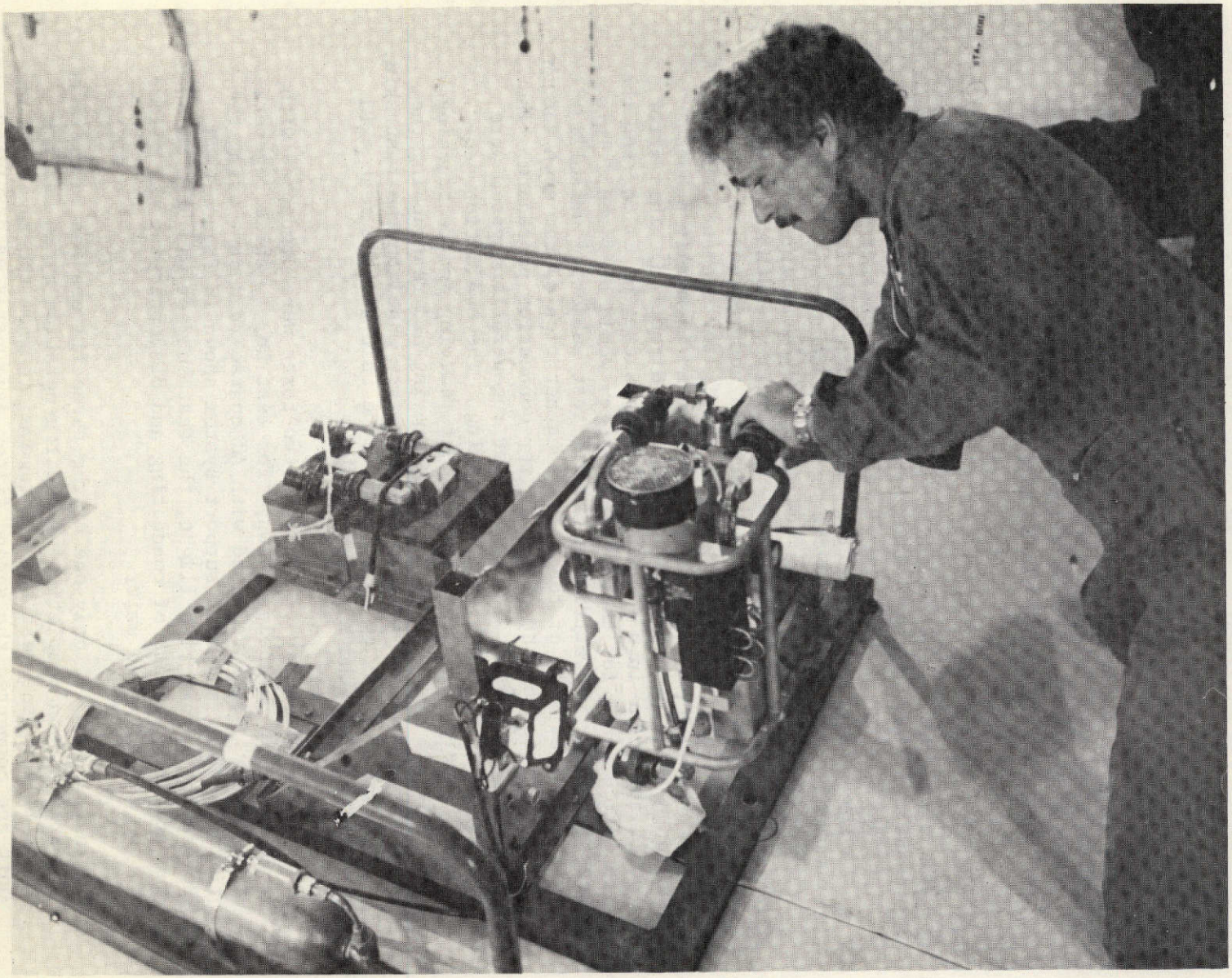

FIGURE V-42 FILTER REGENERATION SYSTEM INSTALLED IN KC-135

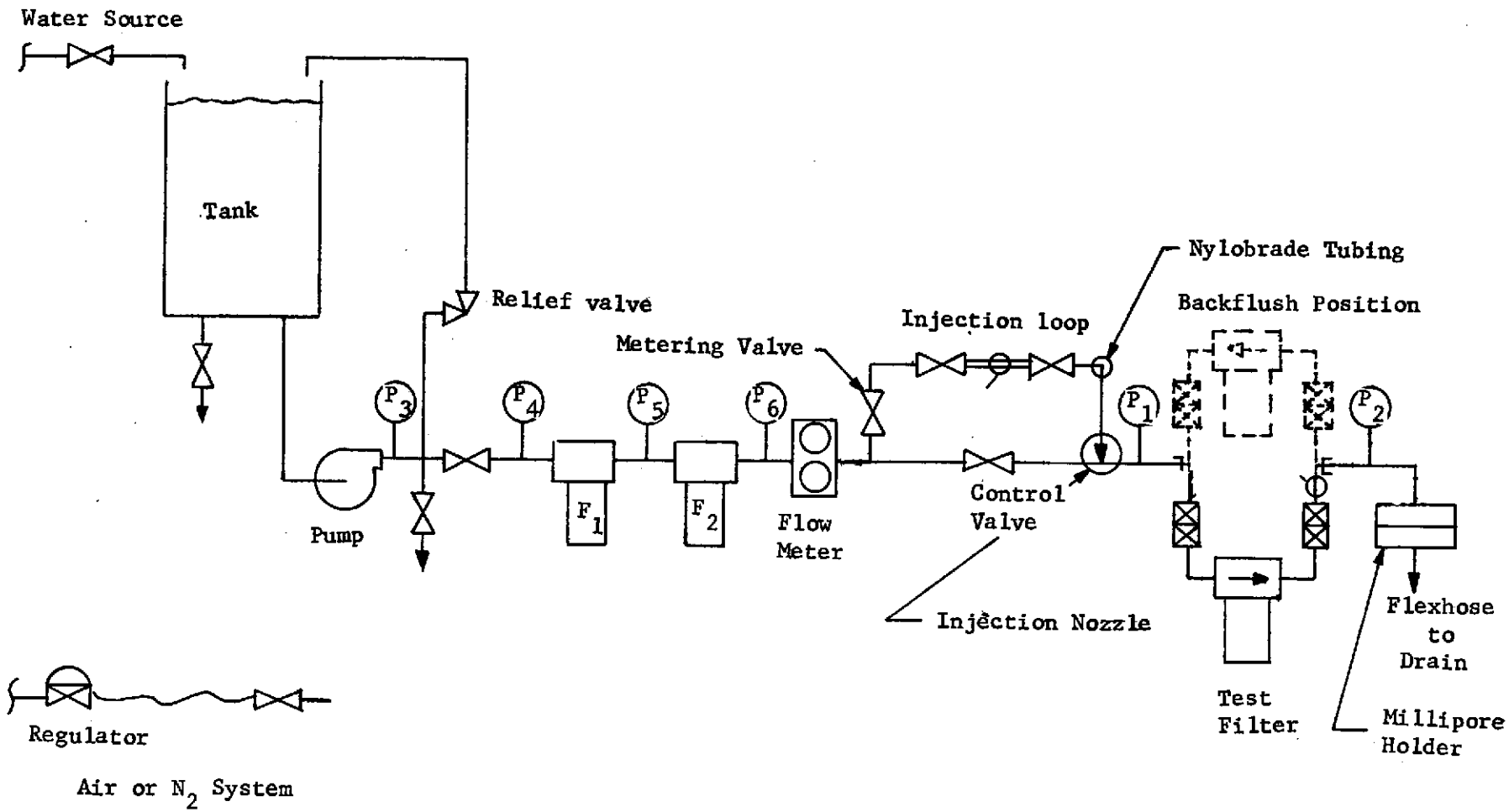

FIGURE V-43 GROUND TEST SUPPORT SYSTEM SCHEMATIC

The third filter was not regenerated due to fluid leakage and subsequent loss of static pump pressure when the test subject attempted to disconnect the second filter from the regeneration unit. This fluid and pressure loss upon disconnection of the second filter was caused by the method the test subject used when disconnecting the filter from the regeneration unit. To prevent fluid leakage, a quick and smooth motion should be used when connecting or disconnecting the regenerative filters. The test subject was briefed on this but he did not achieve the quick and smooth motion during the first day of testing. This was not a problem during the zero-g tests for the Development Unit because of the test subject's familiarity with the quick disconnect operation.

At the completion of test No. 1, the particle separator trap was removed from the regeneration unit and cleaned by ground test engineers. The contaminant retained by the trap was then collected on a .45 micron filter pad and returned to the NASA test facility to be dried in a vacuum oven and weighed. There was an approximate 1 hour turn-around period between tests No. 1 and No. 2. During this turn-around period, one filter was reloaded with AC coarse road dust and returned to the test aircraft for regeneration.

Before test No. 2, the Filter Regeneration Unit was removed from the aircraft and recharged with fluid and pressure to approximately 228 x 10^3 N/m^2 (33 psig). During this test, a total of 18 parabolas were flown, with one filter regenerated with a cumulative regeneration cycle of 1 minute and the second filter regenerated with a cumulative regeneration cycle of 2 minutes. It was concluded from the low efficiencies obtained from the 1 minute regeneration cycles that a 1 minute cyclic regeneration cycle is not sufficient to properly regenerate (clean) the regenerative filters.

After both filters had been regenerated in zero-g, the test subject performed the human factors tasks. When the separator trap was removed from the regeneration unit no apparent fluid leakage was noted. However, the test subject was unable to reconnect the separator trap during the same 20 second parabola and, therefore, had to hold the trap during the 2-g environment. During this time he noted a couple of drops of fluid spilled on his hand. The removal of the trap was much easier during this test than in the previous zero-g tests of the Development Unit where a V-band clamp, used to attach the trap to the separator, required the use of both hands in

a zero-g environment.

The test subject was able to remove and reattach the Filter Regeneration Unit to the interface panel easily in one parabola (20 sec period). There was no apparent human factor problems associated with this task. The latch mechanism is used to attach the filter regeneration unit to the interface panel. This is accomplished by a cam-lock that extends from the regeneration unit and engages a pin in the filter panel. The cam-lock is actuated by turning a T-Handle 3.14 radians (180 degrees). The latch mechanism was easy to operate in zero-g but it appeared that foot restraints would have enhanced this task.

At the completion of test No. 2, the separator trap was removed and cleaned and its contaminant retained on a .45 micron filter pad. Also, at the end of this test, the secondary filter was removed from the regeneration unit and cleaned. The contaminant retained from the secondary filter backflush was proportioned for each of the 3 filters regenerated. The contaminant from the backflush of the three filters cleaned during the first day was retained on .45 micron pads. Table V-15 shows the amount of contaminant recovered from the separator trap, filter bowl, and secondary filter as compared to the amount of contaminant retained on the filter elements for the 4 zero-g test runs. The subsystem efficiencies were determined by comparing the amount of contaminant recovered from the separator trap and filter bowls to the amount of contaminant originally retained on the filter elements. As can be seen from Table V-15, the subsystem efficiency for test No. 1 was 72.5% while the subsystem efficiency for test No. 2 was only 45.3%. The lower efficiency for test No. 2 was caused by the one minute filter regeneration cycle. A one minute, cyclic, regeneration cycle is not sufficient to clean the fluid filters in either 1-g or zero-g environments.

During test No. 3, three filters were regenerated with a cumulative regeneration cycle of 2 minutes each for a total of 20 parabolas. Test No. 4 was conducted with two filters regenerated with a cumulative regeneration time of one minute each. The results of the contaminant recovered, and the subsystem efficiencies for these two tests are given in Table V-15. Twenty parabolas were accumulated on test No. 4.

Table V-15 Filter Regeneration Unit Zero-G Performance Tests

Test No.	Filter	Test Duration Minutes	Contaminant Added (Grams)			Contaminant Recovered (Grams)				Efficiency	
			Total Added to System	Recovered on Millipore	Retained on Filter Element	Separator Trap	Wash from Filter Bowl	Secondary Filter Backflush	Net Contaminant Recovered	Sub-system	Recovery
			A	B	C = A-B	D	E	F*	G = D+E+F	Eff = $\frac{D+E}{C}$	Eff = $\frac{G}{C}$
1	9-A	2 Min	3.0442	.7055	2.3387	1.6721	.0238	.0585	1.7544	72.5	75%
2	7-C 9-A	1 Min 2 Min	8.2754	1.3978	6.8776	2.4602	.6559	.1720	3.2881	45.3	47.8%
3	9-A 8-B 7-C	2 Min	9.2098	1.8967	7.3131	4.3492	.7154	.2160	5.2806	69.2	72.2%
4	9-A 8-B	1 Min	6.1988	1.0605	5.1383	2.0011	.5865	.1517	2.1528	50.4	91.9%

* Secondary Filter Backflush Proportioned for each Test.

After completion of the regeneration cycles for test No. 4, the human factor tasks were performed with no problems noted. There was no fluid leakage upon removing the separator trap, and the Filter Regeneration Unit was easily removed and attached to the interface panel.

The low subsystem efficiencies, indicated by Table V-15, were caused by various factors. First of all, it was shown during the zero-g tests on the Development Unit that there is approximately a 12.23% efficiency loss due to the 20-second cyclic mode of operation inherent in the KC-135 parabolas. This cyclic operation causes a loss of inertia in the particles during each cleaning cycle, which is not present in a continuous regeneration process, and therefore reduces the filter cleaning efficiency.

A second factor that may have produced the low subsystem efficiencies was the loss of contaminant during handling and transferring the filter pads. After each zero-g test, the contaminant retained by the separator trap was transferred to a .45 micron filter pad and returned to the NASA test facility (approximately 15 miles) to be dried in the vacuum oven. The pads were also handled during the weighing procedures which could have induced some contaminant loss. Some of the filter pads from tests No. 3 and No. 4 did not get completely dry and had to be transported back to Martin Marietta-Denver for drying and weighing.

The fact that the contaminant recovery efficiencies, shown in Table V-15, were very low supports the possibility that there was a loss of contaminant.

Another factor that may have caused the lower subsystem efficiencies was the differences between the NASA vacuum drying oven and the Martin vacuum oven. Since the NASA vacuum drying oven was much larger and had a different drying temperature range than the Martin vacuum drying oven, lower efficiencies could have resulted from differences in moisture content of the filter pads.

VI. QUALITY ASSURANCE, RELIABILITY, AND SAFETY SUMMARY

A. QUALITY ASSURANCE

The quality assurance effort for this contract was conducted by representatives from the Quality Assurance Organization. A quality representative was assigned to the program to coordinate and monitor all quality assurance effort. The local NASA quality assurance representative was in attendance at all internal design reviews and performed an inspection of the flight prototype hardware prior to shipment to NASA-JSC.

Quality assurance effort was involved in the design, procurement, receiving, fabrication, testing, shipping, and final inspection of the deliverable hardware. A quality representative was in attendance at all design reviews and supplied significant input particularly in the areas of controls and processes to be used in the fabrication phase. During the procurement cycle, quality assurance was responsible for specification of the inspection processes and supplier qualification. All of the raw materials, parts, and components were inspected by quality assurance in receiving. Special emphasis was placed upon the selection, build, and testing of the motor/pump assembly which was a major component in the end item. On this component a supplier quality source inspection was conducted prior to awarding the contract. In-process and end item inspection was performed at the suppliers facility by the regional quality assurance group. They were also in attendance and witnessed the final acceptance tests.

During the fabrication and build of the end item, in-process and final inspections were made to assure the proper level of workmanship and quality of the end item. Quality assurance was also responsible for monitoring the packaging and shipment of the end item.

B. RELIABILITY

All of the components in the flight prototype filter regeneration unit are passive with the exception of the cooling fan and the motor/pump. The cooling fan is used to cool the unit during and after operation. As many as three successive two minute regenerations can be conducted without requiring the use of the

fan. The fan has a separate electrical switch and circuit breaker and is independent of the pump electrical circuit. The fan has an inlet screen to prevent any foreign material from entering the fan blades.

The motor/pump assembly is critical to the operation of the regeneration unit and supplies the correct fluid flow and pressure necessary for the regeneration process. The pump is sized to flow 22 percent more flow than is required for the regeneration process and therefore some degradation in performance is permissible. In order for the pump to operate correctly it must have a positive pressure, 6.89×10^3 N/m^2 (10 psig), on the pump inlet prior to start-up. This pressure is provided by a pressurized bellows in the accumulator. Inlet pressure can be verified on the pump pressure gage prior to start-up. The bellows is normally pressurized to 24.13×10^3 N/m^2 (35 psig) which allows for some margin in the event of leakage. The bellows can also be repressurized. Lack of a liquid interface at the pump inlet or ingestion of large amounts of air would cause decreased performance or failure of the pump. Lack of flow or proper pressure can be instantly recognized by a low pump outlet pressure as indicated on the pressure gage. Lack of a fluid interface would be caused by fluid vaporization. This failure mode is prevented by a overtemperature sensor that prevents pump start-up when the fluid temperature rises above 55°C (150°F). The pump life is estimated at 600 hours of operation, or 18,000 filter regenerations. The filter regeneration unit was designed with maintainability as a prime consideration. The unit was designed with open access to all components, component level of repair, commonality in fasteners and fluid fittings, and with minimized tool requirements. The maintainability aspects of the design are described in detail in Section I-B.

C. SAFETY

The safety requirements of this program were assured by the performance of a stress analysis on all components in the fluid system and the selection of materials to meet the stress and environmental requirements. In addition, the test system and the test program were monitored by the safety organization. Prior to the zero-g test program in the KC-135 aircraft all aspects of the test equipment, electrical equipment, and test procedures were reviewed and approved by the cognizant agencies.

On the regeneration unit, the cooling fan is enclosed by an inlet and outlet screen to protect the operator. An over-temperature sensor also prevents the skin temperature from reaching excessive temperatures. The unit is protected from external damage by an enclosing frame. The fluid pump is a centrifugal design and reaches a maximum pressure of 154.7 N/m^2 (220 psig). All electrical circuits are protected by circuit breakers.